The preparation of antigen for the generation of polyclonal antibodies against the capsid subunit, VP1, and the viral protease, $3C^{pro}$, of Theiler's murine encephalomyelitis virus (TMEV)

Dissertation submitted in fulfilment of the requirements for the degree of

Masters of Science in Microbiology

At

Rhodes University

By

Boitumelo Moetlhoa

August 2013

Abstract

The *Picornaviridae* is a family of viruses of economic importance that have a major impact on human and animal health. Some of the major genera found in the *Picornaviridae* family are *Enterovirus* which includes Poliovirus (PV) and Human Rhinovirus (HRV), *Cardiovirus* which includes Theiler's murine encephalomyelitis virus (TMEV) and Saffold virus (SAFV), *Aphthovirus* of which the Foot and Mouth disease virus (FMDV) is a member and *Hepatovirus* which includes Hepatitis A virus (HAV). Picornaviruses have a single stranded, positive sense RNA genome which is approximately 7.5-8.4 kb pairs in size. The picornavirus genome is translated into a large polyprotein and is proteolytically cleaved by viral proteases namely $2A^{pro}$, $3C^{pro}$ and $3CD^{pro}$ into mature viral structural and non-structural polypeptides encoded by the P1, P2 and P3 domains. Picornaviruses utilise host cell machinery and cellular pathways for entry and uncoating, genome replication and capsid assembly. In our laboratory, we are studying the mechanisms by which TMEV interacts with host cell components and our recent research shows that molecular chaperones are required for a production infection. To follow up on this observation, the overall aim of this study was to prepare antigen for the generation of polyclonal antibodies against the TMEV VP1 and $3C^{pro}$ proteins. To this end, the TMEV VP1 and $3C^{pro}$ amino acid sequences were analysed to identify hydrophobic, hydrophilic and antigenic regions. Homology modelling was performed in order to predict linear B cell epitopes exposed on the surface of the protein structures. The full length coding sequences of VP1 and $3C^{pro}$ were selected for amplification by the PCR and cloning into pQE-80L for expression in a bacterial system. Time course induction studies of recombinant VP1 and $3C^{pro}$ showed that the proteins were maximally expressed at 6 hrs and 4 hrs respectively. Recombinant VP1 was solubilised using the detergent, Sarcosyl and purified by Nickel affinity chromatography under native conditions. Because recombinant VP1 co-purified with an unidentified protein, the pET expression system was used. Although no protein of the estimated size was observed by SDS-PAGE analysis in the time course induction study, Western analysis using anti-His_6 (2) antibodies detected a signal of ~35 kDa. Solubility studies resulted in the presence of two protein bands in the insoluble fraction resolved between 35 and 40 kDa.

Recombinant $3C^{pro}$ expressed in a bacterial system was predominantly present in the insoluble fraction. Treatment with Sarcosyl had no effect on the solubility of the recombinant protein and it was therefore purified under denaturing conditions using 8M urea. Following dialysis, $3C^{pro}$ was used for immunisation of rabbits.

Crude anti-TMEV $3C^{pro}$ antibodies were able to detect as little as 107 ng of bacterially expressed antigen at a dilution of 1:100 000 by Western analysis. The presence of contaminating proteins was reduced using pre-cleared anti-TMEV $3C^{pro}$ antibodies. The antibodies were unable to detect virally expressed $3C^{pro}$ in BHK-21 cell lysate supernatant. In an attempt to determine whether TMEV $3C^{pro}$ is present in the insoluble fraction, anti-TMEV $3C^{pro}$ antibodies were tested using total protein prepared from infected and mock-infected cell lysates. Once again, no protein band the size of $3C^{pro}$ was detected. The antibodies were further tested for detection of $3C^{pro}$ in TMEV-infected cells by indirect immunofluorescence and confocal microscopy. A diffuse cytoplasmic and perinuclear distribution, as well as nuclear staining, was observed in infected BHK-21 cells. This staining pattern resembled that observed for the HRV, FMDV and EMCV $3C^{pro}$ in similar experiments. Further experiments are required to confirm specificity of these antibodies for virally-expressed $3C^{pro}$ by Western analysis and indirect immunofluorescence.

Declaration

I, Boitumelo Moetlhoa, hereby declare that this MSc dissertation is my own unaided work completed in fulfilment of the requirements for the degree masters of Science at Rhodes University.

Signature:..... Date:.....

Table of Contents

List of figures

List of tables

List of Abbreviations

Viruses

CV: Coxsackievirus

CCHFV: Crimean-Congo Haemorrhagic fever virus

EMCV: Encephalomyocarditis virus

FMDV: Foot and Mouth disease virus

HAV: Hepatitis A virus

HCV: Hepatitis C virus

HIV-1: Human immunodeficiency virus-1

HPV: Human Parechovirus

HRV: Human Rhinovirus

HSV: Herpes simplex virus

PV: Poliovirus

SAFV: Saffold virus

TMEV: Theiler's murine encephalomyelitis virus

General

BHK: Baby hamster kidney

BSA: Bovine serum albumin

CAR: Coxsackievirus-Adenovirus receptor

CD55: Decay accelerating protein

CO_2: Carbon dioxide

CNS: Central nervous system

CPE: Cytopathic effect

DAPI: 4', 6- Diamino-2, phenylindole dihydrochloride

DMEM: Dulbecco modified Eagle's medium

DNA: Deoxyribonucleic acid

ELISA: enzyme-linked immunosorbent assay

ER: Endoplasmic reticulum

FCA: Freund's complete adjuvant

FIA: Freund's incomplete adjuvant

FCS: Fetal calf serum

h.p.i: Hours post-infection

hrs: Hours

Hsc70: Heat-shock cognate 70

Hsp40: Heat shock protein 40

Hsp70: Heat Shock protein 70

Hsp90: Heat shock protein 90

Hsps: Heat shock proteins

ICAM-1: Intracellular adhesion molecule-1

IF: Immunofluorescence

IPTG: Isopropyl-β-D-1-thiogalactopyranoside

IPV: Inactivated poliovirus vaccine

IRES: Internal ribosome entry site

MBP: maltose binding protein

Min: Minute

MOI: Multiplicity of infection

mRNA: Messenger RNA

MTOC: Microtubule organising centre

NTP: Nucleotide triphosphate

OD_{600nm}: Optical density at 600nm

OPV: Oral poliovirus vaccine

ORF: Open reading frame

PBS: Phosphate buffered saline

PBP: Poly (A) binding protein

PCR: Polymerase chain reaction

PDB: Protein databank

PMSF: Phenylmethyl-sulfonyl fluoride

Poly (A): Polyadenalated

PSF: Penicillin, streptomycin and fungizone

PVR: Poliovirus receptor

RdRp: RNA-dependent RNA polymerase

RNA: Ribonucleic acid

RER: Rough endoplasmic reticulum

RT: Reverse transcriptase

Sarcosyl: N-lauroylsarcosine

SDS-PAGE: Sodium dodecyl sulphate polyacrylamide gel electrophoresis

Sec: Seconds

TBS: Tris buffered saline

TPR: Tetratricopeptide repeats

UTR: Untranslated region

UV: Ultra violet

VPg: Virus protein of the genome

WHO: World Health Organisation

Units and symbols

α: alpha

β: beta

bp: base pairs

%: percentage

°C: degrees Celcius

cm^2: square centimetre

g: gram

x g: times gravity

kDa: kilo Daltons

mM: millimolar

mg: milligrams

ng: nano grams

µg: microgram

µl: micro litres

V: Volts

List of outputs

Local Conferences Proceedings:

Moetlhoa B, van Marwijk J, Edkins A, Mutsvunguma L and Knox C. The generation and testing of polyclonal antibodies against the structural capsid protein VP1. Poster presentation SASM 2011 conference, held at the Southern Sun Cape Sun Hotel, Cape Town November 6-9.

Research articles:

Mutsvunguma LZ, **Moetlhoa B,** Edkins AL, Luke AG, Blatch GL & Knox C, (2011) Theiler's murine encephalomyelitis virus infection induces a redistribution of heat shock proteins 70 and 90 in BHK-21 cells, and is inhibited by novobiocin and Geldanamycin. *Cell stress and chaperones* **15**, 505-515

Acknowledgements

I would like to take this time and extend my sincere thanks and appreciation to the following people:

- My supervisor, Dr Caroline Knox, for the motivation, guidance and encouragement. I am truly grateful for all valuable things you have taught me. Thank you for your time and patience during the writing of my thesis
- My co-supervisor, Prof. Rosemary Dorrington for the guidance and support
- Dr J van Marwijk for the support and assistance throughout this study, you were God sent
- Lab 425 members (Brittany, Michael, Fatima and Dora) for the support and always making it a great pleasure to work with you guys
- To Lorraine for your never ending patience and assistance and for always being there when I thought I would never make it to the end
- Isago and Sanele for being my motivation and support throughout.
- My family and friends for the love, motivation and encouragement I received during the course of this study. To mommy and daddy, you have been my pillars of strength and I thank you for believing in me
- The South African National Research Foundation and Medical Research Council for funding
- Above all, I would like to thank the Almighty for making my wish come true and for guiding me throughout this study

Chapter 1: Literature Review

1.1 The Picornaviridae family

The *Picornaviridae* is a family of viruses which infect humans, animals and some plant species. The word *pico* is Italian for 'small', which is one of the main characteristics of these viruses. Picornaviruses have a single stranded, positive sense RNA genome which is approximately 7.5-8.4 kb pairs in size. The size of the non-enveloped viral capsid is between 28-30 nm in diameter and is icosahedral in shape. Picornaviruses are of economic importance worldwide and include some of the most widely studied agricultural and human pathogens such poliovirus (PV), foot-and-mouth disease virus (FMDV), an important pathogen of livestock, human rhinovirus (HRV), a cause of the common cold and the human hepatitis A virus (as reviewed by Bedard and Semler, 2004; Racaniello, 2007).

Currently the *Picornaviridae* family comprises of seventeen genera: *Enterovirus, Cardiovirus, Aphthovirus, Hepatovirus, Parechovirus, Erbovirus, Kobuvirus, Teschovirus, Sapelovirus, Senecavirus, Tremovirus, Aquamavirus, Cosavirus, Dicipivirus, Megrivirus, Salivirus and Avihepatovirus* (Knowles *et al*., 2012; Adams *et al*., 2013). Table 1.1 below gives examples of some significant viruses within the family and the diseases they cause.

Table 1.1: Genera of the *Picornaviridae* family and examples of viruses and their resulting diseases (adapted from Knowles *et al*., 2012).

Genus	Virus Examples	Diseases caused
Enterovirus	Poliovirus, Human rhinovirus	Poliomyelitis, Common cold
Cardiovirus	Theiler's virus	Mouse encephalomyelitis
Aphthovirus	Foot-and-mouth disease Bovine rhinitis A and B disease	Foot and disease in livestock Bovine rhinitis A and B virus
Hepatovirus	Hepatitis A virus	Liver disease
Parechovirus	Human Parechovirus	Chronic meningoencephalitis
Teschovirus	Porcine teschovirus	Teschen-Talfan neurological disease
Kobuvirus	Bovine kobuvirus, Aichi virus	Enteric disease Human gastroenteritis

1.1.1 Economic Importance of Picornaviruses

As mentioned above, diseases caused by picornaviruses have varied economic and health effects. This section focuses on three economically important viruses namely, FMDV, HRV and PV.

FMDV which belongs to the genus *Aphthovirus* is well known for its negative impact on economically important livestock. FMDV is an acute infectious disease causing fever which is followed by blisters on the feet and mouth of cloven hooved animals such as sheep, goats, cattle and pigs. The outbreak of FMDV in 2001 did not only affect the farming industry but also the tourism industry causing a decrease in the economic growth of the United Kingdom (UK). The total losses were estimated to be between US $ 12.3 billion and $13.8 billion (as reviewed by Grubman and Baxt, 2004). Countries affected by FMDV are unable to participate in livestock trade in order to avoid the spreading of the virus to FMD-free nations (Domingo *et al*., 2002). Some European countries were faced with traumatic financial problems in 2001 when millions of livestock suspected of being infected with FMDV were slaughtered (Thompson *et al*., 2002).

HRV is classified under the genus *Enterovirus* and is known for causing the common cold. This virus is of economic importance as it causes companies billions of dollars due to people taking leave of absence from work because of viral infection or to take care of others infected with the virus. More than 500 million cases of the common cold are reported each year in the USA and this then leads to billions of dollars being lost annually (Fendrick *et al*., 2003). No effective vaccine or cure has been established to date for HRV infection possibly due to the rapid antigenic drift observed in the virus (Savolainen *et al.*, 2002).

PV is an acute infectious virus which belongs to the genus *Enterovirus*. PV is responsible for causing severe poliomyelitis which has affected millions of humans in the past, (as reviewed by Bedard and Semler, 2004). The first isolation of PV in 1908 was followed by years of research on the virus leading to the production of two effective vaccines. The first vaccine was produced in 1950s and was an inactivated poliovirus vaccine (IPV) developed by Jonas Salk. The vaccine consisted of a mixture of three wild type poliovirus strains inactivated with formalin to destroy infectivity of the virus without affecting antigenic properties of the capsid. The second vaccine was a live attenuated oral poliovirus vaccine (OPV) developed by Albert Sabin in the 1960s for vaccination in underdeveloped countries. OPV led to the

elimination of PV from entire continents by the 1980s (as reviewed by Racaniello, 2007). The World Health organisation (WHO) aimed in 1988 to eradicate PV completely by the year 2000 using OPV because of its low cost and its ability to interrupt virus transmission. By the year 2002 the occurrence of PV infections had significantly decreased on a global scale (as reviewed by Racaniello, 2007; World Health Organisation, 2002). The discovery of two vaccines against PV initially led to the thought that PV would be completely eradicated in most countries across the world by 2005, but with some countries such as India, Afghanistan and Pakistan still reporting cases of people being infected and affected by PV suggests that the total eradication of the virus has not been achieved (as reviewed by Racaniello, 2007).

A number of studies have been done in order to further understand the mechanisms used by these economically and clinically important viruses during replication, assembly and viral-host interactions. Although members of the picornavirus family have a similar genome organisation, the proteins they express may perform different functions in the virus life-cycle. The following sections will discuss the genomic organisation, polyprotein processing, replication and assembly of picornaviruses using PV as a model.

1.2 Picornavirus Genome Organisation

A schematic representation of PV genome organisation is shown in Figure 1.1 below. As seen in the figure, a viral protein, VPg is covalently linked to the 5' untranslated region (UTR) of the viral genome. This protein plays a role in the initiation of viral RNA replication (as reviewed by Bedard and Semler, 2004). The 5' UTR also contains a cloverleaf structure known as the internal ribosome entry site (IRES). The IRES is a sequence which promotes translation initiation of the viral RNA while the host cell protein translation machinery is shut off, and is also responsible for recognizing the 40s ribosomal unit and forming a secondary structure that stabilizes the RNA required for translation (Belsham and Nahum, 2000; as reviewed by Bedard and Semler, 2004; Racaniello, 2007). All picornaviruses have a polyadenylated (poly-A) tail characteristic of a eukaryotic mRNA attached to the 3' end of the genome (as reviewed by Bedard and Semler, 2004). The poly (A) region is thought to be involved in the translation and RNA replication, how the virus does this however is not fully understood.

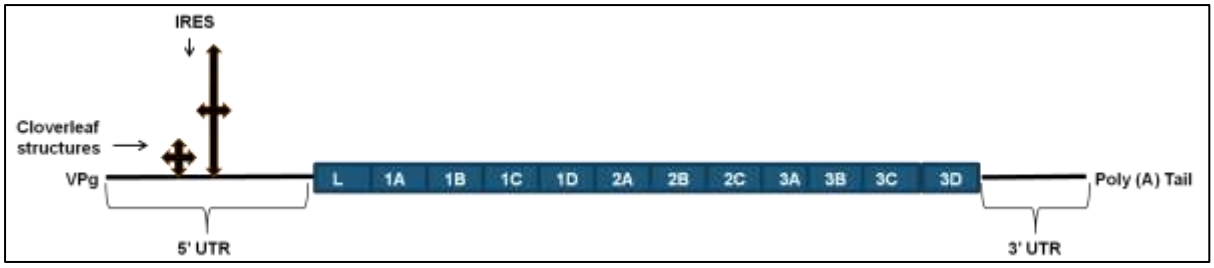

Figure1.1: Schematic diagram showing the genome organisation of picornaviruses. The VPg is located at the far end of the 5' UTR. The IRES is located within the 5' UTR of the genome followed by the coding region of the viral proteins. The poly (A) tail is present at the 3' UTR (adapted from Bedard and Semler, 2004).

1.2.1 Polyprotein Processing

Picornavirus genomes consist of one open reading frame (ORF) which is translated in the host cytoplasm to form a single large polyprotein. The polyprotein is proteolytically cleaved by virus-encoded proteases into mature viral structural and non-structural polypeptides which are encoded by the P1, P2 and P3 precursors (Figure 1.2). The first cleavage involves the separation of the P1 domain from the P2 and P3 domains by $2A^{pro}$ and the remaining cleavages are conducted by $3C^{pro}$ and its precursor $3CD^{pro}$ (as reviewed by Bedard and Semler, 2004; Racaniello, 2007).

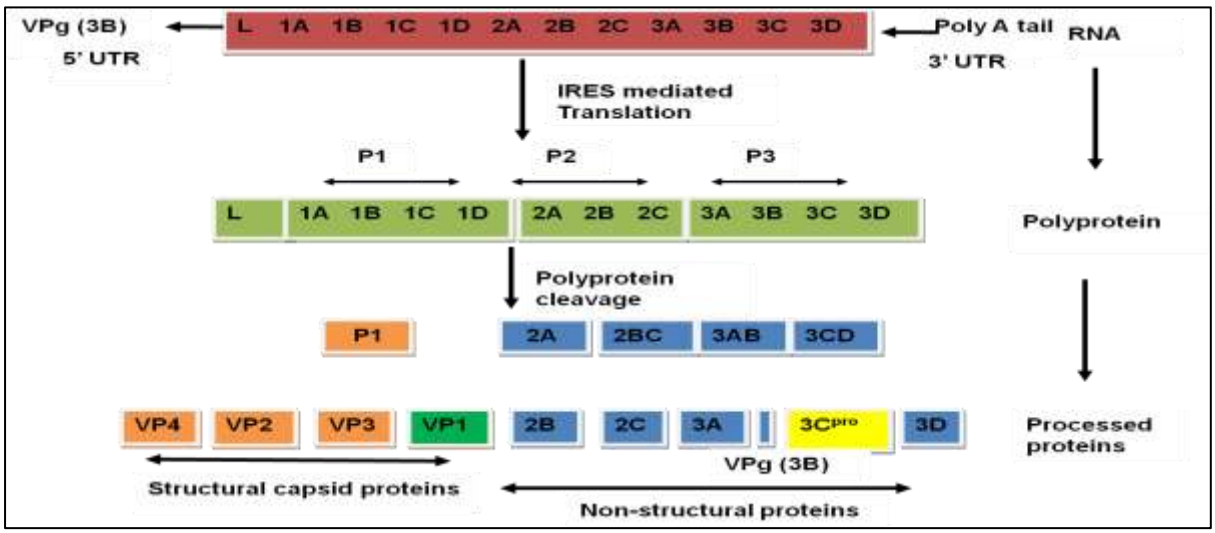

Figure 1.2: Schematic diagram of picornavirus polyprotein processing. The single ORF is translated into a single large polyprotein which gets cleaved by proteases in three domains P1, P2 and P3 respectively. The P1 gives rise to structural proteins (VP1-VP4) and the P2 and P3 domains give rise to non-structural proteins (2A-3D) which play a role in the viral replication process (adapted from Buenz and Howe, 2004).

Mature viral proteins are classified into two groups, the structural and non-structural proteins. The structural proteins, VP1, VP2, VP3 and VP4 are responsible for forming the viral capsid. The viral capsid comprises of 60 copies of each of the structural proteins, VP1-4. These proteins initiate viral infection by binding to the receptor found on the cell surface of the host and are also responsible for virion assembly. For example, the capsid subunit protein, VP1 has been found to bind to host cell receptors such as intracellular adhesion molecule-1 (ICAM-1) for rhinovirus and poliovirus receptor (PVR) for poliovirus (Olson *et al*., 1993; as reviewed by Racaniello, 2007). The properties and functions of VP1 will be discussed in detail in a later section.

The non-structural proteins, with the exception of the leader (L) protein of aphtho- and cardioviruses which is encoded on the 5' region of the ORF, are found within the P2 and P3 domain and are responsible for virus replication, these proteins have been found to be more conserved across the *Picornaviridae* family than the structural proteins (Stanway, 1990; Hughes, 2004; Buenz and Howe, 2004; Bedard and Semler, 2004). The non-structural proteins are known to be responsible for targeting and rearranging cellular membranes in order to create membranes on which replication takes place (Bienz *et al*., 1990; Aldabe and Carrasco 1995; Knox *et al*., 2005; Moffat *et al*., 2005). The section below gives a brief description of the function of each non-structural protein including precursors.

The L protein is found only in aphthoviruses and cardioviruses and there is a great sequence deviation in the peptide across viruses which have this protein within their genome (Aminev *et al*., 2003). The L protein is a protease which helps in the inhibition of cap-dependant translation through the cleavage of translation initiation factors such as elF4GI and elF4GII (Buenz and Howe, 2004). In TMEV, this protein has been suggested to inhibit the host immune response by interfering with the production of α / β interferon (van Pesch *et al*., 2001).

$2A^{pro}$ is a protease which cleaves the P1 domain from the P2 and P3 domains. In hepatoviruses, aphthoviruses and parechoviruses, the $2A^{pro}$ does not have a proteolytic function and the primary cleavage between the P1, P2 and P3 domains is carried out by $3C^{pro}$ (as reviewed by Racaniello, 2007). During PV infection, $2A^{pro}$ works along with the other viral proteases to cleave the endogenous translation initiation factor, elF4GI, in order to inhibit host cell translation (Zamora *et al*., 2002; Buenz and Howe, 2004).

The 2B protein has been identified as a viroporin, which are a class of transmembrane proteins that alter the permeability of membranes thus leading to the disassembly of the Golgi complex. This protein is implicated in inhibition of the cellular secretory pathway in PV-infected cells (Sandoval and Carrasco, 1997; Buenz and Howe, 2004). The 2BC protein is a precursor of 2B and 2C proteins. 2BC together with 2C protein are believed to migrate to the rough endoplasmic reticulum (RER) where they induce the formation of smooth membranes which bud off to become the site of RNA synthesis (Bienz *et al*., 1990, 1992; Cho *et al*., 1994).

The 2C protein is the most conserved non-structural protein within the *Picornaviridae* family. The secondary structure of 2C comprises of three domains, a nucleoside triphosphate (NTP) binding domain, RNA binding domain and the membrane binding domain (Rodriguez and Carrasco, 1995; Carrasco *et al*., 2002; Banerjee *et al*., 2004). 2C has many functions associated with viral replication including, uncoating, host cell membrane association, NTPase activity, RNA replication, and encapsidation, but the role that 2C plays in these functions is yet to be discovered (Li and Baltimore, 1990; Wimmer *et al*., 1993; Cho *et al*., 1994; Mirzayan and Wimmer, 1994; Vance *et al*., 1997). 2C has also been shown to control viral protease activities. Multiple sequence alignments of 2C with protease inhibitors have shown that 2C contains serine protease motifs scattered throughout its sequence, suggesting that 2C plays a regulatory role in protease activity. PV 2C was found to co-immunoprecipitate with viral 3C protease which resulted in the inhibition of proteolytic activity of 3C both *in vivo* and *in vitro* (Banerjee *et al*., 2004). Antibodies generated against TMEV 2C have localised the protein to the Golgi apparatus where it forms part of the replication complex (Jauka *et al*., 2010). Studies conducted with FMDV have indicated that at early stages of infection 2C locates to a diffuse punctate pattern to one side of the nucleus and is concentrated into larger structures next to the nucleus during later stages (Knox *et al*., 2005). Expression of FMDV 2C in Vero cells showed some endoplasmic reticulum (ER) localisation, however most of the protein was located in punctate structures within the Golgi (Moffat *et al*., 2005). In a similar study, V5-tagged TMEV 2C was also localised to the Golgi apparatus when expressed alone in BHK-21 cells using anti-β-COP antibodies (Murray *et al*., 2009). PV 2C was localised to the perinuclear membrane region and in a pattern characteristic of the ER in infected HeLa cells with no presence of other viral proteins (Echeverri and Dasgupta, 1995).

The 3A protein is one of the products from the cleavage of the 3AB protein and plays a role virion replication (Buenz and Howe 2006). PV 3A is known to play a role in altering ER to Golgi trafficking which leads to the evasion of the host immune response by the inhibition of interleukins and interferon (Dodd *et al*., 2001; Buenz and Howe, 2006).

The 3B protein is also known as the VPg protein of picornaviruses and is covalently bound to the 5' end of the viral genome. The uridylylation of 3B causes the protein to act as a primer which initiates RNA synthesis, implying that 3B is a factor in regulating viral replication (Buenz and Howe, 2004; Pathak *et al*., 2007).

3CD is a precursor protein for $3C^{pro}$ and 3D and acts as a protease during the second cleavage of the polyprotein alongside $3C^{pro}$ (Bedard and Semler, 2004). The properties and functions of $3C^{pro}$ will be described in detail in an upcoming section. The 3D protein is the RNA-dependant RNA polymerase which plays a role in the RNA chain elongation during the viral RNA synthesis (as reviewed by Racaniello, 2007; Flint *et al*., 2009).

1.2.1.1 VP1 capsid subunit protein

The viral capsid of picornaviruses is known to assist with viral attachment and entry into the host cell. The capsid subunit protein, VP1 has been suggested to be the protein responsible for aiding the attachment and entry of picornaviruses by binding to host cell receptors. Receptors which interact with VP1 include the intracellular adhesion molecule-1 (ICAM-1) for HRV, poliovirus receptor (PVR) for PV, Coxsackievirus-adenovirus receptor (Car) for Coxsackie B1-6 virus and the vitronectin receptor for FMDV (Olson *et al*., 1993; as reviewed by Racaniello, 2007; Lin *et al*., 2009). Capsids of most enteroviruses have been found to have canyons which have been suggested to be the sites of interaction with host cell receptors. The interaction of PV canyon with its receptor, PVR causes structural changes in the virus exposing the lipophilic N-terminus of VP1. This region has an affinity for membranes and moves towards the host cell membranes where it forms a pore through which viral RNA can enter into the cell and make its way to the cytoplasm (as reviewed by Racaniello, 2007).

Picornaviral VP1 consists of eight-stranded antiparallel beta barrels cores also called a beta-barrel jelly roll or a Swiss-roll beta-barrel, which are similar to those found in VP2 and VP3 (figure 1.3). This beta structure forms a wedge shaped structure which is known to assist in

the packaging of structural units to form a rigid protein shell, suggested to be essential for the stability of the virion (as reviewed by Racaniello, 2007).

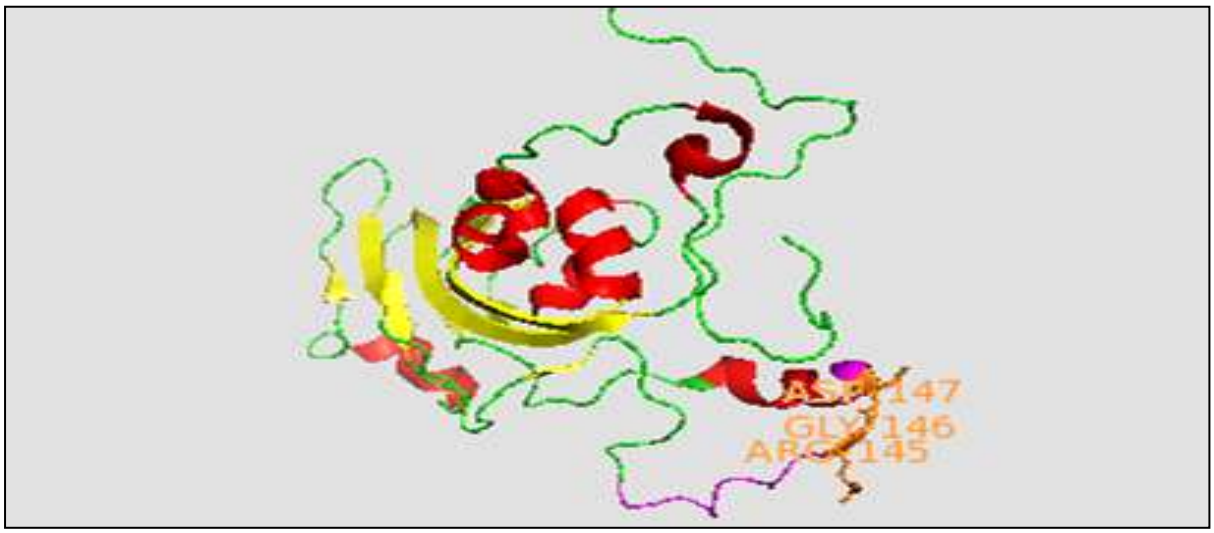

Figure 1.3: Crystal structure of FMDV VP1 serotype 01. The eight-stranded anti-parallel beta barrel is shown in yellow, the loops are shown in green and alpha helices are shown in red. The beta barrels form a wedge shaped structure which is known to assist in the packaging of structural units to form a rigid protein shell, suggested to be essential for the stability of the virion. The GH loop is indicated in magenta with the arginine-glycine-aspartic acid (R-G-D) tripeptide motif indicated in orange (adapted from Burman *et al*., 2006).

VP1 is known to be the most dominating antigen among the capsid proteins. A number of neutralising epitopes have been identified within this protein in most picornaviruses including PV, FMDV, HRV and TMEV (Wychowski *et al*., 1983; Inoue *et al*., 1993; Mason *et al*., 1994; Oberste *et al*., 1999). For example, computer analyses revealed that amino acids 93-103 in the primary sequence of PV-1 VP1 are hydrophilic. The synthesised VP1 (93-104) peptide reacted specifically with the PV-1 monoclonal neutralising antibody, C3, and no reaction was observed between VP1 and other PV-1 antibodies suggesting that the C3 epitope is present within this region (Wychowski *et al*., 1983). Similarly, three antigenic sites with neutralising activity have been determined on various regions of PV-1, 2 and 3 VP1 for the Sabin vaccine (Minor *et al*., 1986). Additionally, crystal structure analyses on the seven FMDV serotypes have revealed the presence of a long, conformational flexible loop on the outer capsid surface of all serotypes. The loop was identified as the G-H loop of VP1 and was found to include a highly conserved arginine-glycine-aspartic acid (R-G-D) tripepetide motif, as shown in figure 1.3 above. This motif is known to bind to integrin receptors and facilitate the internalisation of FMDV into host cells (Mason *et al*., 1994; Jackson *et al*., 1996; Wang *et*

al., 2003). The G-H loop of VP1 has been found to be the major antigenic site for antibody neutralisation in FMDV and hence antibody generation for vaccination against FMDV is based on this epitope (Collen *et al*., 1991; Liu *et al*., 2011). Vaccination of mice with BacVP1 (recombinant EV71 VP1 expressed in a baculovirus system), illustrated effective VP1 antibody specificity, and an *in vitro* neutralisation assay revealed cross-neutralisation of BacVP1 sera against heterologous and homologous EV71 strains (Premanand *et al*., 2012). Studies on TMEV strain DA have shown that epitopes which are responsible for the activation of CD4+ helper T cells to the demyelinated neurons are found on the surfaces of VP1, VP2 and VP3 with VP1 containing the majority of these epitopes (Kim *et al*., 1992; Inoue *et al*., 1994; Cameron *et al*., 2001).

VP1 has also been shown to play a role in picornavirus pathogenicity and determining the virulence of a virus. Studies done on the group B coxsakieviruses (CVB) have revealed that a single amino acid alteration within the exposed region of VP1 leads to a change in the cytolytic and apoptotic abilities of CVB2, suggesting that VP1 is involved in the pathogenesis of CVB (Gullberg *et al*., 2010; Wang *et al*., 2012). Similarly, amino acid 101 of loop II of VP1 has been shown to be an essential determinant of TMEV DA virulence in mice. A single nucleotide change in this position has shown to lower the neurovirulence of the virus. When oligonucleotide-directed-site-specific mutagenesis was utilised to change cytosine to thymine within the loop area, the presence of mutagenised virus *in vivo* in mice showed minor neurovirulence compared to the wild-type virus (Zurbriggen *et al*., 1989).

1.2.1.2 3C protease ($3C^{pro}$)

$3C^{pro}$ is responsible for the majority of cleavages during the processing of capsid and non-structural protein precursors (reviewed by Ryan and Flint, 1997; Buenz and Howe, 2006). However, *in vivo* experiments have illustrated that the $3C^{pro}$ precursor protein, 3CD, rather than $3C^{pro}$ is responsible for most steps of PV polyprotein processing (Ypma-Wong *et al*., 1988; Marcotte *et al*., 2007). Since the early 1990s, only five $3C^{pro}$ structures have been determined, namely those for, HRV-14, HRV-2, PV-1, HAV and FMDV. Bioinformatic analyses of picornavirus $3C^{pro}$ sequences have revealed that the protease has a chymotrypsin (serine protease)-like fold and consists of a cysteine nucleophile residue instead of a serine residue on the catalytic site, as shown in figure 1.4 (Mosimann *et al*., 1997; Sweeney *et al*., 2007). The catalytic triad of picornavirus $3C^{pro}$ comprises of cysteine, histidine, glutamic or

aspartic acid residues which are conserved in all picornaviruses. $3C^{pro}$ is known to cleave the polyprotein specifically at the region where glutamine-glycine (QG) dipeptides occur (Clark *et al*., 1991; Curry *et al*., 2007).

Figure: 1.4: Crystal structure of EV 93 $3C^{pro}$. The protease fold into two β barrels (the first one in orange tone and the second one in blue tone), forming the chymotrypsin-like fold. The catalytic triad residues are highlighted in hot pink. The nucleophilic Cys^{147} (from the second barrel and the general acid/base pair His^{40} and Glu^{71} (from the first barrel) form the catalytic triad (adapted from Norder *et al*., 2011).

Apart from playing a major role during polyprotein processing, picornavirus $3C^{pro}$ is known to have several effects on the host cell during infection. Firstly, it is responsible for the inhibition of host-cell transcription (Weidman, 2003). A study by Sharma *et al*., (2004), indicated that the nuclear localisation signal (NLS) present in the RNA polymerase, 3D, and PV infection are required for entry of the 3CD precursor protein into the nucleus. $3C^{pro}$ then uses this mechanism to enter the nucleus in the form of the precursor, 3CD. $3C^{pro}$ is processed through autoproteolysis, processed $3C^{pro}$ then inhibits host cell transcription through the cleavage of host cell nuclear proteins. Similarly, HRV $3C^{pro}$ has been shown to have intrinsic nuclear protein targeting potential where it can passively or actively disrupt the transportation of nuclear proteins to the cytoplasm by altering the permeability of the nuclear pore (Ghildyal *et al*., 2009). Additionally, studies have shown that cleavage of the TATA-binding protein (Clark *et al*., 1993), Oct-1 and CREB-transcription factors (Yalamanchili *et al*., 1997b;

Yalamanchili *et al*., 1997c) and the IIIC transcription factor by PV $3C^{pro}$ decreases their activities and transcription by polymerase II (Aminev *et al*., 2003). *In vitro* experiments where Hela cells were infected with PV suggested that the cleavage of the transcription factors, TFIIIB and TFIIIC, by $3C^{pro}$ results in the inhibition of DNA polymeraseIII transcription by decreasing the activity of each transcription factor, with TFIIIC's activity being highly influenced by the protease (Clark *et al*., 1991; Ryan and Flint, 1997). Furthermore, FMDV $3C^{pro}$ has been found to play a role in the down regulation of host-cell transcription by removing the first 20 amino acids found on the N-terminal region of histone H3. This region has been found to correspond to the regulatory domain for the transcriptional activation of chromatin. Histones are proteins found in the nuclei and associated closely with DNA. Histones are responsible for the structure of the chromatin and play a major role in the regulation of gene expression (Falk *et al*., 1990; Weidman *et al*., 2003; Curry *et al*., 2007).

Secondly, $3C^{pro}$ has been found to be responsible for the inhibition of host-cell translation. PV $3C^{pro}$ is known to inhibit translation of host mRNA by cleaving the poly (A) binding protein (PBP). The interaction of $3C^{pro}$ and PBP alters the interaction between PBP with eukaryotic initiation factor (eIF) 4G *in vitro* (Joachims *et al*., 1999). Similarly, *in vitro* studies on *Enterovirus* $3C^{pro}$ and PV $3C^{pro}$ have been shown to inhibit host-cell translation by cleaving PBP thus altering the interaction between PBP with eukaryotic initiation factor (eIF) 4B (Bushell *et al*., 2001).

Lastly, picornaviruses have been shown to alter cell morphology and rearrange cytoplasmic membranes in order for viral replication to occur. PV and FMDV $3C^{pro}$ has been shown to modify the cytoskeleton of host cells. *In vivo* and *in vitro* studies have illustrated that PV $3C^{pro}$ cleaves the microtubule associated protein 4 (MAP-4) causing depolymerisation of the microtubule network (Joachims *et al*., 1995). Similarly, the expression of FMDV proteins in transfected cells has revealed that only $3C^{pro}$ induces the loss of γ-tubulin from the microtubule organising centre (MTOC) region in the cells, implying that $3C^{pro}$ also plays a role in FMDV cytoskeleton alteration (Armer *et al*., 2008).

1.2.2 Picornavirus replication

Picornavirus replication occurs in the cytoplasm of infected host cells. The cycle of infection is initiated by attachment in which the virus attaches to the host cell membrane by binding to a host cell receptor. Various receptors are used by different viruses, for example, the

Coxsackie B1-6 virus uses the coxsackievirus-adenovirus receptor (Car), PV uses the poliovirus receptor PVR or CD155, HRV uses the intracellular adhesion molecule-1 (ICAM-1), encephalomyocarditis virus uses the vascular cell adhesion molecule-1 (VCAM-1), and FMDV uses a vitronectin receptor for attachment. The attachment process is followed by receptor-mediated endocytosis and uncoating to release viral genome (as reviewed by Racaniello, 2007; Lin *et al*., 2009). The second and third steps involve the translation of viral mRNA to produce the 3D protein, a RNA-dependent RNA polymerase which replicates the viral genome using 3B (VPg) as a primer for the synthesis of the negative-strand RNA. This is then used as a template for positive-sense RNA synthesis. Replication occurs on membrane-bound vesicles which are thought to be formed by various viral proteins, primarily the 2C protein (Bienz *et al*., 1992). Lastly, once a significant amount of viral capsid proteins have been produced, encapsidation begins and new viral capsids and virions will exit the cell through cell lysis (as reviewed by Racaniello, 2007; Bienz *et al*., 1992). Figure 1.5 below illustrates an overview of the picornavirus replication.

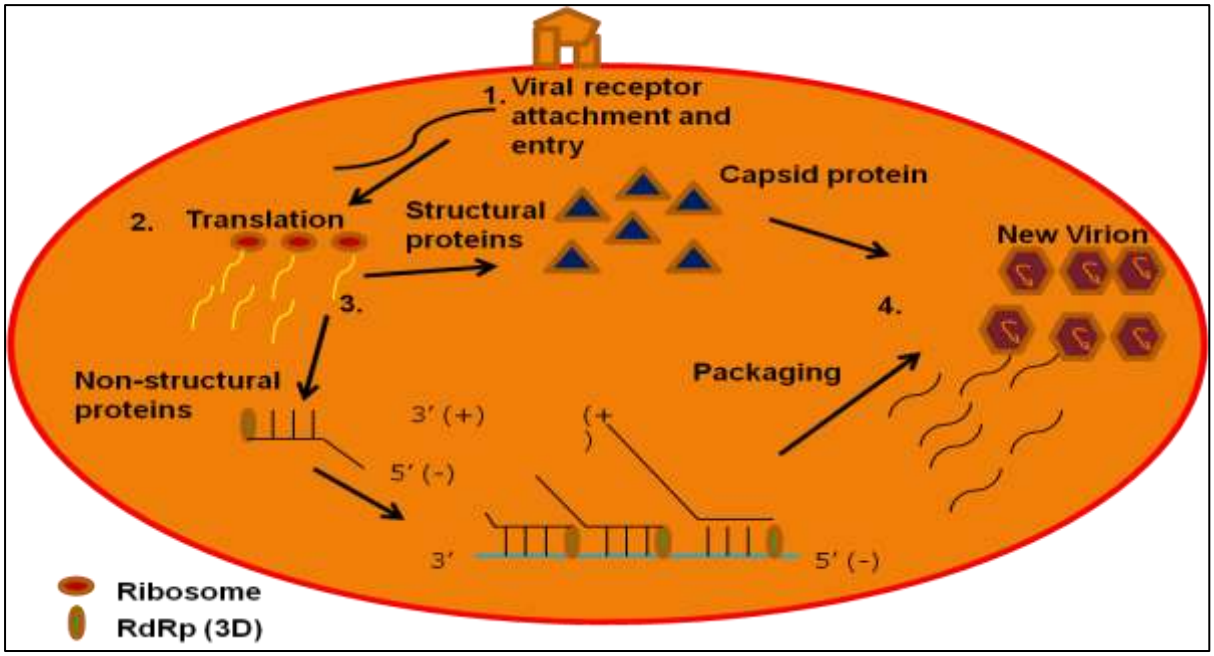

Figure 1.5: Overview of picornavirus life cycle: Step 1: Receptor-mediated attachment to the host cell membrane, followed by penetration and uncoating to release viral RNA into the cytoplasm. **Step 2:** Translation of the RNA is accomplished by utilising the host cell machinery to produce the polyprotein, which is cleaved into various viral proteins. **Step 3:** The structural proteins form viral capsids, while non-structural proteins are responsible for synthesising negative-strand RNA which will be used as a template to produce more positive-strand RNA. **Step 4:** newly synthesised positive-strand RNA is then packaged into the newly formed viral capsids which exit the cells *via* cell lysis (adapted from Andino *et al*., 1999).

1.2.3 Viral assembly

Viral assembly begins with the cleavage of the P1 precursor encoding VP1-VP4 by $2A^{pro}$ (Figure 1.6). In enteroviruses, heat shock protein (Hsp) 70 and Hsp 90 interact with the P1 precursor and maintain the protein in a processing conformation such that it can be recognised and cleaved by viral proteases (Macejak and Sarnow, 1992; Geller *et al*., 2007). The $3C^{pro}$ and its precursor, $3CD^{pro}$ cleave the region between the β-barrels of VP0-VP3 and VP3-VP1 bonds. This cleavage is essential for the formation of the protomer subunit. Five protomers are formed by the interaction of VP1, VP3 and VP0. Each protomer contains a single copy of the three protein subunits which combine to form a pentamer. The next step of assembly involves the formation of a provirion, which occurs when 12 pentamers join to produce an immature viral capsid. Encapsidation of the positive sense viral RNA strand occurs by an unknown mechanism. This is followed by the cleavage of VP0 into VP2 and VP4 leading to the formation of a mature icosahedral virion consisting of 60 copies of each of the four capsid subunits with VP1-3 being located on the surface of the capsid where interaction with host cell receptors occurs, and VP4 being located on the inside of the capsid where it keeps the capsid stable (as reviewed by Racaniello, 2007).

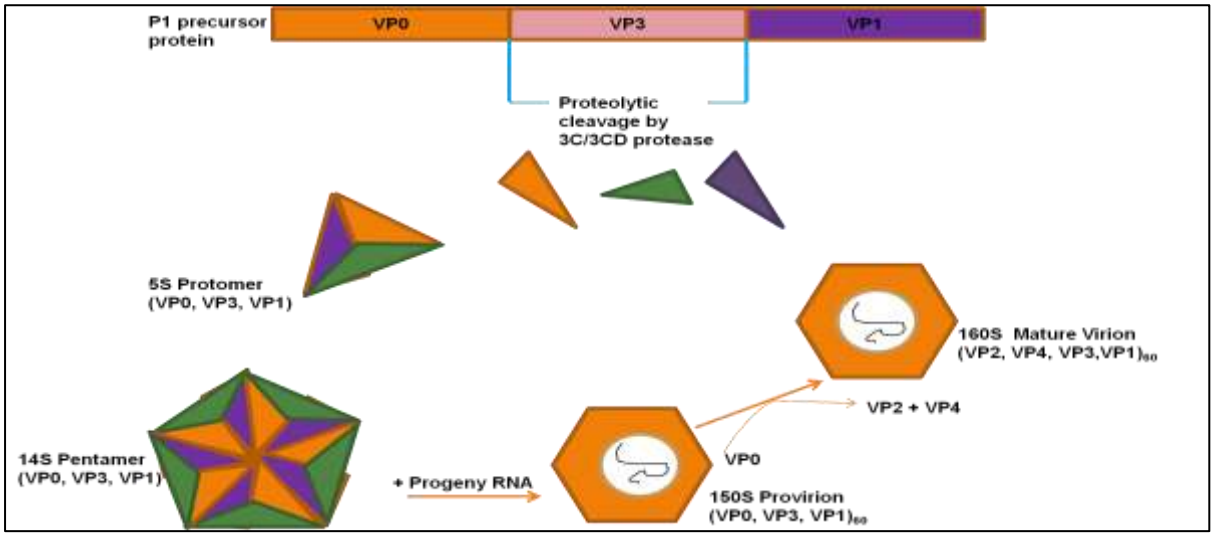

Figure 1.6: Processing and assembly of the picornavirus virion. The P1 domain is cleaved into VP1, VP3 and VP0 by $3C/3CD^{pro}$. The capsid subunits form a 5S protomer and five of these protomers form a 14S pentamer. Twelve pentamers form a 150S provirion in which the viral RNA is encapsidated. VP0 is cleaved to form VP2 and VP4 to form the mature virion consisting of 60 copies of each of the four capsid subunits with VP1-3 being located on the surface of the capsid and VP4 being located on the inside of the capsid (adapted from Semler, 2011).

1.3 Theiler's Murine Encephalomyelitis Virus (TMEV)

TMEV, the picornavirus used in this study, belongs to the genus *Cardiovirus* and causes central nervous system infections in mice. Other cardioviruses are encephalomyocarditis virus (EMCV) and Saffold virus (SAFV), a newly described human virus which is closely related to TMEV (Borghese and Michiels, 2011).

TMEV strains are subdivided into two groups based on neurovirulence and the type of disease caused due to intra-cerebral inoculation of mice. The two groups are GDVII and Theiler original (TO). The GDVII group comprises two strains, GDVII and FA, which are more virulent than the TO strains and cause fatal encephalomyelitis in mice (Theiler and Gard, 1940). TMEV causes central nervous system infections in mice and can encourage the development of a chronic demyelinating disease leading to inflammatory demyelinating lesions in the spinal cord of mice (Lipton, 1975). The TO group is characterised by several strains namely, BeAn, DA, WW, TO4 and Yale. These strains are less virulent than those from the GDVII group and are responsible for causing chronic inflammatory demyelinating disease (Lipton and Friedman, 1980). This demyelinating disease has been found to resemble multiple sclerosis, thus making mice infected with TO strains the most suitable experimental animal models for this disease (Oleszak *et al*., 2004).

TMEV was chosen as a model for this study as it is only pathogenic to mice and thus is safe to use in the laboratory for analysis of virus-host interactions. TMEV has also been shown to infect and replicate within Baby Hamster Kidney 21 (BHK-21) cells (Lipton and Friedman, 1980; Kong *et al*., 1994; van Pesch *et al*., 2001). A replication system has been developed in our laboratory to study virus-host interactions. In one study, the subcellular distribution of P2 proteins, and the effect of amino acid substitution on the conserved region of 2C on virus replication were investigated. Analysis of cells expressing mutant 2C proteins indicated that the distribution of 2C was affected by substituting lysine in position 14, tryptophan in position 18 and isoleucine in position 23 for alanine (Murray *et al*., 2009). In a second study, polyclonal antibodies have been generated against TMEV 2C protein and used to localise the protein to the Golgi apparatus of infected BHK-21 cells where it assists with the formation of replication complexes (Jauka *et al*., 2010). More recently, our studies have shown that molecular chaperones, Hsp 70 and Hsp 90 play a role in the lifecycle of TMEV. Immunofluorescence analysis revealed that Hsp 90 redistributes from the cytoplasm into the

viral replication complex in TMEV-infected cells where it co-localised with the non-structural 2C protein. Hsp 70 redistributed from the cytoplasm into the vicinity of the replication complex. In addition, Hsp 90 inhibitors, novobiocin and geldanamycin, were found to reduce virus growth as there was no development of the cytopathic effect (CPE) on treated cells compared to untreated cells. Furthermore, Western analysis experiments revealed that treatment with novobiocin inhibits the production of the non-structural 2C protein (Mutsvunguma *et al*., 2011).

Viruses utilise host cell machinery during various stages of their lifecycle. Molecular chaperones are an example of such host cell factors utilised by viruses during viral entry, replication, assembly and exit.

1.4 Molecular Chaperones

Molecular chaperones are a group of unrelated protein families which direct the correct conformation of other proteins but do not form part of the final product (as reviewed by Ellis, 1987). Molecular chaperones have a number of functions within cells which include protein folding/unfolding, protein transport across membranes, protein degradation, cell survival and regulating the apoptosis process (as reviewed by Ellis, 1987; Frydman, 2001; Hartl and Hayer-Hartl, 2002). Mutations in molecular chaperones have been associated with various human diseases such as cancer, cardiovascular diseases and neurodegenerative diseases (as reviewed by Xiao *et al*., 2010). Approximately 20 different protein families which display chaperone activity are known and Hsps are the best-studied out of these protein families.

Hsps are highly conserved and are classified into six families based on their molecular size, for example small Hsps (9-43 kDa molecular mass), Hsp 40 (40 kDa), Hsp 60 (60 kDa), Hsp 70 (70 kDa), Hsp 90 (90 kDa) and Hsp 100 (100 kDa). Hsps are mostly stress-induced and located in both the cytosol and ER of most cell types where they assist in protein folding and assembly. There are two major groups of ER chaperones namely, the glucose-regulated proteins (GRPs) and the calnexin/calreticulin chaperones. The GRP 78, also known as BiP, is an ER homologue of Hsp 70 and is known to assist in protein folding by associating with proteins that contain hydrophobic residues in their misfolded regions. The GRP 94 is an ER homologue of Hsp 90 and has been suggested to assist in the assembly of large ER chaperone complex under conditions of ER stress although its role in ER protein quality control is not fully understood. Calnexin is a type I ER membrane protein and calreticulin is a soluble ER

lumen protein, both these chaperones assist in protein folding and assembly by interacting with proteins which contain *N*-linked glycans (as reviewed by Xiao *et al*., 2010).

1.4.1 Viruses-Chaperone Interactions

Many studies have shown that viruses utilise host cell factors including molecular chaperones to support their lifecycle in a host cell. The roles played by chaperones during lifecycles of a wide array of viruses have been widely documented and these proteins have been shown to participate during viral entry, replication and assembly processes (as reviewed by Sullivan and Pipas, 2001; as reviewed by Xiao *et al*., 2010).

Chaperones play a role during the entry of viruses into host cells by acting as viral receptors or participating in the viral uncoating process. As an example, rotavirus entry depends on the interaction with the heat shock cognate protein 70 (Hsc 70) at a post-attachment stage. This brings about a conformational change to the viral capsid to facilitate entry of the virus into the cytoplasm (Guerrero *et al*., 2002; Zarate *et al*., 2003). Other examples of virus-chaperone interactions which facilitate viral entry include, Hsp 70/ Hsp 90 and Dengue virus (Reyes-Del Valle et al., 2005), Hsp 90 and Japanese encephalitis virus (Das *et al*., 2009) and the Hsp 70 homologue, GRP78 and Coxsackievirus (CV) A9 (Triantafilou et al., 2002).

Host chaperones also facilitate replication of viral genome and gene expression of viral proteins. For example, Hsp 90 has been identified as a host factor which induces the activity of the RNA polymerase of Influenza A virus, leading to efficient transcription and replication of viral RNA (Momose *et al*., 2002). Similarly, Hsp 70 and Hsp 40 have been suggested to indirectly enhance replication of papillomavirus by improving the binding of the replicator initiator E1 helicase to the origin of replication on viral DNA (Liu *et al*., 1998). The requirement of DnaJ, DnaK (Hsp 70) and GrpE for initiation of bacteriophage replication has been indicated in *E. coli* using *in vitro* experiments (Alfano and McMacken, 1989; Zylicz *et al*., 1989). The importance of these chaperones has been illustrated in previous studies where the mutated forms of DnaJ, DnaK and GrpE resulted in no replication initiation when introduced into an *in vivo* system containing the lambda DNA replication system (Zylicz and Georgopoulos, 1984; Zylicz *et al*., 1985). Additionally, Hsp 90 is known to play a role in the maturation and activity of the Hepatitis C virus (HCV) non-structural 2/3 (NS2/3) protease which is essential for viral replication (Waxman *et al*., 2001). The HIV-1 Nef protein has been associated with viral infectivity, replication and gene expression. Studies have shown

that the Nef protein induces the expression of Hsp 40 in HIV-1 infected cells. This interaction is essential for increased Hsp 40 translocation into the nucleus of infected cells which then mediates viral gene expression by forming part of the cyclin-dependent kinase 9-associated transcription complex, regulating long terminal repeat-mediated gene expression (Kumar and Mitra, 2005).

Not only are chaperones involved in facilitating viral entry and replication, they also play a role during the viral assembly process. For example, Hsc 70 has been found to incorporate itself within the HIV-1 virions suggesting an interaction between the chaperone and virus during viral assembly (as reviewed by Brenner and Wainberg, 1999). Similarly, Hsc 70 has been shown to bind to the VP1 capsid protein during polyomavirus infection and, this event has been shown to regulate the quality and location of viral assembly (Chromy *et al*., 2003). Furthermore, Calnexin, an ER chaperone, is known to be involved in the formation of the HCV envelope glycoproteins E1 and E2 (Dubuisson and Rice, 1996; Choukhi *et al*., 1998; Dubuisson, 1998). Picornaviruses are also known to utilise molecular chaperones during their life cycle although only three studies have been conducted. In enteroviruses, PV, CV and HRV, Hsp 70 and Hsp 90 are known to be involved in the viral assembly process (Geller *et al*., 2007). Studies conducted on *Enterovirus* assembly have shown that Hsp 70 and Hsp 90 interact with the capsid precursor protein, P1, and maintain the protein in a processing conformation during virus assembly such that it can be recognised and cleaved by viral protease, $3C^{pro}$ (Macejak and Sarnow, 1992; Geller *et al*., 2007). As described in section 1.3 above, Hsp 70 and Hsp 90 play a role in the lifecycle of TMEV (Mutsvunguma *et al*., 2011).

1.5 Motivation

The family *Picornaviridae* contains economically important viruses such as PV, HRV and FMDV. These viruses have a single polyprotein which is cleaved by proteases into mature structural and non-structural proteins which form the viral capsid and play a role in viral replication respectively. The role played by molecular chaperones during viral entry, replication, assembly and exit has been widely researched on a variety of viruses including picornaviruses. In *Enteroviruses*, Hsp 90 and Hsp 70 have been shown to maintain P1 in a processing conformation during virus assembly such that it can be recognised and cleaved by viral protease, $3C^{pro}$ (Macejak and Sarnow, 1992; Geller *et al*., 2007). Only one study has been conducted on the role played by Hsp 90 and Hsp 70 in the replication of TMEV (Mutsvunguma *et al*., 2011). No study has been conducted to investigate interactions between

molecular chaperones and TMEV P1 during virus assembly. In order to study these specific interactions, antibodies against the antigenic capsid subunit, VP1 and $3C^{pro}$ are required.

1.6 Aims and objectives

Overall Aims

The overall aim of this study was to generate polyclonal antibodies against TMEV VP1 capsid protein and $3C^{pro}$ in order to study the role played by molecular chaperones and other host factors in the lifecycle of TMEV.

Objectives

The specific objectives of this study were:

1. To conduct a bioinformatic analysis to determine the predicted hydrophobic, antigenic and linear B cell epitopes exposed on the molecular surface of TMEV GDVII VP1 and $3C^{pro}$
2. To PCR-amplify and clone the full length coding sequences of VP1 and $3C^{pro}$ into the bacterial expression vector, pQE-80L
3. To express VP1 and $3C^{pro}$ in a bacterial system by Isopropyl-β-D-1-thiogalactopyranoside (IPTG) induction and conduct solubility studies
4. To purify the recombinant proteins using ion Nickel affinity chromatography and prepare the purified antigen for immunisation
5. To test the antibodies for detection of bacterial antigen and virally-expressed protein by Western analysis
6. To localise VP1 and $3C^{pro}$ in TMEV-infected cells by indirect immunofluorescence and confocal microscopy

Chapter 2: Bioinformatic analysis and cloning of TMEV VP1 and 3C^{pro} sequences into pQE-80L

2.1 Introduction

Firstly, this chapter describes a bioinformatic analysis of TMEV VP1 and 3C^{pro} sequences in order to predict hydrophobic, hydrophilic and antigenic regions of the proteins. Secondly, structural analyses of VP1 and 3C^{pro} were performed in order to predict linear B cell epitopes exposed on the surface of three-dimensional protein structures. Finally, the cloning of the full length coding sequences of VP1 and 3C^{pro} into pQE-80L and confirmation of the integrity of the recombinant plasmids by restriction analysis and Sanger sequencing is described.

In order to delineate predicted hydrophobic and hydrophilic regions on VP1 and 3C^{pro} primary sequences, a Kyte and Doolittle Hydropathy plot was generated. The programme uses an algorithm which determines the buried hydrophobic and exposed hydrophilic regions of a protein depending on the R-groups of the protein. The programme works by assigning each of the 20 amino acids a hydrophobicity score between -4.6 and 4.6 where a score of -4.6 represents the most hydrophobic amino acids. A window size is set, this is the number of amino acids whose hydrophobicity is averaged and assigned to the first amino acid in the window. The default window size is 9. Setting a window size between 5 and 7 is suggested to be a good value for finding regions which are assumed to be exposed on the surface, whereas a window size of between 19 and 21 results in a plot exposing transmembrane domains (Kyte and Doolittle, 1982).

A Hopp and Woods Hydrophilicity plot was also conducted in order to delineate predicted antigenic regions on VP1 and 3C^{pro} primary sequences. The programme predicts antigenic regions of a protein by determining hydrophilic regions which are most likely to be exposed on the molecular surface of a folded protein (Hopp and Woods, 1981). The programme works by assigning each of the 20 amino acids a hydrophilicity factor. A window size is set in order to average hydrophilicity factors and assign them to the first amino acid in the window. A positive peak in the hydrophilicity profile will be assumed to correspond with an antigenic determinant. Regions with negative hydrophilicity do not correspond with an antigenic determinant (Fraga, 1982).

In order to determine the predicted linear B cell epitopes exposed on the surface of VP1 and $3C^{pro}$ structures, homology modelling was conducted. This technique is based on aligning the amino acid sequence of a target protein whose structure has not been resolved with an amino acid sequence of a protein that has its structure resolved (template) in order to predict the 3D model of the target protein. The predicted structure of the target protein is then determined by the template amino acid sequence which has the highest similarity percentage to the target protein sequence (Centeno *et al*., 2005). HHpred was used for determining homologous templates of VP1 and $3C^{pro}$. The programme provides a sensitive method for sequence searching and structure prediction by identifying homologous sequences of a known protein structure with the target sequence (Söding *et al*., 2005). TMEV DA VP1 was identified as the homologous template of TMEV GDVII VP1. No crystal structures have been resolved for TMEV $3C^{pro}$. FMDV A10 (61) was found to be the homologous template of TMEV GDVII $3C^{pro}$.

In order to determine the percentage of identical, conserved and similar amino acid residues between the TMEV GDVII VP1 and its template (TMEV DA VP1, PDB id: 1TME), and to determine whether the VP1 is conserved within the various TMEV strains, a multiple sequence alignment was performed. A similar analysis was conducted for TMEV GDVII $3C^{pro}$ and its template (FMDV A10 (61), PDB id: 2BHG) and TMEV DA and BeAn $3C^{pro}$ sequences. Amino acid residues which are not identical but share the same properties are known as similar amino acid residues. Conserved amino acid residues are functionally equivalent but are not necessarily identical, these amino acids have similar residue properties such as charge or hydrophobicity (Doolittle, 1981; Schueler-Furman and Baker, 2003).

Structural models for VP1 and $3C^{pro}$ were generated using MODELLER, which generates three-dimensional structures of proteins used for homology or comparative modelling (Eswar *et al*, 2008). The predicted linear B cell epitopes exposed on the surface of the structural models of VP1 and $3C^{pro}$ and their homologous templates were determined using the DNAStar Protean3D system and PyMOL programmes. The predicted linear B cell epitopes regions were mapped to the primary sequences of VP1 and $3C^{pro}$.

Forward and reverse oligonucleotides flanking the desired nucleotide sequences were designed for the amplification of TMEV VP1 and $3C^{pro}$ coding sequences using the PCR. TMEV VP1 and $3C^{pro}$ coding sequences were cloned into the expression vector, pQE-80L using the restriction endonucleases, *Bam*HI and *Sal*I to produce pBMVP1 and pBM$3C^{pro}$. The

integrity of the recombinant plasmids was confirmed by restriction analysis and Sanger sequencing.

A second expression vector system was used for VP1 (as discussed in chapter 3). pETVP1 (1-741) was constructed by Dora Mwangola (B.Sc Honours student, Rhodes University). The recombinant plasmid consists of nucleotides 1-741 of the VP1 coding sequence cloned into pET22b+. The integrity of pETVP1 (1-741) was confirmed by restriction analysis using *Xho*I and *Xba*I and Sanger sequencing.

The specific objectives were:

- To determine predicted hydrophobic, hydrophilic and antigenic regions within the VP1 and the $3C^{pro}$ amino acid sequences using the Kyte and Doolittle Hydropathy plot and the Hopp and Woods Hydrophilicity plot respectively

- To use the internet-based modeling server, HHpred to search for homologous protein templates of TMEV GDVII VP1 and $3C^{pro}$ for structural analysis

- To conduct a multiple sequence alignment in order to determine the percentage of identical, conserved and similar amino acid residues between TMEV GDVII VP1 and its template, 1TME, and determine whether VP1 is conserved within the various TMEV strains in order to conduct structural analysis of VP1

- To conduct a multiple sequence alignment in order to determine whether $3C^{pro}$ is conserved within various TMEV strains and a sequence alignment to determine the percentage of identical, conserved and similar amino acid residues between the TMEV GDVII $3C^{pro}$ and its template, 2BHG, in order to conduct structural analysis of $3C^{pro}$

- To generate structural models of VP1 and $3C^{pro}$ and determine linear B cell epitopes predicted to be exposed on the surface of VP1 and $3C^{pro}$ and their respective homologous templates

- To design forward and reverse oligonucleotides using the nucleotide sequences of TMEV GDVII VP1 and $3C^{pro}$ and amplify them using the PCR

- To clone the PCR-amplified coding sequences into pQE-80L to produce pBMVP1 and pBM$3C^{pro}$ and confirm the integrity of pBMVP1, pBM$3C^{pro}$ and pETVP1(1-741)

by restriction analysis and Sanger sequencing

2.2 Methods and Materials

2.2.1 Prediction of hydrophobic, hydrophilic and antigenic regions of VP1 and 3C^{pro}

In order to determine the amino acids predicted to be hydrophobic, hydrophilic and antigenic, a Kyte and Doolittle Hydropathy and a Hopp and Woods Hydrophilicity plots were generated. The full length amino acid sequences of VP1 and 3C^{pro} were subjected to the internet based programme Protscale on the ExPASytool website (www.expasytool.com) which uses the Kyte and Doolittle method to predict hydrophobic amino acids and the Hopp and Woods method to predict hydrophilic amino acids which are suggested to have antigenic properties. The window size was set at 5 for both plots.

2.2.2 Multiple Sequence alignments of VP1 and 3C^{pro} of the various TMEV strains using Clustal W

In order to determine the percentage of identical, similar and conserved amino acid residues of VP1 and 3C^{pro} within the various TMEV strains, a multiple sequence alignment was performed using the Clustal W algorithm (www.genome.jp/tools/**clustalw**/), with Blosum62 scoring matrix and default parameters. The accession numbers for VP1 and 3C^{pro} sequences used in the alignments were TMEV GDVII complete genome sequence (GenBank accession number: AAA62147); TMEV DA complete genome sequence (GenBank accession number: AAA93172); TMEV BeAn complete genome sequence (GenBank accession number no: AAC02657).

2.2.3 Sequence alignment of TMEV GDVII 3C^{pro} and 2BHG

A sequence alignment was performed on TMEV GDVII 3C^{pro} sequence (GenBank accession number: AAA62147) and its homologous template (FMDV A10 (61), PDB id: 2BHG) sequence (GenBank accession number: 2BHG.A) in order to determine the percentage of identical, conserved and similar amino acid residues of the two proteins.

2.2.4 Homology modeling and prediction of linear B cell epitopes

TMEV GDVII VP1 and $3C^{pro}$ primary sequences (GenBank accession number: AAA62147) were submitted into the modelling server HHpred (Söding *et al*., 2005) to identify suitable templates with resolved structures. Models for TMEV GDVII VP1 and $3C^{pro}$ were generated using the MODELLER software (Sali *et al*., 2009) using (TMEV DA VP1, PDB id: 1TME) and (FMDV A10 (61), PDB id: 2BHG) as their templates respectfully. The structural models of the proteins were analysed using PyMOL v1.1 (2008 DeLano Scientific LLC).

For the prediction of linear B cell epitopes on VP1 and $3C^{pro}$, PDB files of the identified homologous templates were downloaded from the Protein Data Bank (Protein Data Bank, http://www.rcsb.org/pdb/home/home.do) and were opened using DNAStar Protean3D system. The complete primary sequences of the models and their templates were analysed in order to map the predicted linear B cell epitopes in the primary sequence. The predicted epitope regions were mapped on the structure surfaces of the proteins using PyMOL v1.1 (2008 DeLano Scientific LLC).

2.2.5 Growth media

Luria Bertani broth (LB: 0.5% NaCl, 0.5% yeast extract, 1% tryptone powder) and Luria Bertani agar (LA: LB supplemented with 3% bacteriological agar) were used as growth media. Growth of the bacterial strains was carried out at 37°C in LB or LA supplemented with ampicillin (Amp) at a final concentration of 100µg/ml. The growth medium will be referred to as LB/Amp and LA/Amp throughout the study.

2.2.6 Polymerase Chain Reaction of TMEV VP1 and $3C^{pro}$ coding sequences

Forward and reverse oligonucleotides were designed based on the TMEV GDVII complete genome sequence (GenBank accession number: AAA62147) in order to amplify the full-length coding sequences of VP1 (828 bp) and $3C^{pro}$ (649 bp). *Bam*HI (GGATCC) and *Sal*I (GTCGAC) restriction endonuclease recognition sequences were incorporated at the 5’ end

of the forward and 3' end of the reverse oligonucleotides respectively for cloning into pQE-80L. Table 2.1 below indicates the forward and reverse oligonucleotides used for cloning.

Table 2.1: Forward and reverse oligonucleotides designed for the amplification of TMEV VP1 and $3C^{pro}$ showing *Bam*HI in green, *Sal*I in orange and the first codon of each protein sequence in red.

Primer	**Nucleotide sequence**
VP1 forward	5'GGATCCGGAATTGACAATGCTGAGAAG 3'
VP1 reverse	5' GTCGACTCACTCGAACTC 3'
$3C^{pro}$ forward	5' GGATCCGAGGCGGGAAGGTTCTAG 3'
$3C^{pro}$ reverse	5' GTCGACTCATTGCGGTTCCAGCGC3'

The MJ Mini™ Personal Thermal Cycler (Bio-Rad, USA) was used for the amplification of the full-length VP1 and $3C^{pro}$ coding sequences. The reaction mixtures were set up as follows: 25 µl 2 x ready mix with Mg^{2+} (KAPA Biosystems, USA), 2 µl of 10µM forward and reverse oligonucleotides, 1 µl DNA template (~70 µg) and 20 µl ddH_2O. A negative control reaction was set up in the same way using deionised water (ddH_2O) instead of the DNA template. The PCR parameters used were 1 cycle of initial denaturation at 95°C for 1 min followed by 30 cycles of denaturation at 95°C for 1 min, annealing at 60°C for 1 min and initial elongation at 72°C for 45 sec. A final cycle of elongation at 72°C for 5 min was performed. The full length TMEV VP1 (828 bp) and $3C^{pro}$ (649 bp) coding sequences were PCR amplified and analysed using 1 % agarose gel electrophoresis (AGE) as described in the section below.

2.2.7 Agarose gel electrophoresis (AGE)

DNA was analysed by 1 % AGE prepared in 1x TAE buffer [40 mM Tris (pH8.0), 0.1 % glacial acetic acid, 1 mM EDTA] containing 0.5 µg/ml ethidium bromide. DNA samples were thoroughly mixed with 6x loading dye (KAPA biosystems, USA) prior to loading onto the gel. Agarose gels were electrophoresed for 30 min at 90 V in 1x TAE buffer. The gel was visualised by illumination with UV light and images captured using the Gel Bio-Rad

VersaDoc™ Model 4000 imaging system (Biorad, USA). The λ*Pst*1 DNA ladder was used throughout the study in order to determine the sizes of the recombinant plasmids. The ladder was created by restricting 20 µg λ DNA (Fermentas, USA) with 20 units (U) of *Pst*I restriction endonuclease for 2 hrs at 37°C.

2.2.8 Cloning of amplicons into the pGEM®-T Easy vector

VP1 and $3C^{pro}$ amplicons were ligated into pGEM®-T Easy (Promega, USA) in order to create pGEM®-VP1 and pGEM®-$3C^{pro}$. In a total volume of 10 µl, reactions contained 1 U T4 DNA ligase, 1 µl 2x rapid ligation buffer, 1 µl DNA (~70 µg) and 1 µl pGEM®-T Easy (~50 µg) and 6 µl ddH_2O. A negative control reaction was set up in the same way using deionised water (ddH_2O) instead of the DNA template. Ligation reactions were carried out overnight at 4°C. Ligations were transformed into competent JM109 *E. coli* cells using standard procedures. Transformants were grown overnight on LA/Amp, IPTG, X-gal plates (LA/Amp supplemented with X-gal to a final concentration of 80 µg/ml and IPTG to a final concentration of 0.5 µM) for blue/white screening. After an overnight incubation, six white colonies were selected from each of the overnight plates and grown overnight in 5 ml LB/Amp. A plasmid extraction of the overnight culture was performed using the QIAprep® Spin Miniprep kit, (Qiagen, USA) according to manufacturer's instructions and the samples were analysed using 1 % AGE. Plasmids containing inserts were termed pGEM®-VP1 and pGEM®-$3C^{pro}$ and restricted with *Bam*HI and *Sal*I as described below.

2.2.9 Restriction analysis and cloning of VP1 and $3C^{pro}$ into pQE-80L

VP1 and $3C^{pro}$ genes were isolated from pGEM®-T Easy by restriction analysis using *Bam*HI and *Sal*I which had been engineered on the 5' and 3' ends of the nucleotide sequences of the proteins respectively. AGE was performed to analyse the restricted plasmids. The suspected VP1 insert at approximately 880 bp and the suspected $3C^{pro}$ insert at approximately 649 bp were excised from the agarose gel under UV light and purified using the Wizard® SV Gel and PCR Clean-up System (Promega, USA) according to manufacturer's instructions. Purified VP1 and $3C^{pro}$ inserts were ligated into linearised pQE-80L (Qiagen, USA) using *Bam*HI and *Sal*I to produce pBMVP1 and pBM$3C^{pro}$. In a total volume of 10 µl, reactions contained 1 U T4 DNA ligase, 1 µl 10x ligase buffer, 1 µl DNA (~70 µg) and 1 µl linearised pQE-80L (~50 µg) and 6 µl ddH_2O . A negative control reaction was set up in the same way

using deionised water (ddH_2O) instead of the DNA template. The reactions were mixed by pipetting and incubated for 1 hr at 37°C. Ligations were transformed into competent JM109 *E. coli* cells using standard procedures. Transformants were grown overnight on LA/Amp plates at 37°C. A single colony was selected from each overnight plate and grown overnight at 37°C in 5 ml LB/Amp. Plasmid DNA was extracted from overnight cultures using the QIAprep® Spin Miniprep plasmid extraction kit (Qiagen, USA) according to manufacturer's instructions. Samples were analysed by 1 % AGE.

2.2.10 Confirmation of integrity of pBMVP1, pBM3C^{pro} and pETVP1 (1-741) by restriction analysis and Sanger sequencing

The integrity of pBMVP1 and pBM3C^{pro} was confirmed by restriction analysis with *Bam*HI and *Sal*I restriction endonucleases. In a total volume of 20 µl, reactions contained 1 U *Bam*HI and *Sal*I, 1 µl 1x restriction enzyme buffer D, 10 µl recombinant plasmid DNA (~70 µg) and 7 µl ddH_2O. For pETVP1 (1-741) restriction analysis, 1 U *Xho*I and *Xba*I were used instead of *Bam*HI and *Sal*I restriction endonucleases. The restriction analysis was carried out at 37°C for 1 hr and analysed by 1 % AGE. Secondly, the integrity of recombinant plasmids was confirmed by Sanger sequencing (Inqaba Biotec™, South Africa), in order to confirm whether the open reading frames were intact and that no mutations were generated during the PCR reaction procedure. QE Promoter and QE reverse oligonucleotides were used for the sequencing of pBMVP1 and pBM3C^{pro}. The T7 promoter and T7 reverse oligonucleotides were used for the sequencing of pETVP1 (1-741).

2.3 Results

2.3.1 Prediction of hydrophobic, hydrophilic and antigenic regions of VP1

The VP1 amino acid sequence was analysed in order to predict, hydrophobic, hydrophilic and antigenic regions of the protein using the internet based program Protscale in the ExPASytool website (www.expasytool.com). The results are shown in Figure 2.1 A and B below.

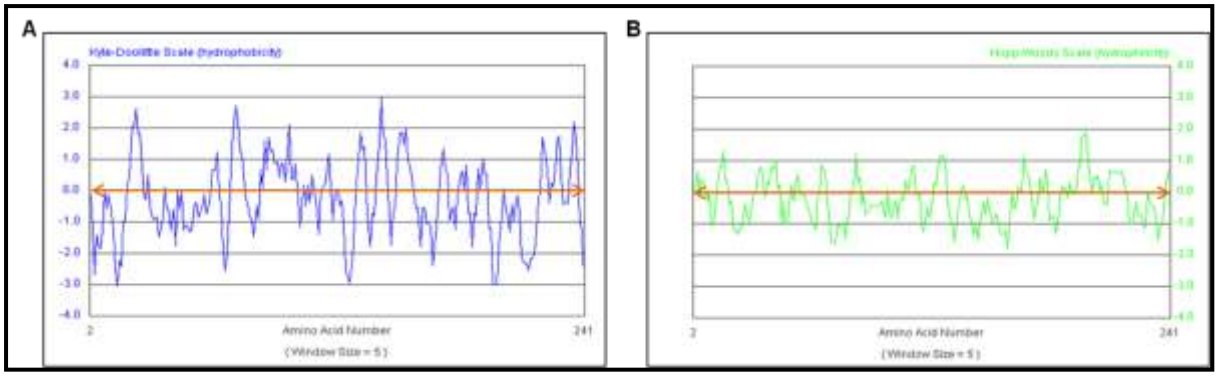

Figure 2.1 A: **Kyte and Doolittle Hydropathy plot of VP1.** Peaks below zero are predicted to be hydrophilic regions and those above zero are predicted to be hydrophobic regions. **B**: **Hopp and Woods Hydrophilicity plot of VP1.** Peaks below zero are predicted to have non-antigenic properties and hydrophobic regions and those above zero are predicted to have antigenic properties and hydrophilic regions.

It can be observed from the Hydropathy plot in Figure 2.1 A that there is distribution of predicted hydrophobic and hydrophilic regions across the VP1 protein as shown by the peaks above and below the zero axis respectively. Amino acids 0-20 on the N-terminus were predicted to be hydrophilic as shown by peaks below the zero axis. The middle region of the amino acid sequence appears to have a distribution of amino acids predicted to be hydrophobic and hydrophilic as shown by the peaks above and below the zero axis throughout the middle region of the protein sequence. The Hopp and Woods Hydrophilicity plot in figure 2.1 B indicates that amino acids 0-20 on the N-terminus are predicted to have antigenic properties as shown by the peak above the zero axis whilst some amino acids on the C-terminus contained peaks which were predicted to have non-antigenic properties as shown by the peaks below the zero axis within this region. The middle region of the protein shows distribution of regions predicted to have antigenic and non-antigenic properties as shown by the peaks above and below the zero axis.

In order to determine whether there was a correlation between the Hydropathy and Hydrophilicity plot, an overlap of both plots was performed, (Figure 2.2).

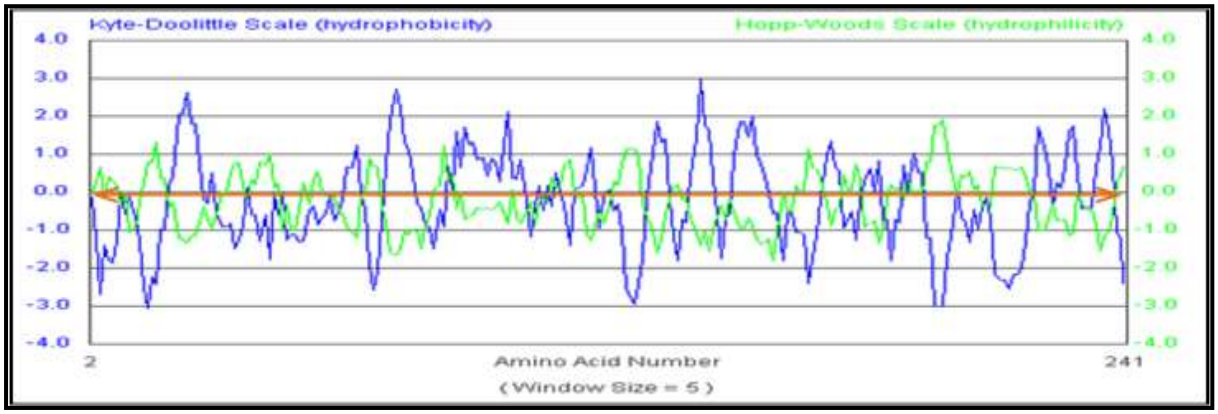

Figure 2.2: An overlap of the Kyte-Doolittle Hydropathy plot (blue) and the Hopp and Woods Hydrophilicity plot (green) for VP1.

The overlap of the Kyte and Doolittle plot (blue) and the Hopp and Woods plot (green) shows a correlation between hydrophilic and antigenic peaks. The amino acids in the Hydropathy plot predicted to be hydrophilic are shown to have antigenic properties in the Hydrophilicity plot. Amino acids 0-20 in the N-terminus which are predicted to be hydrophilic in the Kyte and Doolittle plot have been predicted to have antigenic properties in the Hopp and Woods plot and hydrophobic amino acids on the C-terminus of the protein have been predicted to have non-antigenic properties in the Hydrophilicity plot. Distribution of predicted antigenic (hydrophilic) and non-antigenic (hydrophobic) regions were observed across the middle region of the protein.

2.3.2 Prediction of hydrophobic, hydrophilic and antigenic regions of 3C^{pro}

The 3C^{pro} amino acid sequence was analysed in order to determine the predicted hydrophobic, hydrophilic and antigenic regions of the protein using the internet based program Protscale in the ExPASytool website (www.expasytool.com). The results are shown in Figure 2.3 A and B below.

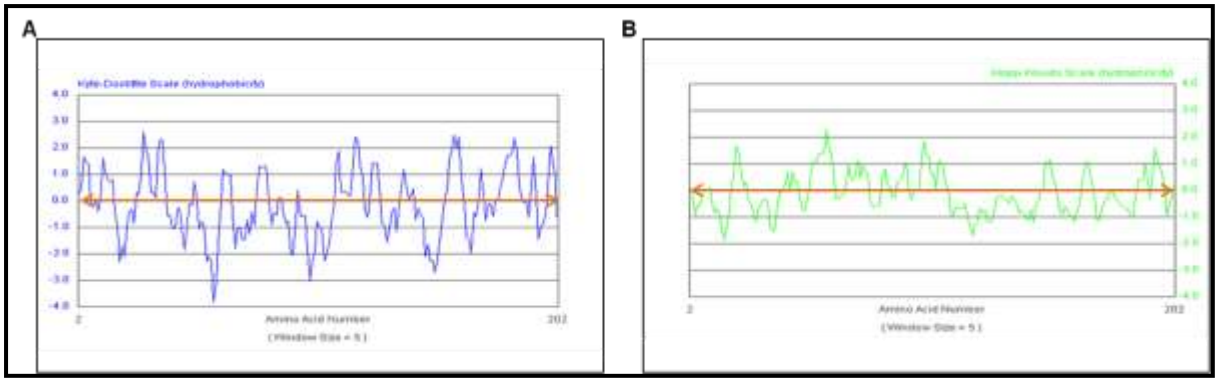

Figure 2.3 A: **Kyte and Doolittle Hydropathy plot of 3C^{pro}.** Peaks below zero are predicted to be hydrophilic regions and those above zero are predicted to be hydrophobic regions. **B**: **Hopp and Woods Hydrophilicity plot of 3C^{pro}.** Peaks below zero are predicted to have non-antigenic properties and hydrophobic regions and those above zero are predicted to have antigenic properties and hydrophilic regions.

It can be observed in figure 2.3 A that amino acids 0-30 of 3C^{pro} are predicted to be hydrophobic as shown by the peaks above zero. There is distribution of predicted hydrophobic and hydrophilic amino acids across the middle region of the 3C^{pro} amino acid sequence as shown by peaks above and below zero respectively. The Hopp and Woods Hydrophilicity plot in Figure 2.3 B indicates that amino acids 0-30 on the N-terminus are predicted to have non-antigenic properties as shown by the peak below zero axis. The middle region of the protein shows a distribution of amino acids predicted to have antigenic and non-antigenic properties as shown by the peaks above and below the zero axis within this region.

In order to determine whether there was a correlation between the Hydropathy and Hydrophilicity plot, an overlap of both plots was performed, (Figure 2.4).

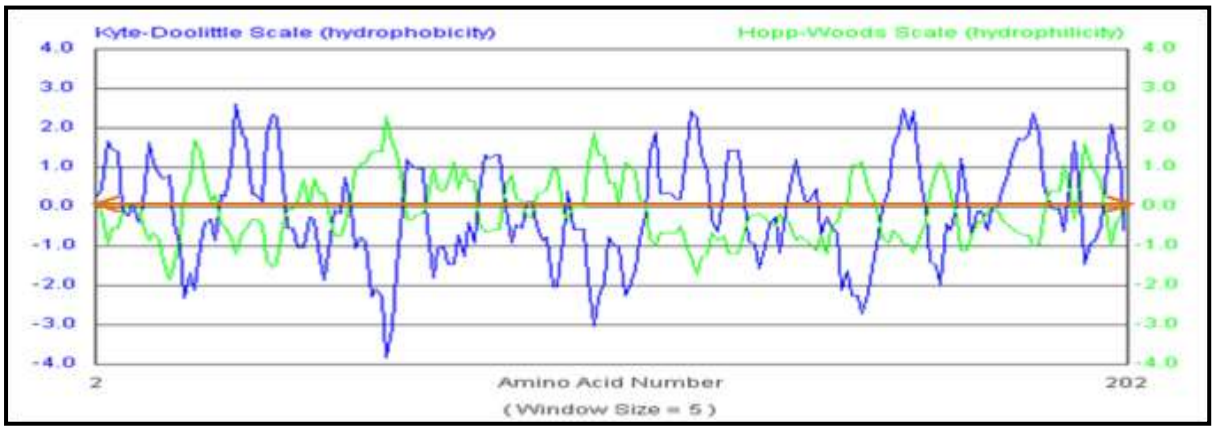

Figure 2.4: An overlap of the Kyte-Doolittle Hydropathy plot (blue) and the Hopp and Woods Hydrophilicity plot (green) for 3C^{pro}.

The overlap of the Kyte and Doolittle and Hopp and Woods plots shows a correlation between the plots. The N-terminal amino acids 0-30 predicted to be hydrophobic in the Hydropathy plot are predicted to have non-antigenic properties in the Hydrophilicity plot. A distribution of predicted antigenic (hydrophilic) and non-antigenic (hydrophobic) regions are observed across the middle region of the protein.

In order to further understand the physico-chemical properties of VP1 and $3C^{pro}$, linear B cell epitopes predicted to be on the surface of the proteins were identified.

2.3.3 Multiple Sequence alignments of VP1 and $3C^{pro}$ within different TMEV strains using Clustal W

In order to generate the predicted three-dimensional models for TMEV GDVII VP1 and $3C^{pro}$, homologous templates of the proteins must be identified. HHpred and PDB were used in order to acquire the homologous protein templates of resolved structures for VP1 and $3C^{pro}$. A multiple sequence alignment was performed using ClustalW in order to determine the percentage of identical, similar and conserved amino acid residues found within TMEV GDVII VP1 and its homologous template, (TMEV DA VP1, PDB id: 1TME) and to determine whether VP1 is conserved within the various TMEV strains. The results are shown in figure 2.5 below.

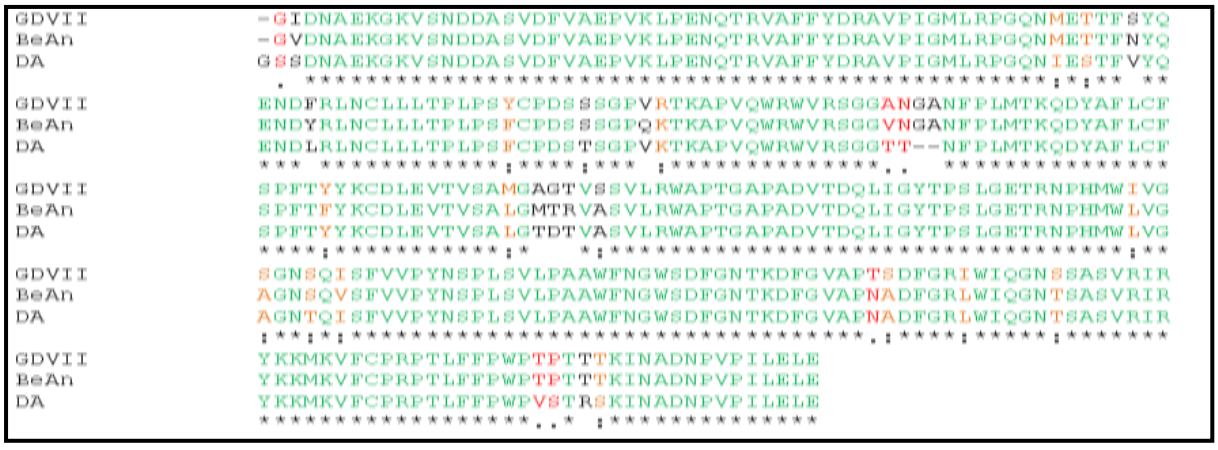

Figure 2.5: Multiple sequence alignment of VP1 amino acid sequences of the various TMEV virus strains. "*" indicates identical amino acid residues (green). ":" indicates different but highly conserved amino acids (orange) and "." indicates different amino acids with similar properties (red). Blanks indicate amino acids which have dissimilar properties.

The multiple sequence alignment of VP1 sequences of different TMEV strains (GDVII, DA, and BeAn) shows a high percentage of amino acid residues which are identical within various

TMEV strains as shown by the amino acid residues highlighted in green. The percentages of conserved and similar amino acid residues of VP1 are lower as shown by the orange and red highlighted amino acids residues respectfully. This indicates that VP1 capsid protein is conserved within the different strains of TMEV. Overall approximately 88 % of the amino acid residues are identical, 5.5 % of the amino acid residues are conserved and 2.3 % of the amino acid residues were found to have similar properties. The homologous template 1TME had an 86 % sequence homology to TMEV GDVII VP1. The sequence homology between TMEV GDVII VP1 and 1TME was high enough to be used for predicting linear B cell epitopes exposed on the surface of the protein structure.

A multiple sequence alignment was performed in order to determine the percentage of identical, similar and conserved amino acid residues found within $3C^{pro}$ of various TMEV strains. Results are shown in figure 2.6 below.

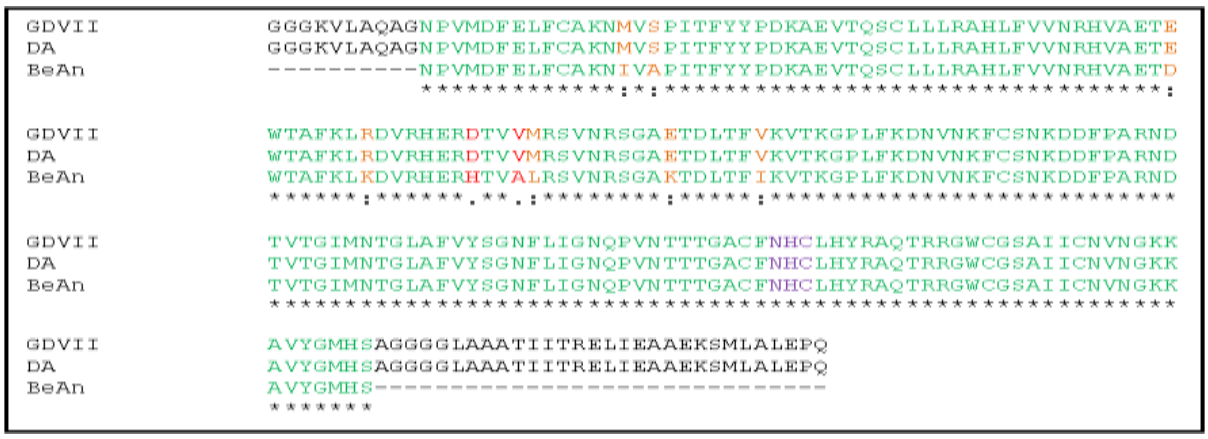

Figure 2.6: Multiple sequence alignment of $3C^{pro}$ amino acid sequences of the different TMEV strains. "*"indicates identical amino acid residues (green). ":" indicates different but highly conserved amino acids (orange) and "." indicates different amino acids with similar properties (red). The catalytic triad of the protease is highlighted in purple. Blanks indicate amino acids which have dissimilar properties.

The multiple sequence alignment of $3C^{pro}$ amino acids sequence of various TMEV strains shows that there is a high percentage of identical amino acid residues (green) compared to the conserved (orange) and similar (red) amino acid residues. The catalytic triad of the protease is indicated in purple. This indicates that $3C^{pro}$ is conserved within the different strains of TMEV. Overall approximately 90 % of the amino acid residues are identical, 3.3 % of the amino acid residues are conserved and 0.2 % of the amino acid residues were found to have similar properties.

Since there is no resolved structure for $3C^{pro}$ within the genus *Cardiovirus*, a sequence alignment was performed in order to determine the percentage of identical, similar and conserved amino acid residues found between TMEV GDVII $3C^{pro}$ and its homologous template (FMDV A10 (61), PDB id: 2BHG). The results are shown in figure 2.7 below.

```
GDVII           GGGKVLAQAGNPVMDFELFCAKNMVSPITFYYPDKAEVTQSCLLLRAHLFVVNRHVAETE
FMDV            -------ESGAPPTDLQKMVMG-NTKPVELILDGKTVAICCATGVFGTAYLVPRHLFAEQ
                       ::* *  *:: :    .. *: :   .*: .  ..  : .  ::* **:   :

GDVII           WTAFKLR----DVRHERDTVVMRSVNRSGAETDLTFVKVTKGPLFKDNVNKFCSNKDDFP
FMDV            YDKIMLDGRAMTDSDYRVFEFEIKVKGQDMLSDAALMVLHRGNKVRDITKHFRDTARMKK
                :  : *        . *   .  .*: ..  :* ::: : :*  .:* .::* ..

GDVII           ARNDTVTGIMNTGLAFVYSGNFLIGNQPVNTTTGACFNHCLHYRAQTRRGWCGSAIICNV
FMDV            GTPVVGVVNNADVGRLIFSGEALTYKDIVVSMDGDTMPGLFAYKAATRAGYAGGAVLAKD
                .   . .        :::**: *  :: * :  *  :   : *:* ** *:.*.*::.:

GDVII           NGKKAVYGMHSAGGGGLAAATIITRELIEAAEKSMLALEPQ
FMDV            GADTFIVGTHSAGGNGVGYCSCVSRSMLQKMKAHVEH----
                .... : * *****.*:. .: ::*.:::  :  :
```

Figure 2.7: Sequence alignment of TMEV GDVII $3C^{pro}$ and 2BHG. "*"indicates identical amino acid residues (purple). ":" indicates different but highly conserved amino acids (red) and "." indicates different amino acids with similar properties (green). Blanks indicate amino acids which have dissimilar properties.

The sequence alignment of TMEV GDVII $3C^{pro}$ and its homologous template (2BHG) shows that there is a higher percentage of conserved amino acid residues (red) compared to identical and similar amino acid residues in purple and green respectively. Overall approximately 42.8 % of the amino acid residues are conserved, 22.8 % of the amino acid residues are identical and 19.46 % of the amino acid residues were found to have similar properties. The homologous template 2BHG had a 40.6 % sequence homology to TMEV GDVII $3C^{pro}$. The sequence homology between TMEV GDVII $3C^{pro}$ and 2BHG was high enough to be used for predicting linear B cell epitopes exposed on the surface of the protein structure

2.3.4 Homology modeling and prediction of linear B cell epitopes

HHpred and PDB were used in order to acquire a homologous protein template of resolved structures for TMEV GDVII VP1. Models for TMEV GDVII VP1 and $3C^{pro}$ were generated using Modeller software, 1TME was identified as the homologous template for TMEV GDVII VP1 with a sequence homology of 86 %. The generated model was viewed using the open-source software PyMOL v1.1. For the linear B cell epitope prediction, the primary amino acid sequences of TMEV GDVII VP1 and 1TME were analysed using DNAStar

Protean3D system in order to determine the predicted linear B cell epitopes on the molecular surface of the proteins. The predicted linear B cell epitopes were mapped on the molecular surface of the models using PyMOL v1.1. The results are shown in figure 2.8 A and B below.

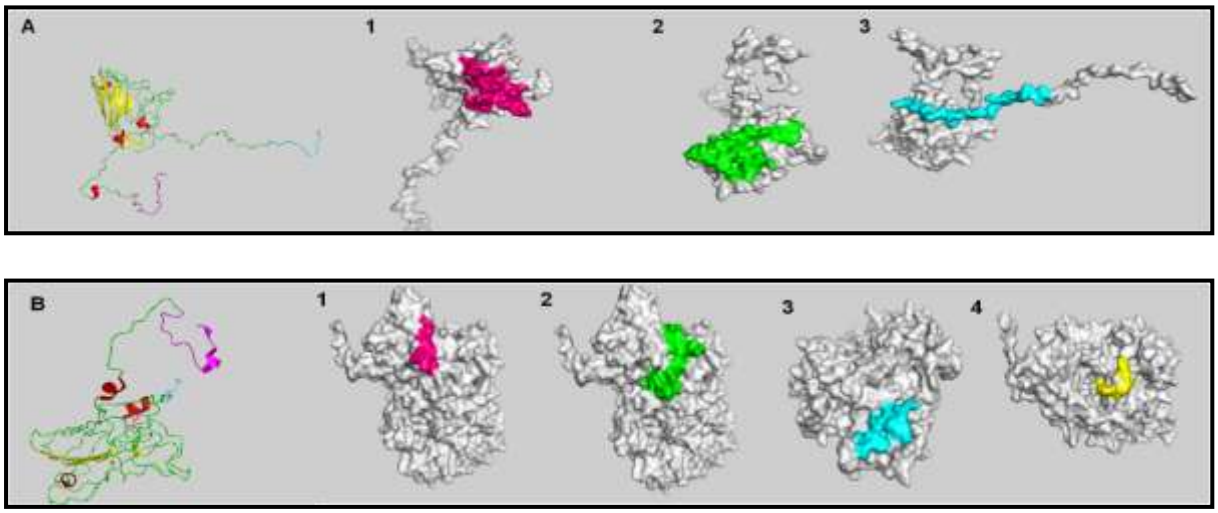

Figure 2.8 Panel A: Secondary structural model of TMEV GDVII VP1 and the predicted linear B cell epitopes of VP1 capsid protein displayed on the molecular surfaces. The secondary structural model of VP1 displays beta sheets, alpha helices and loops in yellow, red and green respectively. Three linear B cell epitopes were mapped on the molecular surface of TMEV GDVII VP1, 1 (amino acids 52-78) hot pink, 2 (amino acids 195-209) green, 3 (amino acids 250-275) cyan. **Panel B: Secondary structure of the 1TME homologous template and the predicted linear B cell epitopes of VP1 capsid protein displayed on the molecular surfaces.** The secondary structural model of 1TME displays beta sheets, alpha helices and loops in yellow, red and green respectively. Four linear B cell epitopes were mapped on the molecular surface of 1TME, 1 (amino acids 56-68) hot pink, 2 (amino acids 78-114) green, 3 (amino acids 164-174) cyan and 4 (amino acids 205-213) yellow.

The secondary structure of TMEV GDVII VP1 in Panel A shows that the protein consists of an eight-stranded anti-parallel beta-barrel structure (yellow), alpha helixes (red) and loops (green). The N-terminal and C-terminal region of the protein is indicated in magenta and cyan respectively. There are three predicted linear B cell epitopes mapped on the molecular surface of TMEV GDVII VP1, 1 (amino acids 52-78), 2 (amino acids 195-209) and 3 (amino acids 250-275). The secondary structure of the 1TME template in Panel B shows that the protein consists of an eight-stranded anti-parallel beta-barrel structure (yellow), alpha helixes (red) and loops (green). The N-terminal and C-terminal region of the protein are indicated in magenta and cyan respectively. There are four predicted linear B cell epitopes mapped on the

molecular surface of 1TME, 1 (amino acids 56-68), 2 (amino acids 78-114), 3 (amino acids 164-174) and 4 (amino acids 205-213).

HHpred and PDB were used in order to acquire the homologous protein templates of resolved structures for TMEV GDVII $3C^{pro}$. Models for TMEV GDVII $3C^{pro}$ were generated using Modeller software, 2BHG was identified as the homologous template for TMEV GDVII $3C^{pro}$ with a sequence homology of 40.6 %. The generated models were viewed using the open-source software PyMOL v1.1. For the linear B cell epitope prediction, the primary amino acid sequences of TMEV GDVII $3C^{pro}$ and 2BHG were analysed using DNAStar Protean3D system in order to determine the predicted linear B cell epitopes on the molecular surface of the proteins. The predicted linear B cell epitopes were mapped on the molecular surface of the models using PyMOL v1.1. The results are shown in figure 2.9 A and B below.

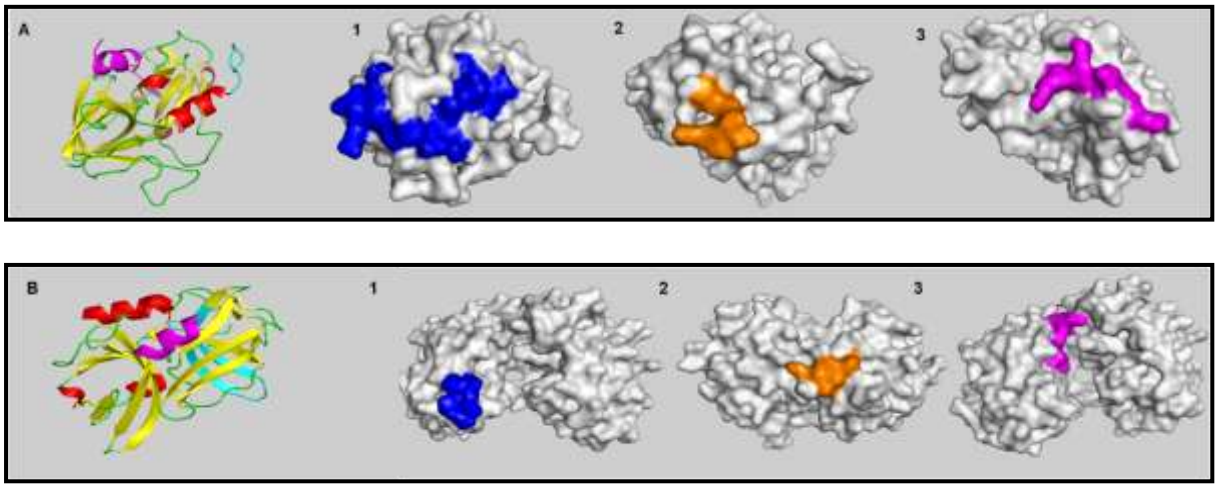

Figure 2.9 Panel A: Secondary structural model of TMEV GDVII $3C^{pro}$ and the predicted linear B cell epitopes of $3C^{pro}$ displayed on the molecular surfaces. The secondary structural model of TMEV GDVII $3C^{pro}$ displays beta sheets, alpha helices and loops in yellow, red and green respectively. Three linear B cell epitopes were mapped on the molecular surface of TMEV GDVII $3C^{pro}$, 1 (amino acids 90-107) blue, 2 (amino acids 130-136) orange and 3 (amino acids 145-152) magenta. **Panel B: Secondary structure of 2BHG homologous template and the predicted linear B cell epitopes of protein displayed on the molecular surfaces.** The secondary structure of 2BHG displays beta sheets, alpha helices and loops in yellow, red and green respectively. Three linear B cell epitopes regions mapped on the molecular surface of 2BHG, 1 (amino acids 22-28) blue, 2 (amino acids 107-113) orange and 3 (amino acids 181-192) magenta.

The secondary structure of TMEV GDVII $3C^{pro}$ in Panel A shows that the protein consists of a six-stranded anti-parallel beta-barrel structure (yellow), alpha helixes (red) and loops (green). The N-terminal and C-terminal region of the protein is indicated in magenta and

cyan respectively. There are three predicted linear B cell epitopes mapped on the molecular surface of TMEV GDVII $3C^{pro}$, 1 (amino acids 90-107) blue, 2 (amino acids 130-136) orange and 3 (amino acids 145-152) magenta. The secondary structure of 2BHG in Panel B indicated that the protein consists of a six-stranded anti-parallel beta-barrel structure (yellow), alpha helixes (red) and loops (green). The N-terminal and C-terminal region of the protein is indicated in magenta and cyan respectively. There are three predicted linear B cell epitopes mapped on the molecular surface of 2BHG, 1 (amino acids 22-28) blue, 2 (amino acids 107-113) orange and 3 (amino acids 181-192) magenta.

Based on the results obtained from the bioinformatic analysis and the predicted B cell epitopes on the protein surface, the full length coding sequences of VP1 and $3C^{pro}$ were PCR amplified and cloned into pQE-80L to produce pBMVP1 and $pBM3C^{pro}$. The integrity of the recombinant plasmids was confirmed using restriction analysis and Sanger sequencing.

2.3.5 Confirmation of pBMVP1 by restriction analysis and Sanger sequencing

A restriction digest using *Bam*HI and *Sal*I was performed in order to determine the integrity of pBMVP1. Digests were analysed by 1 % AGE, the results are shown in figure 2.10 below.

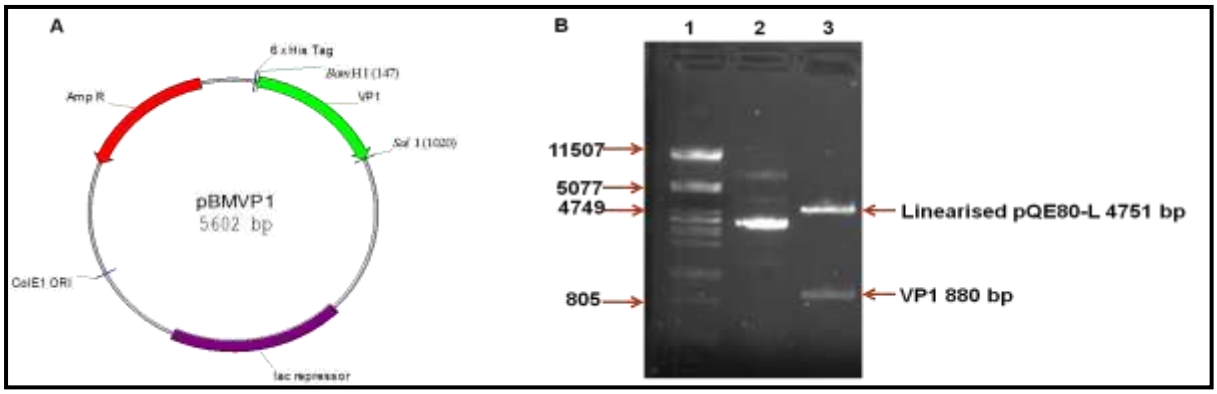

Figure 2.10: A. Schematic map of pBMVP1: The VP1 gene sequence downstream of the 6x His-tag**. B: Restriction analysis of pBMVP1:** Lane 1: *λ pst*1 DNA ladder, lane 2: pBMVP1 uncut, lane 3: pBMVP1 restricted with *Bam*HI and *Sal*I.

Figure 2.10 A shows a schematic map of pBMVP1, which is 5602 bp in size. The pQE-80L expression vector is 4751 bp in size and consists of an optimised promoter-operator element consisting of the phage T5 promoter and two *lac* operator sequences which increase *lac*

repressor binding and ensure efficient repression of the T5 promoter. *E. coli* JM109 cells are used for cloning because this cell strain harbours the *lacI*^{q} mutation and produces enough *lac* repressor to efficiently block transcription in the absence of an inducer such as IPTG. The cell strain is also ideal for storing and propagating pQE plasmids. The pQE-80L vector also consists of a multiple cloning site for convenient preparation of expression constructs. A β-lactamase gene (*bla*) which encodes for ampicillin resistance and a 6x His-tag sequence at the 5' end of the cloning region are also present on the vector (www.**qiagen**.com/Knowledge-and-Support/Resource-Center/, accessed 20-02-2013). Figure 2.10 B shows that when pBMVP1 was restricted with *Bam*HI and *Sal*I, two bands are formed. One band representing linearised pQE-80L is present above the 4749 bp marker and another band representing the VP1 insert is present above the 805 bp marker (lane 3) as expected. This suggests that the VP1 coding sequence was successfully cloned into the pQE-80L.

To further confirm the integrity of pBMVP1 and to ensure that the correct open reading frame was present, Sanger sequencing was performed. The results are shown in figure 2.11 below.

ATGAGAGGATCGCATCACCATCACCATCACGGATCCGGAATTGACAATGCTGAGAAGGGAAAGGTCTCC
AACGATGACGCTTCGGTCGATTTCGTTGCCGAGCCAGTCAAGCTACCCGAGAACCAAACCCGGGTGGCCT
TCTTTTACGACAGAGCTGTCCCCATAGGAATGTTGAGACCCGGCCAAAATATGGAAACCACCTTTAGCTAC
CAAGAGAATGATTTCCGCCTCAATTGTCTTCTGTTGACCCCTCTTCCTTCTTATTGTCCCGACAGTTCCTCCG
GTCCTGTCAGAACGAAGGCTCCCGTCCAGTGGCGATGGGTGCGGTCTGGTGGCGCCAATGGTGCCAACT
TCCCACTCATGACCAAACAGGACTACGCCTTCCTCTGCTTTTCCCCTTTCACCTACTACAAGTGTGACCTTG
AAGTTACCGTTAGTGCTATGGGAGCAGGCACCGTTTCTTCTGTTCTGCGCTGGGCACCCACCGGGGCGCC
CGCGGATGTCACTGACCAGCTGATCGGCTATACTCCTAGTCTTGGTGAAACACGTAACCCCCGCATGTGG
ATCGTTGGCTCTGGAAATTCTCAAATTTCTTTTGTCGTACCTTACAATTCCCCTCTGTCCGTCTTACCCGCTG
CTTGGTTCAATGGATGGTCCGACTTTGGAAACACCAAGGATTTTGGAGTTGCTCCTACGTCGGATTTTGGG
CGCATTTGGATACAGGGTAACAGCTCTGCCTCAGTTCGAATCAGTACAAGAAGATGAAGGTCTTCTGCCC
CCGCCCGACCCTCTTTTTCCCCTGGCCAACGCCCACCACCACCAAGATCAATGCTGACAATCCAGTCCCCAT
TCTTGAGCTTGAGTGACTGGACTTTAATCACAGTGAGTTCGCGTGAGTCGAC

Figure 2.11: Sanger sequencing of pBMVP1: Shown in red and purple are the start and stop codons respectively; in green is the 6x His-tag upstream of the sequence for VP1, the forward and reverse oligonucleotides are underlined. The *Bam*HI and *Sal*I restriction sites are shown in orange and cyan respectfully. The first and the last codons of VP1 coding sequence are shown in blue and burgundy respectively.

The results of the sequence analysis shows that the open reading frame is intact when the codons are read in triplicate from the first ATG shown in red through to the stop codon, TGA in purple. The 6x His-tag sequence upstream of the VP1 sequence is in green, the *Bam*HI and *Sal*I restriction sites are shown in orange and blue respectively at the beginning and end of the VP1 coding sequence. The forward and reverse oligonucleotides are underlined. No mutations were identified when the sequence was subjected to BLAST against the TMEV GDVII complete genome sequence (Acc no: X56019.1)

2.3.6 Confirmation of pETVP1 (1-741) by restriction analysis and Sanger sequencing

The pETVP1 (1-741) is a recombinant plasmid which was constructed by Dora Mwangola and it consists of nucleotides 1-741 of VP1 coding sequence cloned into the pET22b+ expression vector.

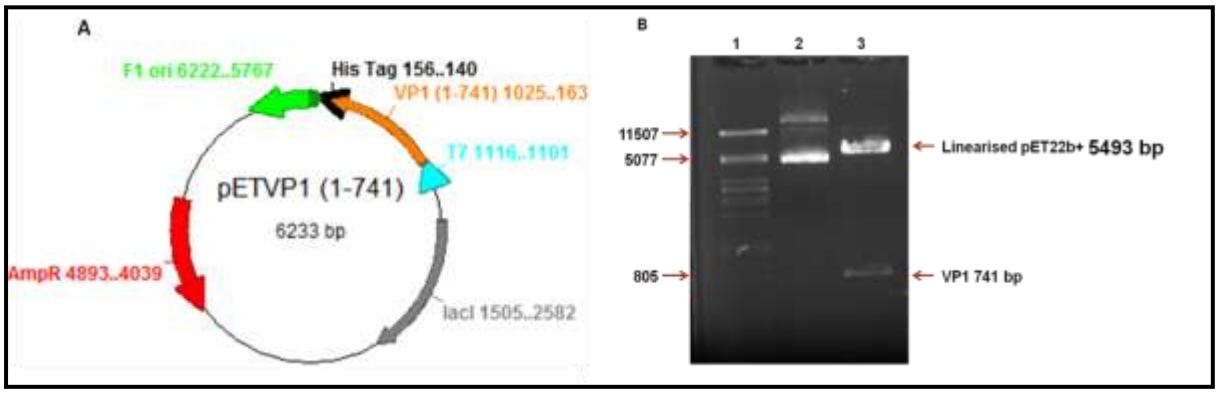

Figure 2.12 A: Schematic map of pETVP1 (1-741): The VP1 (1-741) gene sequence downstream of the 6x His-tag. **B: Restriction analysis of pETVP1 (1-741):** Lane 1: *λ pst*1 DNA ladder, lane 2: pETVP1 (1-741) uncut, lane 3: pETVP1 (1-741) restricted with *Xho*I and *Xba*I**.**

Figure 2.12A shows a schematic map of pETVP1 (1-741), which is 6233 bp in size. The pET22b+ vector is 5493 bp in size and consists of an optimised promoter-operator element consisting of the phage T7 promoter and a *lac* operator sequence downstream from the T7 promoter which increases *lac* repressor binding and ensures repression of the T7 promoter. The T7 promoter is highly specific in that it is only bound to the bacteriophage T7 RNA polymerase. The vector also consists of a multiple cloning site and translational stop codons in all three reading frames for convenient preparation of expression constructs. A β-lactamase gene (*bla*) which encodes for ampicillin resistance and a 6x His-tag sequence 3' to the cloning region are also present in the vector (www.novagen.co.za, accessed: 20-02-2013). *E.*

coli BL21 (DE3) cells are used for cloning into the pET22b+ vector as this cell strain allows for high-efficiency protein expression of genes which are under the control of a T7 promoter. The bacterial strain is lysogenic for λ-DE3 which contains the T7 bacteriophage gene I, encoding T7 RNA polymerase under the control of the *lac UV5* promoter (www.promega.com, accessed: 20-02-2013). The restriction analysis in figure 2.12 B was performed using *Xho*I and *Xba*I. The *Xba*I restriction site is present within the multiple cloning site and restricts VP1 (1-741) at approximately 40 bp downstream from the *Nde*I restriction site, so that the size of the VP1 (1-741) insert observed on the 1 % AGE is 781 bp in size. When pETVP1 was restricted with *Xho*I and *Xba*I, two bands are formed. One band representing linearised pET22b+ is present above the 5077 bp marker and another band representing VP1 (1-741) insert is present below the 805 bp marker (lane 3) as expected. This suggests that the VP1 (1-741) coding sequence was successfully cloned into the pET22b+.

To further confirm the integrity of pETVP1 (1-741) and ensure that the open reading frame was intact, Sanger sequencing was performed and results shown below in figure 2.13.

CATATGGGAATTGACAATGCTGAGAAGGGAAAGGTCTCCAACGATGACGCTTCGGTCGATTTCGTTGCC
GAGCCAGTCAAGCTACCCGAGAACCAAACCCGGGTGGCCTTCTTTTACGACAGAGCTGTCCCCATAGGAA
TGTTGAGACCCGGCCAAAATATGGAAACCACCTTTAGCTACCAAGAGAATGATTTCCGCCTCAATTGTCTT
CTGTTGACCCCTCTTCCTTCTTATTGTCCCGACAGTTCCTCCGGTCCTGTCAGAACGAAGGCTCCCGTCCAG
TGGCGATGGGTGCGGTCTGGTGGCGCCAATGGTGCCAACTTCCCACTCATGACCAAACAGGACTACGCCT
TCCTCTGCTTTTCCCCTTTCACCTACTACAAGTGTGACCTTGAAGTTACCGTTAGTGCTATGGGAGCAGGCA
CCGTTTCTTCTGTTCTGCGCTGGGCACCCACCGGGGCGCCCGCGGATGTCACTGACCAGCTGATCGGCTAT
ACTCCTAGTCTTGGTGAAACACGTAACCCCCACATGTGGATCGTTGGCTCTGGAAATTCTCAAATTTCTTTT
GTCGTACCTTACAATTCCCCTCTGTCCGTCTTACCCGCTGCTTGGTTCAATGGATGGTCCGACTTTGGAAAC
ACCAAGGATTTTGGAGTTGCTCCTACGTCGGATTTTGGGCGCATTTGGATACAGGGTAACAGCTCTGCCTC
AGTTCGAATCACGTACAAGAAGATGAAGGTCTTCTGCCTCGAGCACCACCACCACCACCACTGA

Figure 2.13: DNA sequencing of pETVP1: The start codon is highlighted in green and the stop codon is shown in red, the *Nde*I and *Xho*I restriction sites are shown in burgundy and orange respectively, the reverse and forward oligonucleotides are underlined. The 6x His-tag is shown in blue downstream of the sequence for VP1 (1-741). The first and last codons of VP1 (1-741) coding sequence are shown in purple and cyan respectively.

The results of the sequence analysis shows that the open reading frame is intact when the codons are read in triplicate from the first ATG shown in highlighted in green through to the stop codon, TGA in red. The 6x His-tag sequence downstream of the VP1 (1-741) sequence

is in blue, the *Xho*I and *Nde*I restriction sites shown in burgundy and orange respectively at the beginning and end of the VP1 (1-741) coding sequence. The forward and reverse oligonucleotides are underlined. No mutations were identified when the sequence was subjected to BLAST against the TMEV GDVII complete genome sequence (Acc no: X56019.1).

2.3.7 Confirmation of pBM3C^{pro} by restriction analysis and Sanger sequencing

A restriction digest using *Bam*HI and *Sal*I was performed in order to determine the integrity of pBM3C. Digests were analysed by 1 % AGE. The results are shown in figure 2.14 below.

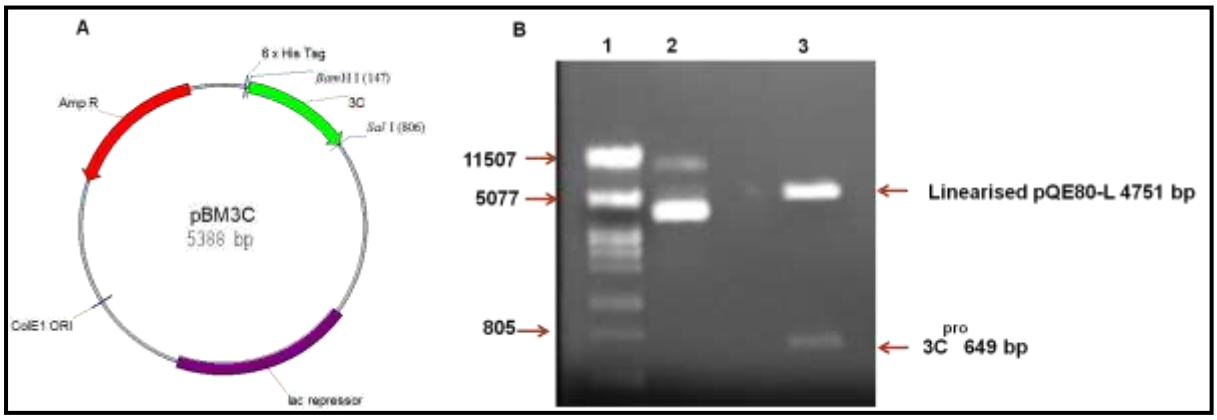

Figure 2.14:A. Schematic map of pBM3C^{pro}: The 3C^{pro} gene sequence downstream of the 6x His-tag**.** B: **Restriction analysis of pBM3C^{pro}:** Lane 1: λ *pst*1 DNA ladder, lane 2: pBM3C^{pro} unrestricted, lane 3: pBM3C^{pro} restricted with *Bam*HI and *Sal*I.

Figure 2.14 A indicates a schematic map of pBM3C^{pro} which is 5388bp in size. The size and essential features of pQE-80L have been previously described in section 2.3.5. Figure 2.14 B shows that when pBM3C^{pro} was restricted with *Bam*HI and *Sal*I, two bands formed. One band representing linearised pQE-80L is present above the 4749 bp marker and another band representing the 3C^{pro} insert is present below the 805 bp marker (lane 3) as expected. This suggests that the 3C^{pro} coding sequence was successfully cloned into the pQE-80L.

To further confirm the integrity of pBM3C^{pro} and to ensure that the open reading frame was intact, Sanger sequencing was performed. The results are shown in figure 2.15 below.

ATGAGAGGATCGCATCACCATCACCATCACGGATCCGGAGGCGGGAAGGTTCTAGCCCAGGCCGGTAAC
CCCGTCATGGACTTTGAGCTTTTCTGTGCCAAAAACATGGTTTCCCCGATTACCTTCTACTATCCTGACAAG
GCTGAAGTGACCCAGAGCTGCTTGCTGCTCCGTGCCCACCTCTTCGTGGTCAACCGCCACGTCGCTGAAAC
GGAATGGACAGCTTTCAAGCTTAGGGATGTGAGGCACGAACGTGACACTGTTGTCATGCGTTCCGTTAAC
CGCTCAGGAGCTGAAACGGACCTTACATTCGTGAAGGTTACTAAAGGACCACTCTTCAAGGACAATGTGA
ACAAGTTTTGCTCAAACAAGGACGATTTTCCTGCTAGGAATGACACTGTTACCGGGATAATGAACACTGG
ATTGGCCTTCGTGTATTCCGGTAACTTTCTGATTGGCAATCAACCTGTGAACACAACAACTGGAGCCTGCT
TCAACCACTGCCTCCACTATCGAGCTCAAACTCGACGTGGTTGGTGTGGTTCTGCCATCATCTGCAATGTT
AACGGCAAAAAAGCTGTTTACGGAATGCACTCTGCTGGAGGCGGAGGCCTTGCCGCCGCTACCATCATCA
CCAGAGAGTTGATTGAAGCAGCTGAGAAGTCTATGTTGGCGCTGGAACCGCAATGAGTCGAC

Figure 2.15: Sanger sequencing of pBM3C^{pro}: Shown in green and cyan are the start and stop codons respectively, in red is the 6x His-tag upstream of the sequence for 3C^{pro}, the forward and reverse oligonucleotides are underlined. The *Bam*HI and *Sal*I restriction sites are shown in blue and orange respectively. The first and last codons of 3C^{pro} coding sequence are shown in purple and burgundy respectively.

The results from the sequence analysis show that the open reading frame is intact when the codons are read in triplicate from the first ATG shown in green through to the stop codon, TGA in cyan. The 6x His-tag sequence upstream of the 3C^{pro} sequence is in red, the *Bam*HI and *Sal*I restriction sites are shown in blue and orange respectfully at the beginning and end of the 3C^{pro} coding sequence. The forward and reverse oligonucleotides are underlined. No mutations were identified when the sequence was subjected to BLAST against the TMEV GDVII complete genome sequence (accession number: X56019.1).

2.4 Discussion

This chapter describes a bioinformatic analysis of TMEV VP1 and 3C^{pro} amino acid sequences and the cloning of the full length coding sequences of VP1 and 3C^{pro} into pQE-80L.

The Kyte and Doolittle Hydropathy plots for both proteins indicated that VP1 and 3C^{pro} have a distribution of amino acids which are predicted hydrophobic and hydrophilic throughout the protein sequence. The Hopp and Woods Hydrophilicity plots indicated that both proteins have a distribution of predicted antigenic and non-antigenic regions throughout the protein sequences. An overlap of both plots indicated a correlation between the predicted

hydrophobic and non-antigenic regions as well as predicted hydrophilic and antigenic regions for the proteins. Based on these results it was decided that the full length coding sequences of VP1 and $3C^{pro}$ would be PCR-amplified and cloned into pQE-80L for expression.

The prediction of linear B cell epitopes exposed on the surface of protein structures was also described. When an antigen is encountered within a living organism, B cells of the immune system recognise the antigen by their membrane bound immunoglobulin receptors. In response to this event antibodies are produced specific to the antigen. The binding region of an antigen to the B cell is known as a B cell epitope (Ponomarenko and van Regenmortel 2009). Two types of B cell epitopes are known, linear or continuous (non-conformational) B cell epitopes and discontinuous (conformational) B cell epitopes. Linear or continuous B cell epitopes are a single stretch of a polypeptide chain on antigens which antibodies formed by B-cells bind. Discontinuous B cell epitopes consist of various parts of the polypeptide chain joined on the protein surface by the folding of the protein (Larsen *et al*., 2006; Ponomarenko and van Regenmortel 2009). Discontinuous B cell epitopes are the most common epitopes found in proteins which cross react with corresponding epitopes whereas only 10 % of linear B cell epitopes cause a cross reaction with corresponding antibodies. Linear B cell epitopes are exposed to the surface and most commonly localised in loop regions of proteins. The loop regions of proteins have been found to be flexible and are composed of hydrophilic polar residues (Odorico and Pellequer, 2003; Larsen *et al*., 2006). Various methods such as X-ray crystallography, enzymatic fragmentation, synthetic over-lapping peptides and site directional mutagenesis to name a few, may be used to determine B cell epitopes, however these methods are time consuming and expensive. Computational methods can be used for the prediction of B cell epitopes, this alternative is less expensive and fast (Sharma *et al*., 2013). Linear B cell epitopes can be predicted by the use of scale methods which analyse the physicochemical properties of amino acids (Larsen *et al*., 2006). The prediction of discontinuous B cell epitopes is based on the knowledge of the three-dimensional structure of the protein. The determination of discontinuous B cell epitopes has proven to be a major challenge with only a few applications available. Previous prediction methods have been based on protein sequences and are not effective (Ponomarenko and van Regenmortel 2009).

Prior to linear B cell epitope prediction, homology modelling was conducted to identify homologous templates for TMEV GDVII VP1 and $3C^{pro}$. These homologous templates were used for the generation of three-dimensional models of TMEV GDVII VP1 and $3C^{pro}$. The

multiple sequence alignment of VP1 TMEV sequences gave an amino acid residue percentage identity of 88 %, suggesting that the protein is highly conserved. The 88 % amino acid residue identity was in agreement with the 86 % sequence homology between TMEV GDVII VP1 and its homologous template, 1TME. Therefore this template was used for the prediction of Linear B cell epitopes exposed on the surface of the protein structure.

The model of TMEV GDVII VP1 and its homologous template 1TME indicated that the protein structures consist of an eight-stranded antiparallel beta barrel structure, alpha helices and loops. Three capsid proteins, VP1, 2 and 3 have been described to consist of a beta barrel structure. The beta structure forms a wedge shaped structure which has been suggested to play a role in stabilising the virion (as reviewed by Racaniello, 2007). Structural analysis of the TMEV DA, homologous template has indicated that the VP1, 2 and 3 viral capsid proteins consist of eight-stranded antiparallel beta barrels cores which are similar to those found in other picornavirus capsid proteins (Grant *et al*., 1992). There were three predicted linear B cell epitopes exposed on the molecular surface of TMEV GDVII VP1, 1 (amino acids 52-78), 2 (amino acids 195-209) and 3 (amino acids 250-275). The third epitope, 3 (amino acids 250-275) was localised on the loop region of the structure where a number of polar residues such as serine, threonine, cysteine and glutamine were identified within this region of TMEV GDVII VP1 secondary structure. Four predicted B cell epitopes exposed on the molecular surface of 1TME, 1 (amino acids 56-68), 2 (amino acids 78-114), 3 (amino acids 164-174) and 4 (amino acids 205-213).

The multiple sequence alignment of $3C^{pro}$ TMEV sequences gave an amino acid identity percentage of 90 %, suggesting that the protein is highly conserved. Since no structure of $3C^{pro}$ has been resolved within the *Cardiovirus* genus, (FMDV A10 (61), PDB id: 2BHG), was identified as a homologous template of the protein. A sequence alignment was conducted between the TMEV $3C^{pro}$ and 2BHG primary sequences. A percentage identity of 22.8 % was obtained. There is a sequence homology of 40.6 % between TMEV GDVII $3C^{pro}$ and 2BHG. TMEV GDVII $3C^{pro}$ has a sequence homology of 25 % with (chain A HRV, PDB id: 1CQQ), a 23 % sequence homology was identified between TMEV GDVII $3C^{pro}$ and (HAV, PDB id: 2HAL) and 30 % homology with (chain A PV, PDB id: 4DCD). Sufficient homology of sequences for predicting a three-dimensional structure can be assumed when there is a 30 % or more sequence identity, when sequences confer a 15 % or lower identity, then homology

cannot be assumed (Hillisch *et al*., 2004). HHpred is more sensitive in determining homology between a target sequence and its template. The Hidden Markov Model (HMM) profile included in HHpred ensures that homology is considered from a structural perspective in addition to the sequence identity being taken into account (Söding *et al*., 2005). The homologous template, 2BHG was used for the prediction of linear B cell epitopes exposed on the protein surface.

Homology modelling was performed in order to generate three-dimensional structures for TMEV GDVII $3C^{pro}$ and 2BHG. The TMEV GDVII $3C^{pro}$ model and its homologous template, 2BHG, indicated that the protease structures consist of an anti-parallel beta-barrel structure, alpha helices and loops. Five crystal structures of picornavirus $3C^{pro}$ have been determined (HRV-14, HRV-2, PV-1, HAV, FMDV).The structure of picornavirus $3C^{pro}$ has been found to consist of a six-stranded antiparallel beta structure which folds into two beta barrels which form the chymotrypsin-like fold. These beta barrels have been found to form an extended groove which allows for substrate binding (as reviewed by Norder *et al*., 2011). There were three predicted B cell epitopes exposed on the molecular surface of TMEV GDVII $3C^{pro}$, 1 (amino acids 90-107), 2 (amino acids 130-136) and 3 (amino acids 145-152) and three predicted B cell epitopes exposed on the molecular surface of 2BHG, 1 (amino acids 22-28), 2 (amino acids 107-113) and 3 (amino acids 181-192).

Based on the results obtained from the bioinformatic analysis and to include the predicted B cell epitopes regions, the full length coding sequences of VP1 and $3C^{pro}$ were PCR amplified and cloned into pQE-80L expression vector to produce pBMVP1 and pBM$3C^{pro}$. The expression vector, pQE-80L was chosen as a vector system because cloning into this vector has been successful in our laboratory. TMEV 2C was cloned and expressed in pQE-80L for preparation of antibodies against the non-structural 2C protein. Staining with anti-TMEV 2C antibodies localised the protein to the Golgi where virus replication is suggested to occur (Jauka *et al*., 2010).

The full length coding sequences of VP1 and $3C^{pro}$ were successfully cloned into pQE-80L. A second expression vector system was used for VP1 (as discussed in chapter 3). pETVP1 (1-741) is a plasmid created by Dora Mwangola (B.Sc Honours student, Rhodes University). The integrity of the recombinant plasmids was confirmed by restriction analysis and Sanger sequencing. The open reading frames of pBMVP1, pBM$3C^{pro}$ and pETVP1 (1-741) were intact and no mutations were identified when the sequences were subjected to BLAST against the TMEV GDVII complete genome sequence (Acc no: X56019.1).

The next chapter describes the expression and purification of recombinant VP1, $3C^{pro}$ and VP1 (1-247) in order to produce antigen for immunisation purposes.

Chapter 3: Preparation of antigen for the generation of polyclonal antibodies against TMEV VP1 and $3C^{pro}$.

3.1 Introduction

This chapter describes the expression of recombinant VP1, VP1 (1-247) and $3C^{pro}$ proteins in a bacterial system and purification of recombinant VP1 and $3C^{pro}$ using ion affinity chromatography in order to prepare antigen for immunisation in rabbits.

Recombinant pBMVP1, pBM$3C^{pro}$ and pETVP1 (1-741) previously described in chapter 2 were transformed using standard procedures. A time course induction study was performed using 1 mM IPTG in order to determine the maximum expression time of recombinant VP1, $3C^{pro}$ and VP1 (1-247). Western analysis using mouse monoclonal antibody [clone 2] (anti-His_6 (2)) was conducted in order to confirm whether the expressed proteins identified by SDS-PAGE analysis were recombinant VP1, VP1 (1-247) and $3C^{pro}$ proteins.

Solubility studies were carried out in order to determine whether recombinant VP1, VP1 (1-247) and $3C^{pro}$ were present in the soluble or insoluble fractions. When recombinant proteins were found to be predominantly in the insoluble fraction, treatment with Sarcosyl was carried out in an attempt to release recombinant proteins into the soluble fraction. Sarcosyl is an ionic detergent which is commonly used for protein solubilisation because of its mild effects on tertiary conformations of protein chains (Crossley and Holberton, 1983).

Purification of recombinant VP1 and $3C^{pro}$ was carried out using Protino® NI-IDA 1000 Packed columns kit (Macherey-Nagel, Germany). These columns enable purification of recombinant proteins by immobilised ion affinity chromatography. Protino® NI-IDA resin is pre-charged with Ni^{2+} ions which interact with the 6x His-tag of recombinant proteins thus ensuring efficient binding of the target protein (Macherey-Nagel user manual, 2011). Purification is carried out under native conditions for soluble proteins or denaturing conditions for insoluble proteins. Denaturing conditions involve the solubilisation of insoluble protein with a high concentration of urea, a chemical denaturant which increases solubility of compounds. Urea stabilises the recovery of proteins in the unfolded state where non-polar side chains are exposed, this weakens hydrophobic interactions which occur in insoluble proteins (Rossky, 2008). Based on the solubility studies results, recombinant VP1 was purified under native conditions and recombinant $3C^{pro}$ was purified under denaturing

conditions. Refolding of the proteins was not necessary after denaturation as the antigen did not have to be in its active form for downstream applications. However it was necessary to remove urea for immunisation purposes by dialysis of the purified protein using PBS.

The specific objectives were:

- To conduct a time course induction in order to determine the maximum expression time for recombinant VP1, $3C^{pro}$ and VP1 (1-247)
- To conduct solubility studies of recombinant VP1, $3C^{pro}$ and VP1 (1-247) in order to determine whether recombinant proteins were present within the soluble or insoluble fractions
- To purify recombinant VP1 and $3C^{pro}$ under native and denaturing conditions respectively using ion affinity chromatography to generate antigen for immunisation of rabbits

3.2 Methods and Materials:

3.2.1 Time course induction study of recombinant VP1, $3C^{pro}$ and VP1 (1-247)

E. coli JM109 cells were transformed with pBMVP1, pBM$3C^{pro}$ and pQE-80L. *E. coli* BL21 (*DE3*) cells were transformed with pETVP1 (1-741) and pET22b+ using standard procedures. Transformants were grown on LA/Amp plates overnight at 37°C. A single colony was selected and grown overnight in 5 ml LB/Amp at 37°C with shaking. Following the overnight incubation, a 1:20 dilution was performed by adding 2 ml of the cell culture to 38 ml of LB/Amp and cultures were allowed to grow to log phase (OD_{600}0.6-0.8) at 37°C. The cultures were induced with IPTG at a final concentration of 1 mM and harvested every 2 hrs for 6 hrs for recombinant VP1. Cells were harvested at 2 and 4 hrs for recombinant $3C^{pro}$. Two 1 ml samples were collected from each culture at each time point. One sample was used for SDS-PAGE analysis in order to determine protein expression and the other sample was used to measure the optical cell density at 600 nm using a UV-VIS spectrophotometer (Shimadzu, USA). To determine protein expression, cells were harvested by centrifugation at 11100 x g and the pellet was resuspended in a volume of phosphate buffered saline (PBS) [137 mM NaCl, 2.7 mM Na_2HPO_4, 2 mM KH_2PO_4 (pH 7.4)] using the equation

Volume: PBS µl=A_{600nm}/0.5*150 µl

3.2.2 Solubility studies

To determine whether recombinant VP1, VP1 (1-247) and $3C^{pro}$ were present in the soluble or insoluble fraction, induction studies were carried out as described in the section above. A 40 ml culture was divided into 2 x 20 ml cultures and cells harvested by centrifugation at 13000 rpm in a Beckman ultracentrifuge (Beckman Coulter, USA). One of the pellets was resuspended in 500 µl ice cold PBS and the second pellet was resuspended in 500 µl in PBS containing 7.5 % N-lauroylsarcosine (Sarcosyl; Sigma, USA). The cell suspensions were sonicated 10 times 15 sec using the Vibra Cell apparatus (Sonics and Materials, USA) at 4°C. A 100 µl aliquot of sample was taken to represent total protein (TP) and the remainder of the sample was harvested by centrifugation to pellet the insoluble fractions. The soluble fraction or supernatant (S) was collected and the insoluble fraction or pellet (P) was resuspended in 500 µl PBS. The total protein (TP), supernatant (S) and pellet (P) samples were analysed by SDS-PAGE.

3.2.3 SDS-PAGE and Western analysis

Proteins were resolved by 12 % or 15 % SDS-PAGE. Gels were prepared according to manufacturer's instructions (Bio-Rad, USA). Proteins were boiled for 5 min in 5x SDS sample buffer [62.5 mM Tris-HCl (pH 6.8), 10 % glycerol, 1.25 % bromophenol blue, 0.5 % β-mercaptoethanol, 2 % SDS]. Gels were electrophoresed at 100V for 2 hrs in 1x SDS running buffer [1.44 % glycine, 25 mM Tris (pH 8.3), 0.1 % SDS] and stained with Coomassie brilliant blue [6.25 % Coomassie (R125), 50 % methanol, 10 % acetic acid] and incubated overnight in destaining solution (40 % methanol, 7 % acetic acid).

Western analysis was conducted using the BM Western blotting kit chemiluminescence mouse/rabbit kit (Roche, Mannheim, Germany). Proteins separated by SDS-PAGE were transferred onto nitrocellulose membrane (Bio-Rad, USA) in transfer buffer [25 mM Tris-HCl (pH 8), 192 mM Glycine, 20 % methanol] for 2 hrs on ice with stirring. In order to determine that the transfer was successful the membrane was stained in Ponceau-S stain (0.1 % Ponceau S in 0.1 % glacial acetic acid) for 2 min and the membrane was rinsed in water. The membrane was washed twice for 20 min in TBS-T [Tris-buffered saline (TBS 150 mM NaCl, 50 mM Tris (pH 7) containing 1 % Tween-20]. The membrane was incubated for 2

hrs with shaking in 1 % block solution [1 % Blocking reagent (stock solution) in TBS]. The membrane was incubated overnight with anti-His_6 (2) primary antibodies (1:3000; Roche, Mannheim, Germany) in 0.5 % blocking solution at 4°C. The membrane was washed twice for 20 min in TBS-T and probed with HRP-conjugated mouse/rabbit secondary antibody diluted 1:20 000 in 0.5 % blocking solution for 45 min followed by washing four times for 15 min in TBS-T. Detection was performed according to manufacturers' instructions and proteins visualised with the VersaDoc^{TM}Model 4000 imaging system (Bio-Rad, USA).

3.2.4 Purification of recombinant VP1 under native conditions

In order to obtain sufficient antigen for immunisation purposes, the culture was scaled-up to 1L (4x 250 ml) for induction. Cell cultures were harvested in a Beckman ultracentrifuge at 10 000x g for 10 min and stored at -20°C overnight. For protein purification the Protino® NI-IDA 1000 Packed columns kit (Macherey-Nagel, Germany) was used. Each pellet was resuspended in 5 ml of 1x lysis-equilibration-wash (LEW) buffer [50 mM NaH_2PO_4, 300 mM NaCl (pH 8.0)] and lysozyme to a final concentration of 1 mg/ml. The suspension was kept on ice with stirring for 30 min. Each sample was sonicated in 5 x 1 ml aliquots as described in section 3.2.2. A sample representing total protein (TP) was boiled in SDS sample buffer and stored at -20°C. The rest of the samples were clarified by centrifugation at 13000 rpm for 5 min. A Protino®NI-IDA Packed columns (Macherey-Nagel, Germany) was equilibrated using 2 ml of 1x LEW buffer and allowed to drain. The clear supernatants were pooled and loaded to the pre-equilibrated column and the flow through sample was collected. The column was washed twice with 2 ml of 1x LEW buffer. The recombinant protein was eluted three times with 1.5 ml of elution buffer [50 mM NaH_2PO_4, 300 mM NaCl, and 250 mM imidazole (pH 8.0)]. Flow-through (FT), wash 1 (W1), wash 2 (W2), elution 1(E1) and elution 2 (E2) samples were collected and analysed by 12 % SDS-PAGE.

3.2.5 Purification of recombinant $3C^{pro}$ under denaturing conditions

Cultures were induced as described for VP1 in section 3.2.4. After sonication, the samples were clarified by centrifugation at 10 000x g for 5 min. The supernatants were discarded and the five pellets were resuspended in 5 ml of 1 x denaturing solubilisation buffer (DSB) [50 mM NaH_2PO_4, 300 mM NaCl, 8 M Urea (pH 8.0)]. The suspensions were pooled and centrifuged at 10 000x g for 30 min at 4°C in a Beckman ultracentrifuge. The supernatant

was discarded and the pellet was resuspended in 2 ml of 1x DSB to solubilise the inclusion bodies. The suspension was left to dissolve by stirring on ice for 60 min. The suspension was then centrifuged at 10 000x g for 30 min at 4°C in a Beckman ultracentrifuge and the supernatant was retained for purification. A Protino®NI-IDA packed column (Macherey-Nagel, Germany) was equilibrated with 2 ml of 1x DSB and allowed to drain. The supernatant was passed through the column and the flow through was collected. The column was washed twice with 2 ml with 1x DSB. The recombinant protein was eluted three times with 1.5 ml 1x denaturing elution buffer [50 mM NaH_2PO_4, 300 mM NaCl, 8 M Urea, and 250 mM imidazole (pH 8.0)]. Flow-through (FT), wash 1 (W1), wash 2 (W2), elution 1(E1), elution 2 (E2) and elution 3 (E3) samples were collected and analysed by 15 % SDS-PAGE.

3.2.6 Dialysis of purified 3C^{pro} antigen

SnakeSkin® pleated Dialysis tubing (Thermo Scientific, USA) was used for the dialysis. A 14 cm length was equilibrated by soaking with ddH_2O and 1.5 ml of the purified protein was added to the tubing. Air bubbles were removed from the tubing and the top end was clamped using a plastic clamp. The tubing was placed in 2 L of PBS and incubated with stirring overnight at 4°C with the PBS being replenished at 4 hr intervals. The protein precipitate was removed and a 20 µl sample was set aside for analysis. The dialysed sample was centrifuged at 10 000x g for 5 min. A 20 µl sample of the supernatant was collected before it was discarded. The pellet was dried by aspiration and resuspended in 250 µl PBS and stored at 4°C for immunisation of rabbits. The total protein, supernatant and pellet samples were analysed by 15 % SDS-PAGE. Immunisation was carried out by Prof. Bellstedt at the University of Stellenbosch, South Africa.

3.3 Results:

3.3.1 Time course induction study of recombinant VP1

In order to determine the maximum expression time of recombinant VP1 protein, *E. coli* JM109 cells harbouring pBMVP1 and pQE-80L were grown to mid-log phase and induced with 1mM IPTG for 6 hrs. Samples were collected every 2 hrs and analysed by 12 % SDS-PAGE. Western analysis was conducted using anti-His_6 (2) antibodies (Roche, Mannheim, Germany). The results are shown in figure 3.1 A and B below.

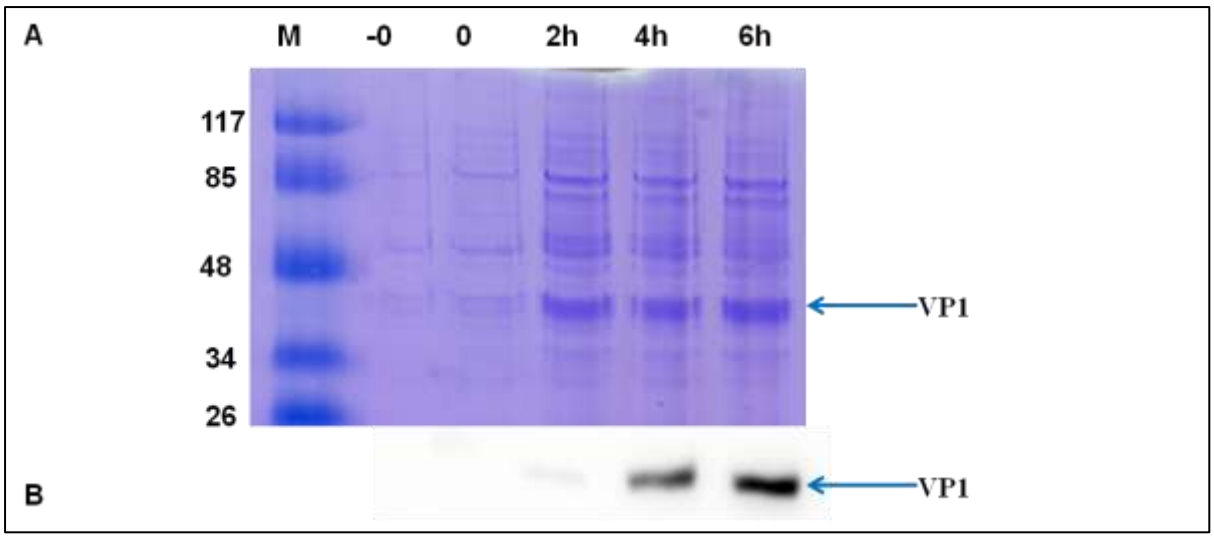

Figure 3.1 Panel A: Time course induction study of recombinant VP1 expression. Cells were induced for 6 hrs, samples were collected every 2 hrs and analysed by 12 % SDS-Page. Coomassie staining was used to visualise the proteins. **Panel B: Western analysis using anti-His_6 (2) antibodies.** Lane M: Prestained protein molecular weight marker in kDa; Lane -0: Uninduced cells harbouring pQE-80L; Lane 0: Cells harbouring pBMVP1 prior to induction; Lane 2h, 4h, 6h: Cells expressing recombinant VP1 at 2 hr, 4 hr and 6 hr post-induction.

The molecular weight of recombinant VP1 was calculated to be 38.04 kDa using the internet based programme ExPASy- compute pI/Mw tool (www.expasy.com). Panel A indicates the SDS-PAGE analysis of the time course induction study for recombinant VP1. Expression is observed from 2 hrs, 4 hrs and 6 hrs post-induction as shown by the protein band resolved at approximately 38 kDa in lanes 2h, 4h and 6h respectively. The negative control in lane -0 consists of cells harbouring pQE-80L and no expression of recombinant VP1 is observed in this lane as expected. Lane 0 shows cells harbouring pBMVP1 prior to induction and no recombinant protein band is observed at this time point. In order to confirm if the expressed protein was recombinant VP1, Western analysis was conducted using anti-His_6 (2) antibodies (Panel B). Recombinant VP1 was detected at 2, 4, and 6 hrs post-induction and the signal increased in intensity at each time point. This suggests that protein expression was increasing with an increase in hours post-induction. A 6 hr induction of recombinant VP1 will be carried out for solubility studies and purification.

3.3.2 Time course induction study of recombinant $3C^{pro}$

In order to determine the maximum expression time of recombinant $3C^{pro}$, *E. coli* JM109 cells harbouring pBM$3C^{pro}$ and pQE-80L were grown to mid-log phase and induced with 1

mM IPTG for 4 hrs. Samples were collected every 2 hrs and analysed by 15 % SDS-PAGE. Western analysis was conducted using anti-His_6 (2) antibodies (Roche, Mannheim, Germany). The results are shown in figure 3.2 A and B below.

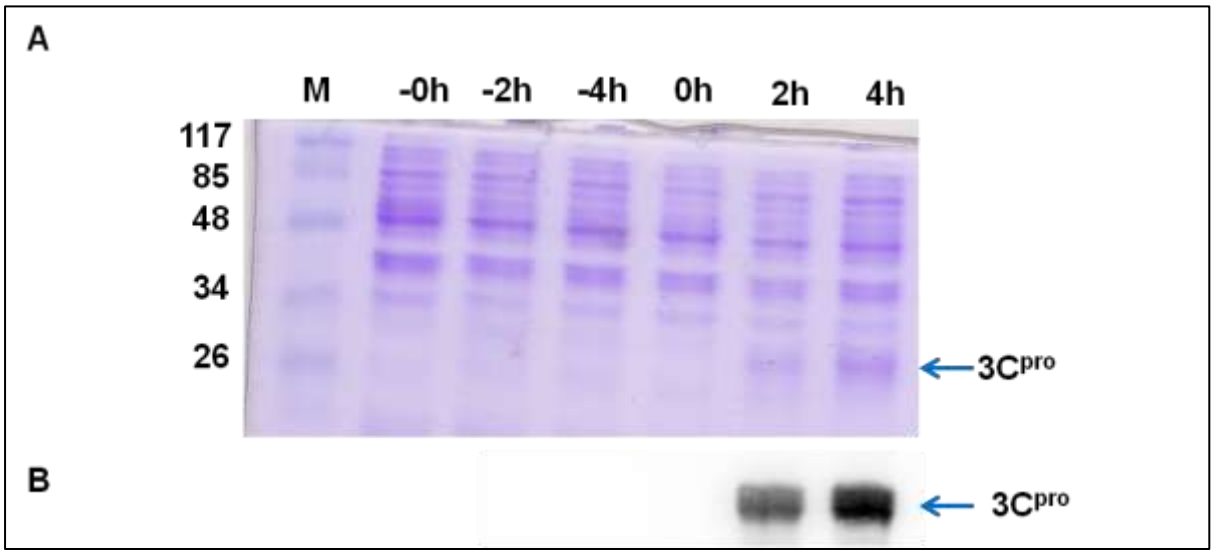

Figure 3.2 Panel A: Time course induction study of recombinant $3C^{pro}$ expression. Cells were induced for 4 hrs, samples were collected every 2 hrs and analysed by 15 % SDS-Page. Coomassie staining was used to visualise the proteins. **Panel B: Western analysis using anti-His_6 (2) antibodies.** Lane M: Prestained protein molecular weight marker in kDa; Lane -0: Uninduced cells harbouring pQE-80L; Lane 0: Cells harbouring pBM$3C^{pro}$ prior to induction; Lane -2h, -4h: Cells expressing pQE-80L at 2 hr and 4 hr post-induction; Lane 2h, 4h: Cells expressing recombinant $3C^{pro}$ at 2 hr and 4 hr post-induction.

The molecular weight of recombinant $3C^{pro}$ was calculated to be 27 kDa using the internet based programme ExPASy- compute pI/Mw tool (www.expasy.com). Panel A indicates the SDS-PAGE analysis of the time course induction study for recombinant $3C^{pro}$. Expression was observed at 2 and 4 hrs post-induction as shown by the protein band resolved at approximately 27 kDa in lane 2h and 4h. No protein band representing the recombinant protein was observed in lanes labelled -0h and 0h as expected. In order to confirm whether the expressed protein was recombinant $3C^{pro}$, Western analysis was conducted using anti-His_6 (2) antibodies (Panel B). The Western analysis showed a signal for recombinant $3C^{pro}$ at 2 hrs and 4 hrs post-induction. An increase in the protein signal was observed with an increase in hours post-induction. This suggests that protein expression was increasing at each time point. A 4 hr induction of recombinant $3C^{pro}$ will be conducted for solubility studies and purification.

3.3.3 Solubility studies of recombinant VP1

A 40 ml culture was induced for 6 hrs. Cell cultures were harvested for solubility studies in order to determine whether recombinant VP1 was present in the soluble or the insoluble fraction. Cells expressing recombinantVP1 were resuspended in PBS without (figure 3.3 A) and with (figure 3.3 B) 7.5 % Sarcosyl and sonicated. A sample was taken to represent the total protein TP, the remaining sample was harvested by centrifugation to obtain the soluble (S) and insoluble (P) fractions. The total protein (TP), supernatant (S), and pellet (P) samples were analysed by 12 % SDS-PAGE. The results are shown in figure 3.3 A and B below

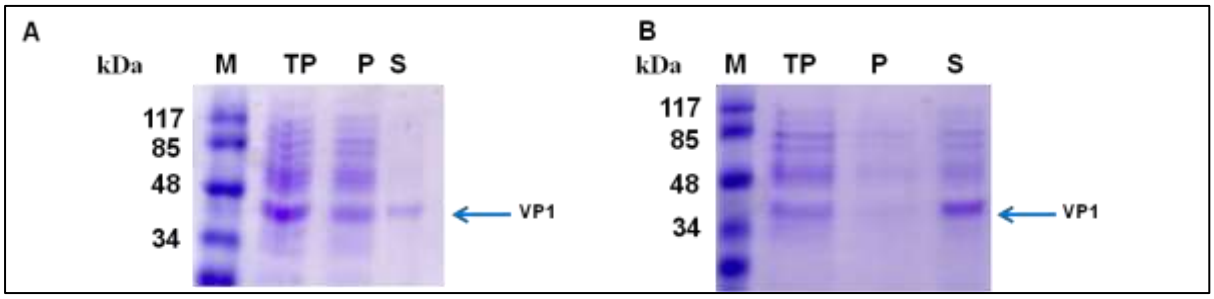

Figure 3.3: Solubility analysis of recombinant VP1. Panel A: Cells expressing recombinant VP1 in the absence of 7.5 % Sarcosyl. Lane M: Prestained protein molecular weight marker in kDa; lane TP: Total protein lysate; Lane P: Pellet (insoluble) fraction; Lane S: Supernatant (soluble) fraction. **Panel B:** Cells expressing recombinant VP1 in the presence of 7.5 % Sarcosyl. Lane M: Prestained protein molecular weight marker in kDa; lane TP: Total protein lysate; Lane P: Pellet (insoluble) fraction; Lane S: Supernatant (soluble) fraction. Coomassie staining was used to visualise the proteins.

Panel A indicates that recombinant VP1 is present equally in the soluble and insoluble fraction as shown by the protein band resolved at approximately 38 kDa in lane P and S. After treatment with 7.5 % Sarcosyl, recombinant VP1 is released into the soluble fraction with trace amounts of recombinant protein still present in the insoluble fraction as shown by the protein band resolved at approximately 38 kDa in lane S and P of panel B. This suggests that treatment with Sarcosyl was successful and recombinant protein is solubilised from the insoluble fraction into the soluble fraction. Based on these results, purification of recombinant VP1 was carried out under native conditions.

3.3.4 Solubility studies of recombinant 3C^{pro}

A 40 ml culture was induced for 4 hrs. Cell cultures were harvested for solubility studies in order to determine whether recombinant 3C^{pro} was present in the soluble or insoluble fraction. Cells expressing recombinant 3C^{pro} were resuspended in PBS without (figure 3.4 A) and with (figure 3.4 B) 7.5 % Sarcosyl and sonicated. After sonication, a sample was taken to represent the total protein TP, and the remaining sample was harvested by centrifugation to obtain the soluble supernatant (S) and insoluble pellet (P) fractions. The total protein (TP), supernatant (S) and pellet (P) samples were analysed by 15 % SDS-PAGE, results are shown in figure 3.4 A and B below.

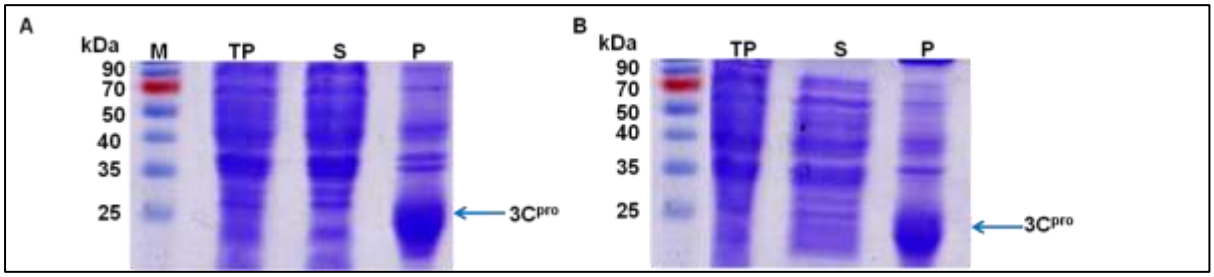

Figure 3.4: Solubility analysis of recombinant 3C^{pro}. Panel A: Cells expressing recombinant 3C^{pro} in the absence of 7.5 % Sarcosyl. Lane M: Prestained protein molecular marker; lane TP: Total protein lysate; Lane S: Supernatant (soluble) fraction; Lane P: Pellet (insoluble) fraction. **Panel B:** Cells expressing recombinant 3C^{pro} in the presence of 7.5 % Sarcosyl. Lane TP: Total protein lysate; Lane S: Supernatant (soluble) fraction; Lane P: Pellet (insoluble) fraction. Coomassie staining was used to visualise the proteins.

Panel A indicates that recombinant 3C^{pro} was present in the insoluble fraction as shown by the protein band resolved at approximately 27 kDa in lane P. Panel B indicates that treatment with Sarcosyl did not affect the solubility of recombinant 3C^{pro} since the protein was still predominantly present in the insoluble fraction. Based on these results, purification of recombinant 3C^{pro} was carried out under denaturing conditions.

3.3.5 Purification of recombinant VP1 under native conditions

A scale up culture of 1 L was induced for 6 hrs and cells were harvested by centrifugation, resuspended in 1x LEW buffer and sonicated at 4°C. Sonicates were clarified by

centrifugation and passed through a Ni-IDA column for purification. TL, FT, W1 and 2 and E1 and 2 samples were collected during purification and were analysed using 12 % SDS-PAGE. The results are shown below in figure 3.5 below.

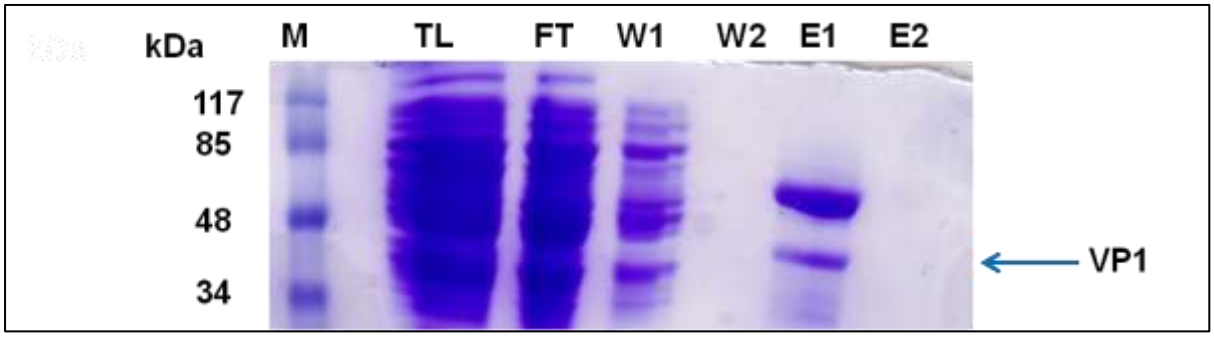

Figure 3.5: SDS-Page analysis of the purification of recombinant VP1 under native conditions. Samples collected at each stage during the purification were resolved by 12 % SDS-PAGE. Lane M: Prestained protein molecular marker; Lane TL: Total protein lysate after sonication; Lane FT: Flow through from the His-tagged column; Lane W1-2: Wash1 and 2 fractions; Lane E1-2: Elution fractions 1-2. Coomassie staining was used to visualise the proteins.

The total protein lysate (TL) indicates proteins present after sonication. Recombinant VP1 is shown by the protein band resolved at approximately 38 kDa. The flow through in lane FT indicates that some of recombinant VP1 protein was passed through the column without being bound to the Ni-IDA column, suggesting that the column may have reached its binding capacity. The column was washed twice in 1x LEW buffer. It can be observed in lane W1 that contaminating proteins were washed off the column including unbound recombinant VP1. Two proteins are eluted from the column (lane E1). The protein resolved at approximately 38 kDa is possibly recombinant VP1. The co-eluting protein resolving between 48 and 85 kDa is unidentified and present at a higher concentration than recombinant VP1. No proteins can be observed in the second elution fraction (lane E2).

3.3.6 Purification of recombinant 3C^{pro} under denaturing conditions

A scale up culture of 1 L was induced for 4 hrs and cells were harvested by centrifugation, resuspended in 1x LEW buffer and sonicated at 4°C. Sonicates were clarified by centrifugation and treated with 1x DSB. The treated samples were passed through a Ni-IDA column for purification under denaturing conditions. TL, FT, W1 and 2 and E1-3 samples

were collected during the purification and analysed by 15 % SDS-PAGE. Results are shown below in figure 3.6 below.

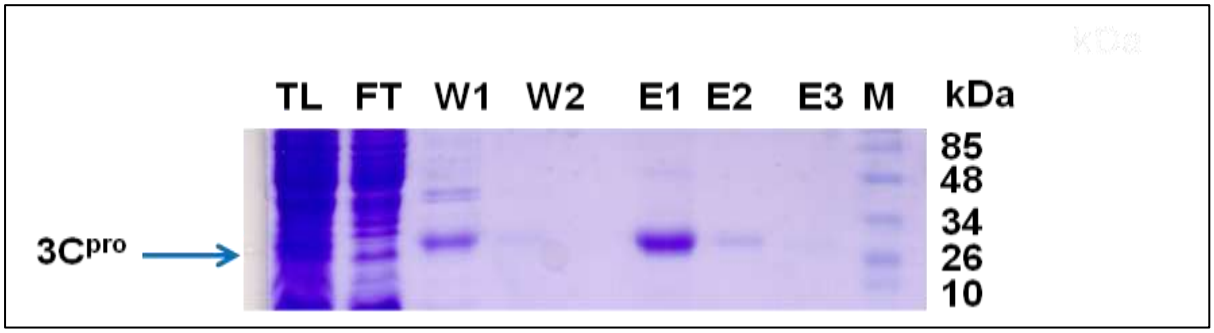

Figure 3.6: SDS-Page analysis of the purification of recombinant 3C^{pro} under denaturing conditions. Lane M: Prestained protein molecular marker; Lane E3-1: Elution fractions; Lane W2-1: Wash fractions; Lane FT: Flow through from the His-tagged column; Lane TL: Total protein lysate after sonication (TL). Coomassie staining was used to visualise the proteins.

The total protein lysate (TL) indicates all protein present after sonication. The flow through in lane FT indicates that some recombinant 3C^{pro} was passed through the column without being bound to the Ni-IDA column as shown by the protein band resolved at approximately 27 kDa, suggesting that the column may have reached its binding capacity. The column was washed twice in 1x DSB and it can be observed in lane W1 that contaminating proteins were washed off the column including unbound recombinant 3C^{pro}. Recombinant 3C^{pro} is eluted in lane E1 as shown by the protein band resolved at approximately 27 kDa with trace amounts of co-eluting proteins. Lane E2 indicates that some of recombinant 3C^{pro} is present in the second elution. Sample E1 was chosen for dialysis and immunisation of rabbits.

3.3.7 Dialysis of purified recombinant 3C^{pro}

In order to remove the urea in the 1.5 ml purified recombinant 3C^{pro} sample, dialysis was performed. The dialysed recombinant 3C^{pro} antigen (1 ml) was centrifuged, a sample of the supernatant was taken for analysis and the pellet was resuspended in 250 µl PBS. BSA standards were analysed alongside the dialysed and undialysed samples in order to determine the concentration of the purified antigen. The results are shown in figure 3.7 below.

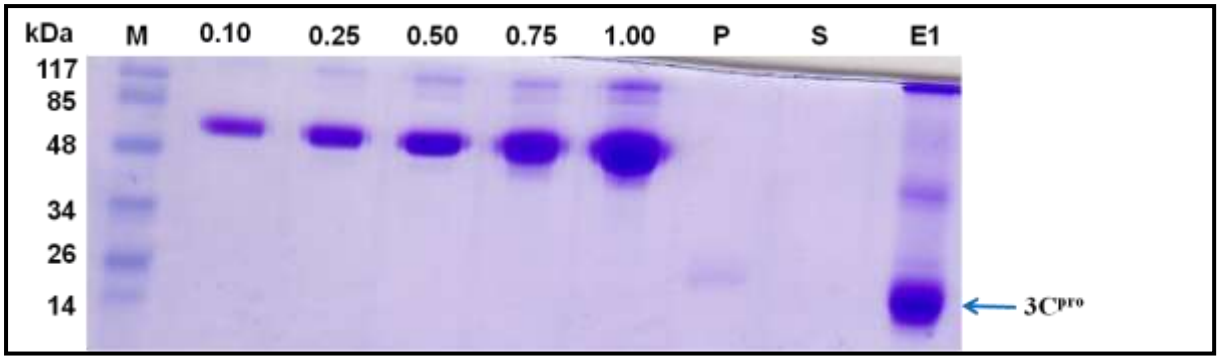

Figure 3.7: SDS-PAGE analysis of the dialysis of purified recombinant 3C^{pro} sample. Lane M: Prestained protein molecular marker; Lane 1-5: BSA standards 0.10-1.00 mg/ml; Lane P: 1:10 dilution of dialysed recombinant 3C^{pro} Pellet; Lane S: Supernatant of dialysed recombinant 3C^{pro}; Lane E1: Elution 1 sample of the purified recombinant 3C^{pro} before dialysis. Coomassie staining was used to visualise the proteins.

During dialysis it was observed that the purified recombinant 3C^{pro} formed a white precipitate. The precipitate was mixed with PBS present within the dialysis tubing to form a 1 ml suspension. The suspension was centrifuged, the supernatant and pellet were analysed by SDS-PAGE. A 1:10 dilution of dialysed pellet was made in order to avoid the sample from precipitating during SDS-PAGE analysis. Dialysed recombinant 3C^{pro} is present in the pellet as shown by the protein band resolved at approximately 27 kDa in lane P. No protein band is observed in lane S. Due to the sample precipitating out of solution, less amounts of the recombinant protein was observed after dialysis making it difficult to measure concentration of the dialysed sample using BSA standards. Likewise a nanodrop reading was performed to determine the concentration of the dialysed pellet and an average concentration reading of 0.35 mg/ml was obtained. However due to the sample precipitating out of solution, the reading from the nanodrop was considered not to be accurate. Because purified recombinant 3C^{pro} was in solution before dialysis, concentration was estimated for the sample using BSA standards. BSA standards in lanes 0.10-1.00 show that the purified sample before dialysis was approximately 0.75 mg/ml.

3.3.8 Time course induction study of recombinant VP1 (1-247)

Because recombinant VP1 co-purified with an unidentified protein, a different bacterial expression system was used. pETVP1 (1-741) was constructed and kindly donated by Dora Mwangola (B.Sc Honours student, Rhodes University). In order to determine the maximum expression time of recombinant VP1 (1-247), *E. coli* BL21 (DE3) cells harbouring pETVP1

(1-741) and pET22b+ were grown to mid-log phase and induced with 1 mM IPTG for 6 hrs. Samples were collected hourly and analysed by 12 % SDS-PAGE. Western analysis was conducted using anti-His_6 (2) antibodies (Roche, Mannheim, Germany). The results are shown in figure 3.8 A and B below.

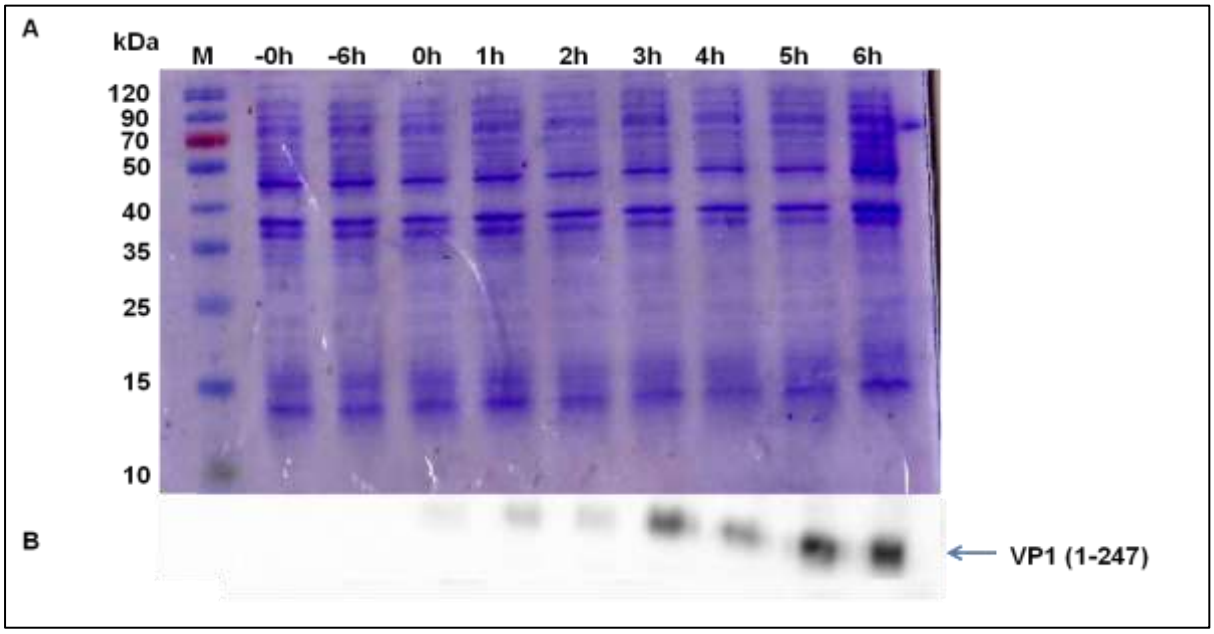

Figure 3.8 Panel A: Time course induction study of recombinant VP1 (1-247) expression. Cells were induced for 6 hrs and samples were collected and analysed with 12 % SDS-Page. Coomassie staining was used to visualise the proteins. **Panel B: Western analysis using anti-His_6 (2) antibodies.** Lane M: Prestained protein molecular weight marker in kDa; Lane -0 and -6h: Cells harbouring pET22b+; Lane 0h: Cells harbouring pETVP1 (1-741) at 0 hr; Lane 1h - 6h: cells expressing recombinant VP1 (1-247) 1 hr - 6 hr post-induction.

The molecular weight of recombinant VP1 (1-247) was calculated to be 35 kDa using the internet based programme ExPASy- compute pI/Mw tool (www.expasy.com). A protein band of this size was not observed by SDS-PAGE analysis as shown in Panel A. Western analysis was performed to detect the presence of recombinant VP1 (1-247) using anti-His_6 (2) antibodies (Panel B). Panel B shows a signal which increases in intensity between 1 and 6 hrs post-induction.

3.3.9 Solubility studies of recombinant VP1 (1-247)

In order to confirm the expression of recombinant VP1 (1-247) and determine if recombinant protein was present in the soluble or the insoluble fraction, a 40 ml induction study was carried out for 6 hrs and cell cultures were harvested for solubility studies. Cells were

resuspended in PBS and sonicated. A sample was taken to represent the total protein TP and the remaining sample was harvested by centrifugation to obtain the soluble (S) and insoluble (P) fractions. The total protein (TP), supernatant (S), and pellet (P) samples were analysed by 12 % SDS-PAGE. Western analysis was conducted using anti-His_6 (2) antibodies (Roche, Mannheim, Germany). The results are shown in figure 3.9 A and B below.

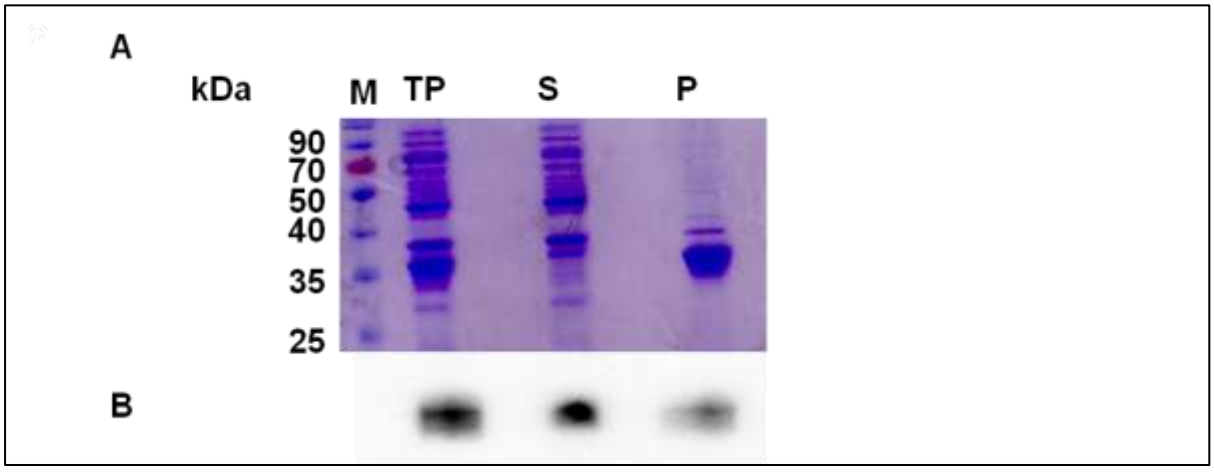

Figure 3.9: Solubility analysis of recombinant VP1 (1-247). Panel A: Cells expressing recombinant VP1 (1-247). Lane M: Prestained protein molecular weight marker in kDa; Lane TP: Total protein lysate; Lane S: Supernatant (soluble) fraction; Lane P: Pellet (insoluble) fraction. Coomassie staining was used to visualise the proteins. **Panel B: Western analysis using anti-His_6 (2) antibodies.** Lane TP: Total protein lysate; Lane S: Supernatant (soluble) fraction; Lane P: Pellet (insoluble) fraction.

The solubility study resulted in the presence of two protein bands being resolved between 35 and 40 kDa in all fractions. The lower protein band is predominantly present in the insoluble fraction with trace amounts of the protein band present in the soluble fraction as shown in lanes P and S. The upper protein band is more concentrated in the soluble fraction than in the insoluble fraction as seen in lane S and P respectively. Western analysis was conducted using anti-His_6 (2) antibodies (Panel B) in order to confirm the presence of a 6x His-tagged protein. A signal is detected in all three lanes. The signal is less intense in lane P, suggesting that more of the recombinant protein is present in the soluble fraction. An attempt was made to solubilise the protein with Sarcosyl and treatment had no effect on the solubility of the protein (data not shown).

Since the two protein bands resolved were similar in size (figure 3.9), an attempt to separate the protein bands by longer electrophoresis time was carried out. A 1:20 dilution was

performed on the insoluble fraction in lane P and increasing volumes (2 µl-8 µl) of the diluted sample were resolved by 12 % SDS-PAGE for an additional 30 min. The gel was transferred onto nitrocellulose membrane and Western analysis using anti-His_6 (2) antibodies was conducted. The results are shown in figure 3.10 A and B below.

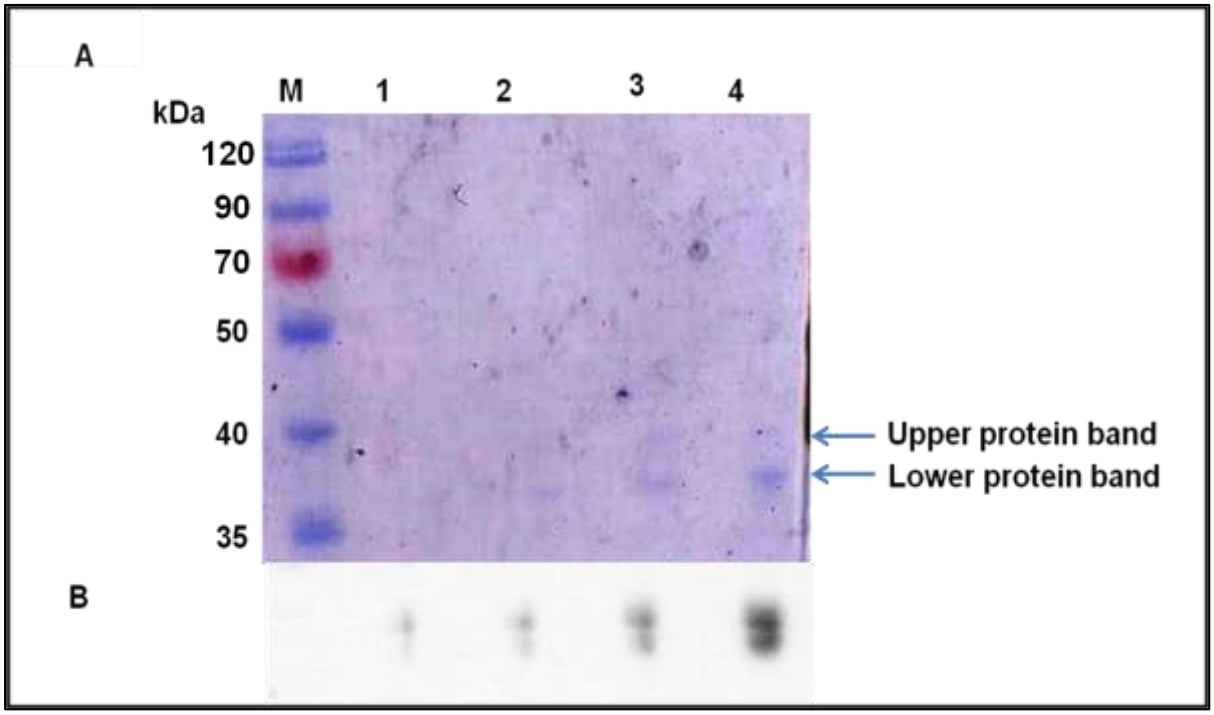

Figure 3.10: Panel A: SDS-PAGE analysis of different volumes of 1:20 dilution of the insoluble fraction. Panel B: Western analysis of the 1:20 dilution of the insoluble fraction using anti-His_6 (2) antibodies. Lane M: Prestained protein molecular weight marker in kDa; Lane 1: 2 µl of 1:20 insoluble fraction dilution; Lane 2: 4 µl of 1:20 insoluble fraction dilution; Lane 3: 6 µl of 1:20 insoluble fraction dilution; Lane 4: 8 µl of 1:20 insoluble fraction dilution.

The longer electrophoresis time results in a greater separation of the two proteins (Panel A). A double signal is detected for both bands by Western analysis using anti-His_6 (2) antibodies in all lanes. The signal for higher molecular weight protein is more intense than that for the lower protein band. An increase in protein signal for both protein bands is observed with an increase in sample volume. It was initially suspected that the lower protein band is recombinant VP1 (1-247) however based on these results, it is still not clear which protein band represents recombinant VP1 (1-247).

3.4 Discussion

This chapter describes the preparation of antigen against recombinant TMEV VP1, VP1 (1-247) and $3C^{pro}$ in order to generate polyclonal antibodies against these proteins.

A time course induction study was performed in order to determine the maximum expression time for recombinant VP1. Expression was observed at 2, 4 and 6 hrs post-induction and Western analysis using anti-His_6 (2) antibodies confirmed the presence of recombinant VP1. A 6 hr induction of recombinant VP1 was conducted for solubility studies and purification. A similar study was carried out for recombinant $3C^{pro}$ and a 4 hr induction of recombinant $3C^{pro}$ was conducted for solubility studies and purification.

Different expression systems can be used for heterologous protein expression. Bacterial, mammalian, and baculovirus expression systems are the most commonly used. Baculovirus vectors are widely used for heterologous expression of protein in insect cells (Luckow, 1991; Miller, 1988). The principle of the system is based on the capability of a baculovirus to infect and multiply in cultured insect cells. Post-translational modifications which are encountered in mammalian cells such as glycosylation and phosphorylation also occurs in insect cells. However the preparation of a baculovirus system is expensive and more challenging than a bacterial system. Mammalian cells are often the best host for expression of recombinant vertebrate proteins even though they have very low expression levels. This system is favoured because it produces the same post-translational modifications and is able to recognise the same signal for synthesis, processing and secretion utilised in the organism from which the sequence was originally obtained. However, a mammalian system yields low levels of protein which is not favoured for some downstream applications (Verma et al., 1998).

Recombinant VP1 and $3C^{pro}$ were successfully expressed in a bacterial system. Bacterial expression systems for heterologous protein production are widely used because of high productivity and low cost (as reviewed by Terpe, 2006). *E. coli* is the most widely used host due to its ability to grow rapidly and at high densities on inexpensive substrates and a large number of vectors and mutant host strains which are easily accessible. (as reviewed by Baneyx, 1999). For these reasons, a bacterial expression system was used in this study. An *E. coli* expression strain should lack most harmful natural occurring proteases, retain the expression plasmid in a stable condition and offer genetic elements which will enable high expression levels of target genes (Sørensen and Mortensen, 2005). There are many advantages of using *E. coli* as a host for production of heterologous proteins, however not every gene can be highly expressed in the bacterium. This may be caused by a number of factors including stability and translation efficiency of mRNA, possible toxicity of protein to host and presence of rare *E. coli* codons on the foreign gene. There are drawbacks in using a

bacterial expression system. The inability to perform post-translational modifications of proteins such as glycosylation is one of the major drawbacks which make it a challenge to produce biologically active proteins. Other drawbacks include the lack of secretion mechanism to release protein into the culture medium efficiently and limited resources to facilitate the formation of disulphide bonds (as reviewed by Jana and Deb, 2005). Because the protein expressed in this study was used for immunisation purposes and not functional assays, these drawbacks did not affect the study.

In order to determine whether recombinant VP1 and $3C^{pro}$ were present in the soluble or insoluble fractions, solubility studies were conducted. Recombinant VP1 was present in approximately equal amounts in the soluble and insoluble fraction before treatment with Sarcosyl. Sarcosyl treatment was successful in releasing the protein from the insoluble fraction into the soluble fraction, suggesting that some of the protein was membrane associated.

Based on the presence of recombinant VP1 protein in the soluble fraction, purification was carried out under native conditions. Two protein bands co-eluted from the column during the first elution. The protein resolved at approximately 38 kDa was suspected to be recombinant VP1. The co-eluting protein resolved between 48 and 85 kDa was unidentified and present at a higher concentration than recombinant VP1.

In an attempt to separate the two proteins, size exclusion chromatography was performed. The technique separates molecules based on pore sizes, depending on the size of the proteins (Yau *et al*., 1937). Different fractions were collected and analysed by SDS-PAGE. No protein bands were observed on the gel and the technique was not repeated due to time constraints. It was suggested that the co-eluting protein may be a molecular chaperone interacting with recombinant VP1 (data not shown). Both Hsp 90 and Hsp 70 have been found to play a role in the picornavirus assembly process. Immunoprecipitation experiments showed that the *Enterovirus* P1 precursor protein co-precipitates with Hsp 90 and 70 (Macejak and Sarnow, 1992; Geller *et al*., 2007). Furthermore, there is redistribution of Hsp 90 and Hsp 70 in TMEV-infected cells and inhibitors of Hsp 90 prevent the development of cytopathic effect (Mutsvunguma *et al*., 2011). However, Western analysis using anti-Hsp 70 antibodies failed to detect the co-eluting protein (data not shown) and its identity still remains unknown.

Recombinant $3C^{pro}$ solubility studies showed that the recombinant protein was abundant in the insoluble fraction before treatment with Sarcosyl. Treatment with Sarcosyl was unable to

release the protein into the soluble fraction presumably because of the formation of insoluble inclusion bodies which are cytoplasmic or nuclear aggregations of proteins in a host cell. The formation of inclusion bodies may be due to a variety of factors such as protein misfolding and over expression (Fink, 1998; Palomares *et al*., 2004). These misfolded or over expressed proteins accumulate in intracellular aggregates by an unknown mechanism (Palomares *et al*., 2004). It is unknown whether inclusion bodies are formed as a result of hydrophobic interactions between exposed regions of an unfolded protein or by grouping mechanisms. Incorrect formation of disulphide bonds for proteins with cysteine residues in the reducing environment of *E. coli* cytoplasm may add to misfolding and formation of inclusion bodies (Carrio and Villaverde, 2002; www.**qiagen**.com/Knowledge-and-Support/Resource-Center/, accessed: 08-03- 2013). There are seven cysteine amino acid residues present in TMEV GDVII $3C^{pro}$ sequence, suggesting that disulphide bonds may occur between cysteine residues leading to protein aggregation. The formation of protein aggregates can be reduced by controlling certain parameters during protein expression such as growth temperature, expression rate and host metabolism. Temperature affects expression levels and protein solubility, a decrease in growth temperature will lead to lower expression levels and higher protein solubility. On the other hand cultures can be grown to a higher cell density before induction, and expression time can be reduced. Expression levels can also be significantly reduced by the reduction in IPTG concentration from 1mM to 0.5mM or less. Finally the host strain can be changed due to the ability of certain host strains to express some proteins better than others in a stable condition and allow for higher expression levels before the formation of inclusion bodies (Jonasson *et al*., 2002).

Based on the presence of recombinant $3C^{pro}$ in the insoluble fraction, purification was carried out under denaturing conditions. The recombinant protein was denatured using 8M urea. Guanidine hydrochloride can also be used for denaturing proteins for purification. Guanidine hydrochloride is a chaotropic protein denaturant, meaning that it disrupts protein structures by transferring apolar groups to water in order to reduce the hydrophobic effect of insoluble proteins. When used at lower concentration, guanidine hydrochloride assists the refolding of denatured proteins (www.scbt.com , accessed 10-03- 2013). Recombinant $3C^{pro}$ was eluted in the first fraction with trace amounts of co-eluting proteins, and this fraction was selected for dialysis and immunisation of rabbits.

For immunisation purposes, it was necessary to remove urea present in the purified $3C^{pro}$ sample. During dialysis the purified $3C^{pro}$ antigen was observed to form a white precipitate.

This complicated protein concentration measurements using BSA standards and SDS-PAGE, and also nanodrop readings. However based on the amount of visible protein present before dialysis, it was decided that the precipitate should be used for immunisation of rabbits. When there is instability between intra- and inter-molecular interactions during protein folding, aggregation will occur during the refolding process. Aggregation normally occurs during dialysis because the protein of interest is exposed to intermediate concentration of denaturant for a certain period of time which may cause the protein to lose its stability. Misfolding of proteins may lead to the exposure of buried hydrophobic regions which cause the insoluble protein to aggregate. Certain methods have been proposed in order to avoid aggregation during the refolding process. These methods include slow continuous or discontinuous addition of protein to refolding buffer whereby there is time given between the additions of protein to allow for folding past the early stages when the protein is found to be at risk of aggregation (as reviewed by Clark, 1998). Another method involves folding the protein by dilution to final concentrations of the denaturant that are high enough to solubilise aggregates but low enough to induce proper folding of the protein, a study using this method was able to show the successful oxidative renaturation of lysozyme at a high concentration of approximately 5mg/ml by the addition of non-denaturing concentration of the chaotropic agent guanidinium hydrochloride (as reviewed by Clark, 1998).

Immunisation companies such as Proteintech^{TM} (www.ptglab.com, accessed: 14-03-2013) and Prosci.inc (http://www.prosci-inc.com, accessed: 14-03-2013) accept precipitated protein antigen for immunisation of rabbits, because immunising with insoluble protein produces antibodies which are more effective than antibodies arising from immunisation with a soluble protein. A precipitated antigen is suspected to provide long-term antigen storage for continuing stimulation of the immune system. It may also be easier for antigen-presenting cells such as macrophages to engulf precipitated antigen (www.ptglab.com, accessed: 14-03-2013). Precipitated $3C^{pro}$ was sent off for immunisation of rabbits.

Because recombinant VP1 co-purified with an unidentified protein, a different bacterial expression system was used. VP1 was C-terminally truncated to produce recombinant VP1 (1-247). The recombinant protein was expressed in the pET22b+ expression vector. The size of the recombinant protein was estimated to be 35 kDa. A protein band of that size was not observed by SDS-PAGE analysis of the time course induction study of the recombinant protein. However Western analysis showed detection of a 6x His-tagged protein at approximately 35 kDa. A signal increasing in intensity was observed at each time point. The

results suggest that recombinant VP1 (1-247) was being expressed in low levels possibly due to the presence of rare *E. coli* codons. The recombinant protein might have been unstable or considered toxic in an *E. coli* host system.

When protein expression is initiated by an inducer, large quantity of heterologous mRNA is produced. *E. coli* uses a precise subset of the 61 amino acid codons for the production of mRNA. Rare codons occur in genes expressed in low levels, whereas major codons occur in highly expressed genes (Kane, 1995). The expression of heterologous proteins may be decreased when the gene encodes numerous rare *E. coli* codons (Novy *et al*., 2001). Presence of rare codons leads to problems such as, delayed translation rates of the target gene and undetectable protein bands of expressed protein during analysis (as reviewed by Chen and Texada, 2006).

The FMDV VP1 gene has been widely studied for development of new vaccines. High expression levels of the protein are important for this application. Previous attempts to express FMDV type A VP1 in a bacterial system resulted in low expression levels of the protein, therefore codon optimisation was carried out in order to achieve maximum expression levels of recombinant VP1 for purification. Codons were optimised using GeneOptimizer software and synthesised taking into account the codon bias of the host. Synthesised products were cloned and expressed in pET-28a. Higher expression levels were achieved with 36 % of recombinant VP1 accounted for. The recombinant protein was successfully purified and used as antigen for further studies. The results from this study revealed that codon optimisation is a useful method in protein expression (Liu *et al*., 2011). Another example is the nucleoprotein antigen for Crimean-Congo Haemorrhagic Fever virus (CCHFV) which was prepared for expression using codon optimisation. The CCHFV nucleoprotein coding sequence was optimised using Optimum Gene software and synthesised. The synthesised gene was expressed in the pCold TF expression vector. The pCold TF expression system expresses protein at a lower temperature and uses a trigger factor (TF) chaperone as a solubilising tag which assists with folding and solubility of expressed protein (www.takarabioeurope.com, accessed: 17-03-2013). Higher expression levels were achieved from the synthesised gene in a bacterial expression system. The expressed protein was found to be insoluble and was purified under denaturing conditions and used as antigen to test for cross-reactivity against antibodies in recovering CCHFV patients by enzyme-linked immunosorbent assay (ELISA) (Samudzi *et al*., 2012). According to Zhang *et al*., 1991, there are eight rare codons of *E. coli* namely arginine (AGG, AGA,

CGA and CGG), isoleucine (AUA), leucine (CUA), proline (CCC) and serine (UCG). Rare *E. coli* codons were identified on TMEV GDVII VP1 coding sequence. Five rare codons for arginine (GGA) and 2 rare codons for CGG were identified. Two rare codons for isoleucine and thirteen rare codons for proline were identified. This suggests that low expression levels of recombinant VP1 (1-247) observed may be due to the presence of these particular rare *E. coli* codons in the TMEV VP1 (1-247) gene, however this is not likely as recombinant VP1 was successfully expressed from pQE-80L in *E. coli* JM109 cells.

There are different types of vector systems which can be used for sufficient expression of recombinant proteins. Fusion protein consists of a partner or a tag which is linked upstream or downstream from the target protein coding sequence by a restriction site. Most fusion partners are utilized for specific affinity purification approaches (Sørensen and Mortensen, 2005). The most commonly used tags are the polyhistidine tag (His-tag), which works efficiently with immobilised metal affinity chromatography and the glutathione S-transferase (GST) tag, which is used for purification on glutathione based resins. Other tags include the *E. coli* maltose binding protein (MBP) and *E. coli* N-utilizing substance A (NusA) which are commonly used when expressing proteins which form inclusion bodies (Sørensen and Mortensen, 2005). The pQE-80L expression vector has been used successfully in our laboratory for the expression of TMEV 2C and 3D. TMEV 2C was cloned and expressed in pQE-80L for preparation of antibodies against the non-structural 2C protein. These antibodies were used to identify the site of replication in TMEV-infected cells (Jauka *et al*., 2010). Therefore pQE-80L was chosen for the expression of recombinant VP1 and $3C^{pro}$. Because recombinant VP1 co-purified with an unknown protein when using pQE-80L, the pET expression system was chosen for expressing recombinant VP1 (1-247). This system has been widely used for cloning and expression of recombinant proteins. The pET expression system was also chosen because it has been widely used for the preparation of recombinant FMDV VP1. Shi *et al*., (2012), were able to successfully clone and express FMDV O-DG-2005 VP1 in pET-28a. FMDV type A VP1 was codon optimised and prepared in pET-28a for purification. The antigen was used for further development studies in vaccination production (Liu *et al*., 2011).

Solubility studies were carried out in order to confirm the expression of recombinant VP1 (1-247) and to determine whether the recombinant protein was present in the soluble or insoluble fraction. The solubility study resulted in the presence of two protein bands being resolved between 35 and 40 kDa. The lower protein band was predominantly present in the

insoluble fraction with less of the protein being present in the soluble fraction. The upper protein band was more concentrated in the soluble fraction with less being present in the insoluble fraction. Initial Western analysis experiments showed detection of a single 6x His-tagged protein in the total protein lysate, supernatant and pellet fractions.

Because the protein bands were of similar size, it was uncertain which of the two protein bands detected by Western analysis represented recombinant VP1 (1-247). A longer electrophoresis time resulted in greater separation of the two proteins. Western analysis showed the presence of two protein signals and the signal for the higher molecular weight protein was more intense than that for the lower protein band.

The presence of two protein bands resolved by SDS-analysis may be due to degradation of recombinant VP1 (1-247) caused by freeze-thawing of sample before analysis. Protein stability is influenced by a number of factors, freeze-thaw cycles being one of the factors. Repeated freeze-thaw cycles degrade proteins by disrupting the stability of the protein structure. It is best to aliquot protein samples used for analysis in order to avoid protein degradation (www.uni-leipzig.com, accessed: 11-03-2013).

The presence of two protein bands resolved may also have been caused by the presence of the reducing agent, β-mercaptoethanol, in SDS-loading buffer. Reducing agents break disulphide bonds in proteins which disrupt the tertiary structure of the protein (www.uni-leipzig.com, accessed: 11-03-2013). In a similar study, it was shown that the denaturation of a recombinant protein in the presence of a reducing agent such as DTT results in the formation of two protein bands of similar size resolved during SDS-PAGE analysis. In the absence of a reducing agent, the recombinant protein is resolved as a single band (Jacqueline van Marwijk, Ph.D. dissertation, University of the Free State, 2010). Due to time constraints, the effect of β-mercaptoethanol on recombinant VP1 (1-247) was not investigated.

In conclusion, purified recombinant $3C^{pro}$ was sent off for immunisation of rabbits. Because recombinant VP1 co-purified with an unidentified protein and recombinant VP1 (1-247) protein band could not be identified by SDS-PAGE and Western analysis, recombinant VP1 or VP1 (1-247) antigen was not sent off for immunisation of rabbits. The next chapter involves the testing of anti-TMEV $3C^{pro}$ antibodies for detection of $3C^{pro}$ by Western analysis and indirect immunofluorescence.

Chapter 4: Testing of anti-TMEV $3C^{pro}$ antibodies for detection of bacterially-expressed antigen and virally-expressed protein in TMEV-infected BHK-21 cells

4.1 Introduction

This chapter describes the testing of anti-TMEV $3C^{pro}$ antibodies for the ability to detect bacterially expressed antigen and virally-expressed protein in TMEV-infected BHK-21 cells.

Recombinant $3C^{pro}$ was successfully expressed, purified under denaturing conditions and used for immunisation as described in chapter 3.

Day 0 (pre-immune), 28 and 43 serum was received and tested for antibody activity. Day 43 antiserum was tested for the detection of bacterially expressed antigen using Western analysis. Increasing amounts of purified recombinant $3C^{pro}$ antigen was resolved by SDS-PAGE and probed with different dilutions of day 43 antiserum. A negative control was prepared using pre-immune serum in order to test for cross reactivity of antibodies against the antigen used for immunisation. Crude and pre-cleared antiserum was used for analysis.

The antibodies were also tested for the detection of virally-expressed $3C^{pro}$ in infected cell lysates by Western analysis. The protein was virally-expressed by infecting BHK-21 cells with TMEV and preparing cell lysates using Triton X-100 at 5 hrs post-infection. Anti-TMEV 2C antibodies were used as a positive control in order to determine if the cells were successfully infected with TMEV. Pre-immune serum was used as a negative control to determine any cross reactivity of antibodies in the serum against virally-expressed $3C^{pro}$.

For localisation of $3C^{pro}$ in infected BHK-21 cells, indirect immunofluorescence (IF) was performed using anti-TMEV $3C^{pro}$ antibodies at dilutions of 1:500 and 1:1000, and Alexa-Fluor 488-conjugated anti-rabbit secondary antibodies at a dilution of 1:500. Proteins were detected by fluorescence and confocal microscopy. Indirect IF is a procedure in which cells are stained with a primary antibody specific for the protein or molecule of interest. The primary antibody is then bound at the constant region by a secondary antibody which is tagged with a fluorescent dye. The cells are then viewed using confocal or fluorescence microscopy to detect the region of staining by the primary antibody (Harlow and Lane, 1988; Johnson *et al*., 1981). Negative controls were performed by staining TMEV-infected cells

with anti-TMEV $3C^{pro}$ antibodies alone and Alexa-Fluor 488-conjugate anti-rabbit secondary antibodies alone. Anti-TMEV 2C and P1 antibodies were used to stain the cells in order to determine if they were successfully infected by the virus.

The specific objectives were:

- To detect bacterially expressed antigen using anti-TMEV $3C^{pro}$ antibodies by Western analysis
- To detect virally- expressed $3C^{pro}$ in infected BHK-21 cell lysates by Western analysis using anti-TMEV $3C^{pro}$ antibodies
- To localise virally-expressed $3C^{pro}$ in infected BHK-21 cells by indirect immunofluorescence and confocal microscopy

4.2 Methods and Materials:

4.2.1 Testing of Day 0 and Day 43 serum

Antiserum collected at day 0 (pre-immune serum), 28 and 43 post immunisation was received 6 weeks after the purified $3C^{pro}$ antigen had been sent off for immunisation of rabbits. The day 43 antiserum (anti-TMEV $3C^{pro}$) was tested for its ability to recognise bacterially expressed $3C^{pro}$. Increasing amounts of purified recombinant $3C^{pro}$ antigen in doubling dilutions were resolved by 15 % SDS-PAGE. The proteins were transferred individually onto nitrocellulose membrane (Bio-Rad, USA), which was probed with pre-immune serum at a dilution of 1:5000, and anti-TMEV $3C^{pro}$ at dilutions of 1:5000, 1:10 000, 1:50 000 and 1:100 000 respectively as described in section 3.2.3.

4.2.2 Pre-clearing of anti-TMEV $3C^{pro}$ using E. coli JM109 cell lysate

E. coli JM109 cells were grown in LB overnight at 37°C. A 2 ml aliquot of cells was collected and sonicated 12 times for 15 sec at 4°C on ice. The cells were harvested by centrifugation at 11100 x g for 2 min. The supernatant was discarded and the pellet was washed with PBS and centrifuged at 11100 x g for 2 min. The pellet was resuspended in a 1:10 dilution of crude day 43 antibody in PBS. The suspension was left to shake for 2 hrs at RT and centrifuged at 11100 x g for 2 min. The supernatant was collected and used for Western analysis of the bacterially expressed antigen as pre-cleared anti-TMEV $3C^{pro}$ antibodies.

4.2.3 Mammalian cell lines and Culture conditions

BHK-21 cells were a kind gift from Professor Martin Ryan (University of St Andrews, UK) and were the cell line used in this study. Cells were maintained in HEPES-buffered Dulbecco modified Eagle's medium (DMEM, Lonza Group Ltd, Basel, Switzerland) containing 5 % fetal calf serum (FCS, Lonza Group Ltd, Basel, Switzerland) and 1 % penicillin, streptomycin and fungizone (PSF, Lonza Group Ltd, Basel, Switzerland) in a 25 cm^3 vented flasks incubated at 37°C with 10 % CO_2.

4.2.4 Subculturing of BHK-21 cells

Cells at 100 % confluency were subcultured by discarding the old medium in the flask and rinsing the cells with 2 ml PBS. Trypsin was added to the cells to interrupt the cell matrix and cell-cell interactions. Cells were incubated at 37°C for 1 min to allow detaching from the surface and 2 ml of complete medium was added to cells. Cells were seeded into 5 ml of fresh complete medium in new 25 cm^3 vented flasks at a dilution of 1:10.

4.2.5 Cryopreservation of BHK-21 cells

Cells were preserved by subculturing a confluent 25 cm^3 flask into 10 x 25 cm^3 flasks. At 100 % confluency, cells were trypsinised and resuspended in 1 ml completed medium per flask. Cells were pooled into a sterile 20 ml Falcon tube and centrifuged at 200 x g for 1 min. The pellet was resuspended in 10 ml cryopreservation solution (20 % FCS, 10 % glycerol, 1 % PSF, 69 % DMEM). Cells were aliquoted into 1 ml cryovials and stored at -80°C.

4.2.6 Preparation of TMEV stock

A 100 % confluent 25 cm^3 vented flask was subcultured into a 75 cm^3 vented flask with 10 ml complete medium. When cells reached 100 % confluency, they were infected with TMEV stock (previously prepared in our laboratory). Cells were incubated at RT with shaking for 1 hr to allow the virus to be adsorbed. 9 ml of serum-free DMEM was added and cells were incubated overnight at 37°C. Cells lysis was accomplished by three cycles of freeze-thawing and then collected in a 15 ml falcon tube. Cell debris was pelleted at 200 x g for 1 min and the supernatant was aliquoted into 1 ml cryovials and stored at the - 80°C.

4.2.7 Preparation of BHK-21 cell lysate supernatants for Western analysis

A 100 % confluent 25 cm^3 flask was subcultured into two 75cm^3 flask with 10 ml complete medium, and incubated at 37°C with 10 % CO_2 until 100 % confluency. Old medium was discarded and cells were rinsed with serum-free DMEM. One flask was infected with 1 ml TMEV at an estimated multiplicity of infection (MOI) of 50 and the other flask was mock-infected with 1 ml of serum-free DMEM. The flasks were shaken at RT for 1 hr and topped up with 5 ml serum-free DMEM before being incubated for a further 5 hrs at 37°C with 10 % CO_2. Cells were collected by trypsinisation and harvested by centrifugation at 200 x g for 1 min. Cells were rinsed with PBS to remove the excess trypsin and resuspended in 100 µl of lysis buffer [50 mM Tris-HCl, (pH 7.5), 150 mM NaCl, 1 % Triton X-100, 1 mM DTT, 1 mM PMSF, 1x EDTA-free protease inhibitor cocktail (PIC) (Roche, Mannheim, Germany)] and kept on ice for 30 min with vigorous vortexing every 5 min. Cells were then passed through a 25-gauge needle 25 times and centrifuged at 11100 x g for 1 min. The supernatant was collected and analysed by 15 % SDS-PAGE and Western analysis using anti-TMEV $3C^{pro}$ antibodies.

4.2.8 Preparation of total BHK-21 cell protein for Western analysis

Cells were prepared as described in section 4.2.7. Cells were rinsed with PBS to remove the excess trypsin and resuspended in 200 µl of PBS. The suspension was boiled for 5 min in 5x SDS sample and analysed by 15 % SDS-PAGE and Western analysis using anti-TMEV $3C^{pro}$ antibodies.

4.2.9 Preparation of BHK-21 cells for indirect immunofluorescence

Cells were grown to 90 % confluency on ethanol-sterilised 13 mm glass coverslips in a 6-well plate with complete medium. Old medium was discarded and cells were rinsed with serum-free DMEM. Cells were infected with TMEV stock diluted 1:10 in serum-free DMEM (final volume of 1 ml) at an estimated MOI of 10. Cells were mock-infected for controls with serum-free DMEM. The cells were incubated at 37°C for 1 hr with shaking. The virus was removed and 2 ml serum-free DMEM was aliquoted into each well and the plates were incubated at 37°C for a further 5 hrs to allow for the expression of viral proteins. The

medium was removed and cells were rinsed with PBS and fixed with 4 % paraformaldehyde for 5 min with shaking at RT. Coverslips were rinsed with PBS and transferred into a 24-well plate for IF staining.

4.2.10 Indirect immunofluorescence staining of BHK-21 cells

Cells were permeabilised with PB (10 % sucrose, 0.5 % NP-40 in PBS) for 20 min with shaking at RT and blocked with 2 % blocking solution (2 % BSA in PBS) for 1 hr with shaking at RT. Cells were washed twice for 10 min in wash buffer (0.1 % Tween-20 in PBS) and incubated with anti-TMEV $3C^{pro}$, anti-TMEV 2C and anti-TMEV P1 antibodies (table 4.1) prepared in blocking solution for 1 hr with shaking at RT. Cells were washed twice for 10 min in wash buffer and incubated in species-specific Alexa-Fluor 488-conjugated secondary antibodies (Molecular probes through Invitrogen, USA) for 30 min. Cells were washed three times with the second wash containing 0.8 µg/ml of 4', 6-Diamino-2, phenylindole dihydrochloride (DAPI, Sigma, St Louise, USA) in order to stain the nucleus. Coverslips were then mounted onto glass slides using Dako fluorescent Mounting Medium (Dako North America, Inc, CA, USA) and stored at 4°C for fluorescence and confocal microscopy. For negative controls, cells were stained with anti-TMEV $3C^{pro}$ antibodies alone at a dilution of 1:1000 and Alexa-Fluor 488-conjugated anti-rabbit secondary antibodies alone at a dilution of 1:500.

Table 4.1: Detailed description of primary antibodies utilised in IF staining.

Antibody	Dilution	Type animal	Source
Anti-TMEV $3C^{pro}$	1: 500; 1: 1000	Polyclonal Rabbit	Boitumelo Moetlhoa (R.U)
Anti-TMEV-2C	1:1000	Polyclonal Rabbit	Jauka *et al.*, 2010
Anti-TMEV P1	1:1000	Monoclonal Mouse	Prof Lipton (U. Of Chicago)

4.2.11 Fluorescence and Confocal microscopy and image acquisition

Cells were visualised using an inverted LSM 510-meta confocal laser scanning microscope and the Zeiss Axiovert.A1 Fluorescence LED microscope (Carl Zeiss, Germany) using the 63x oil immersion objective lens. The Helium/neon and argon lasers at wavelengths 488 nm and 405 nm were used to excite Alexa-Fluor 488 and DAPI respectively. All images were

analysed using the Axiovision LE or SE freeware software (Carl Zeiss, Germany) and processed using Microsoft Office PowerPoint 2007.

4.3 Results

4.3.1 Detection of purified recombinant 3C^{pro} antigen using anti-TMEV 3C^{pro} antibodies

To test for cross reactivity of antibodies against the antigen used for immunisation, Western analysis was conducted using the pre-immune serum at a dilution 1:5000. Crude anti-TMEV 3C^{pro} antibodies were tested by Western analysis using 1:5000, 1:10 000, 1:50 000 and 1:100 000 dilutions on increasing amounts of the purified antigen. The results are shown in figure 4.1 below.

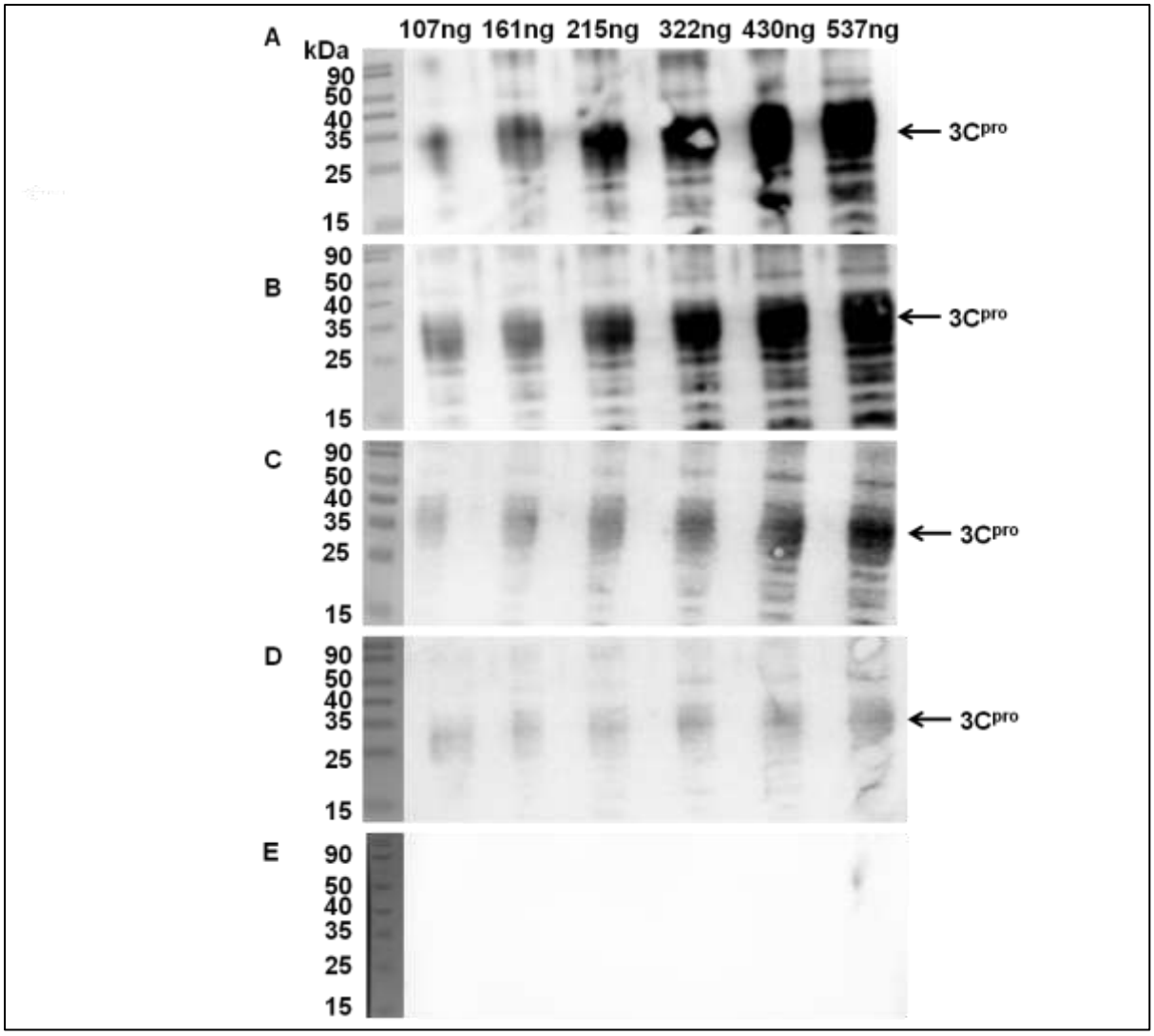

Figure 4.1: Detection of increasing amounts of purified $3C^{pro}$ using crude anti-TMEV $3C^{pro}$ diluted at 1:5000(A), 1:10 000 (B), 1: 50 000 (C), 1:100 000 (D) and pre-immune serum diluted 1:5000 (E).

Figure 4.1 shows detection of a protein of approximately 27 kDa with other contaminating protein bands (Panels A to D). There is an increase in signal intensity with an increase in amount of antigen loaded. The signal decreases in intensity with an increase in antibody dilution. In Panel E, increasing amounts of purified recombinant $3C^{pro}$ antigen were probed using a 1:5000 dilution of pre-immune serum. No detection of bacterial proteins is observed in this panel as expected. The results suggest that anti-TMEV $3C^{pro}$ antibodies can detect 107ng of bacterially expressed antigen after a 1 min exposure at a dilution of 1:100 000.

4.3.2 Detection of purified 3C^{pro} antigen using pre-cleared anti-TMEV 3C^{pro} antibodies

Because contaminating proteins were detected with crude antiserum, pre-clearing with *E. coli* JM109 cell lysates was performed as described in section 4.2.2. This was done in attempt to reduce the detection of non-specific protein bands. The results are shown in figure 4.2 A and B below.

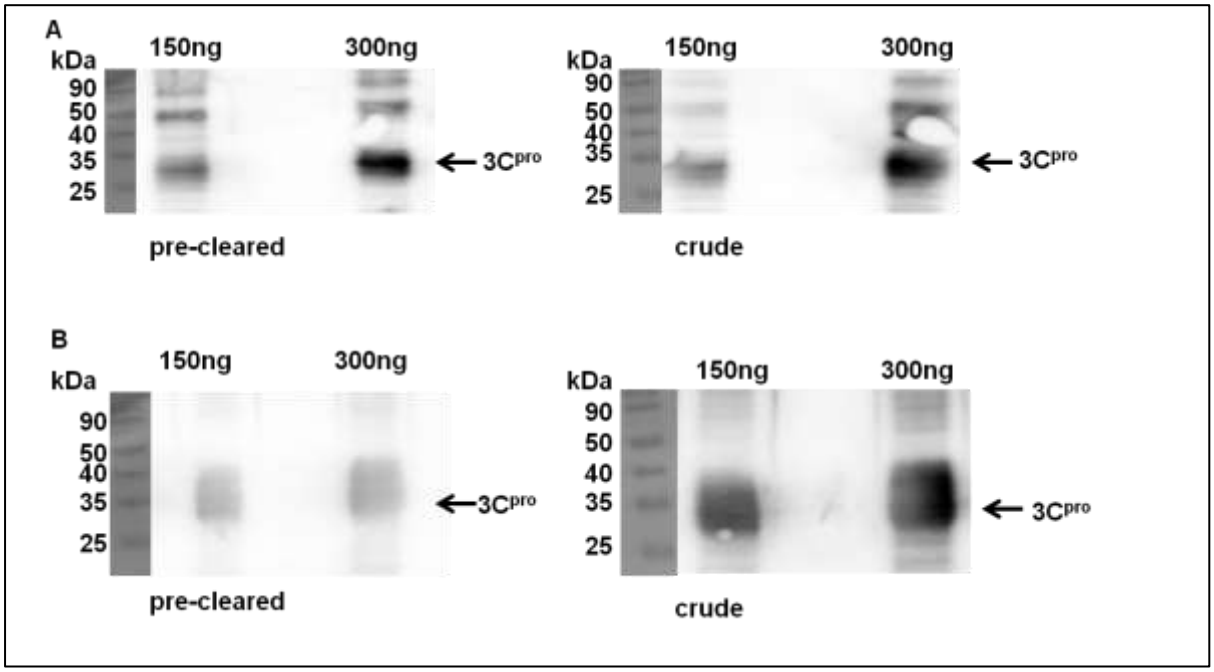

Figure 4.2: Western analysis comparing the detection of purified recombinant 3C^{pro} antigen using pre-cleared and crude anti-TMEV 3C^{pro} antibodies at different dilutions. Panel A: Detection of 150 ng and 300 ng of purified recombinant 3C^{pro} antigen using pre-cleared and crude anti-TMEV 3C^{pro} antibodies at a dilution of 1:1000. **Panel B:** Detection of 150 ng and 300 ng of the purified recombinant 3C^{pro} antigen using pre-cleared and crude anti-TMEV 3C^{pro} antibodies at a dilution of 1:5000

The results show a reduction in the detection of contaminating protein bands at both the 1: 1000 and 5000 dilutions when pre-cleared anti-TMEV 3C^{pro} antibodies were used compared to crude antibodies (Panels A and B). Signal intensity increased with an increase in purified recombinant 3C^{pro} concentration as expected. Signal intensity decreased with an increase in anti- TMEV 3C^{pro} dilution as shown by the decrease in signal intensity from 1:1000 antibody dilution (Panel A) to 1: 5000 antibody dilution (Panel B). These results suggest that the pre-clearing of anti-TMEV 3C^{pro} antibodies was effective as there was a reduction in signal

intensity for contaminating protein bands with pre-cleared antibodies compared to crude antibodies.

4.3.3 Detection of virally-expressed 3C^{pro} in infected BHK-21 cell lysates supernatants using anti-TMEV 3C^{pro} antibodies

Anti-TMEV 3C^{pro} antibodies were tested for detection of virally-expressed 3C^{pro} in infected BHK-21 cell lysates. Anti-TMEV 2C antibodies (Jauka *et al*., 2010) were used as a positive control in order to determine if the cells were successfully infected with TMEV. Cells were infected and mock-infected with TMEV for 5 hrs and resuspended in lysis buffer. The supernatant was analysed by SDS-PAGE and Western analysis using anti-TMEV 2C (1:10 000) and anti-TMEV 3C^{pro} (1:500). The results are shown in figure 4.3 A and B below.

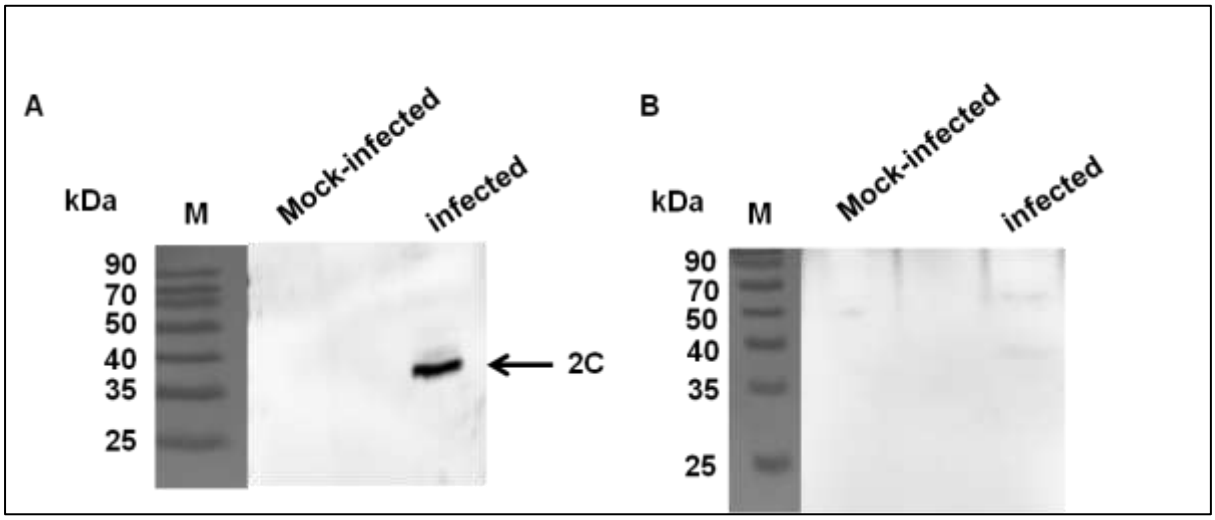

Figure 4.3: Western analysis of infected and mock-infected BHK-21 cell lysates supernatants. Panel A: Detection using anti-TMEV 2C (1:10 000); **Panel B:** Detection using anti-TMEV 3C^{pro} (1:500). Lane mock-infected: Mock-infected BHK-21 cell lysates supernatant, Lane infected: Infected BHK-21 cell lysates supernatant

The predicted size of 2C is approximately 37 kDa. Panel A shows no detection of 2C in the mock-infected lysate as expected. A protein band is resolved between 35 and 40 kDa in the infected lysate, indicating the cells were successfully infected. Panel B shows faint protein bands resolving between 15 and 25 kDa in both mock-infected and infected lysates. No protein band of the predicted size of 3C^{pro} is observed in the infected lysate. Because no signal for virally-expressed 3C^{pro} in TMEV-infected cell lysate supernatants was detected in this assay, total protein was prepared for Western analysis.

4.3.4 Detection of 3C^{pro} in total BHK-21 cell protein samples using anti-TMEV 3C^{pro} antibodies

In an attempt to determine whether TMEV 3C^{pro} is present in the insoluble fraction, anti-TMEV 3C^{pro} antibodies were tested using total protein prepared from infected and mock-infected cell lysates. Once again anti-TMEV 2C antibodies were used as a positive control and pre-immune serum as a negative control. Cells were infected and mock-infected with TMEV for 5 hrs and resuspended in PBS. The total protein was analysed by SDS-PAGE and Western analysis using anti-TMEV 3C^{pro} (1:500), anti-TMEV 2C (1:10 000) and pre-immune serum (1:500). The results are shown in figure 4.4 A, B and C below.

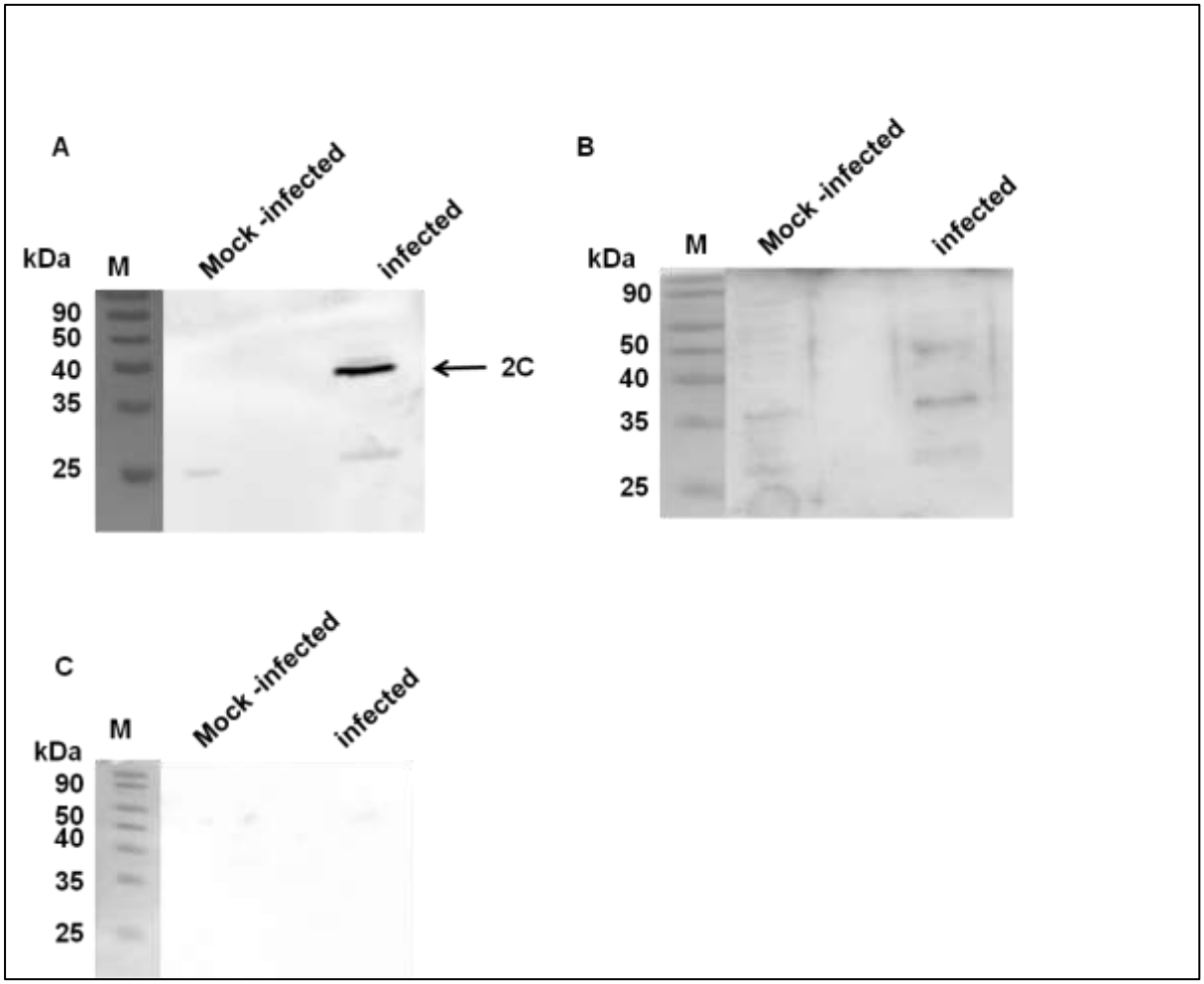

Figure 4.4: Western analysis of total BHK-21 cell protein samples prepared from infected and mock-infected cell lysates. Panel A: Detection using anti-TMEV 3C^{pro} antibodies (1:500); **Panel B:** Detection using anti-TMEV 2C antibodies (1:10 000). **Panel C:** Detection using pre-immune serum (1:500).Lane mock-infected: Total BHK-21 cell protein samples prepared from mock-infected cell lysate, Lane infected: Total BHK-21 cell protein samples prepared from infected cell lysate.

Panel A shows protein bands resolved between 25 and 35 kDa and between 35 and 40 kDa in the mock-infected and infected lysates. No protein band of the predicted size of $3C^{pro}$ is observed in the infected lysate. Panel B shows no detection of 2C in the mock-infected lysate as expected. A protein band is resolved between 35 and 40 kDa in the infected lysate, indicating the cells were successfully infected. No protein bands were detected in both infected and mock-infected lysates as expected in Panel C. These results suggest that anti-TMEV $3C^{pro}$ antibodies are unable detect virally-expressed $3C^{pro}$ in total protein samples prepared from infected and mock-infected cell lysates.

4.3.5 Localisation of virally-expressed $3C^{pro}$ in TMEV-infected BHK-21 cells by indirect immunofluorescence and confocal microscopy

To localise virally-expressed $3C^{pro}$ in infected BHK-21 cells, cells were grown on glass coverslips and infected with TMEV. Cells were fixed with 4 % paraformaldehyde and stained with anti-TMEV $3C^{pro}$ at dilutions of 1:500 and 1:1000. Anti-TMEV 2C and anti-TMEV P1 antibodies were utilised at a dilution of 1:1000. The primary antibodies were detected with species-specific Alexa-Fluor 488-conjugated antibodies. Anti-TMEV 2C and P1 antibodies were used as positive controls in order to confirm that cells were successfully infected with TMEV. The results are shown in figure 4.5 below.

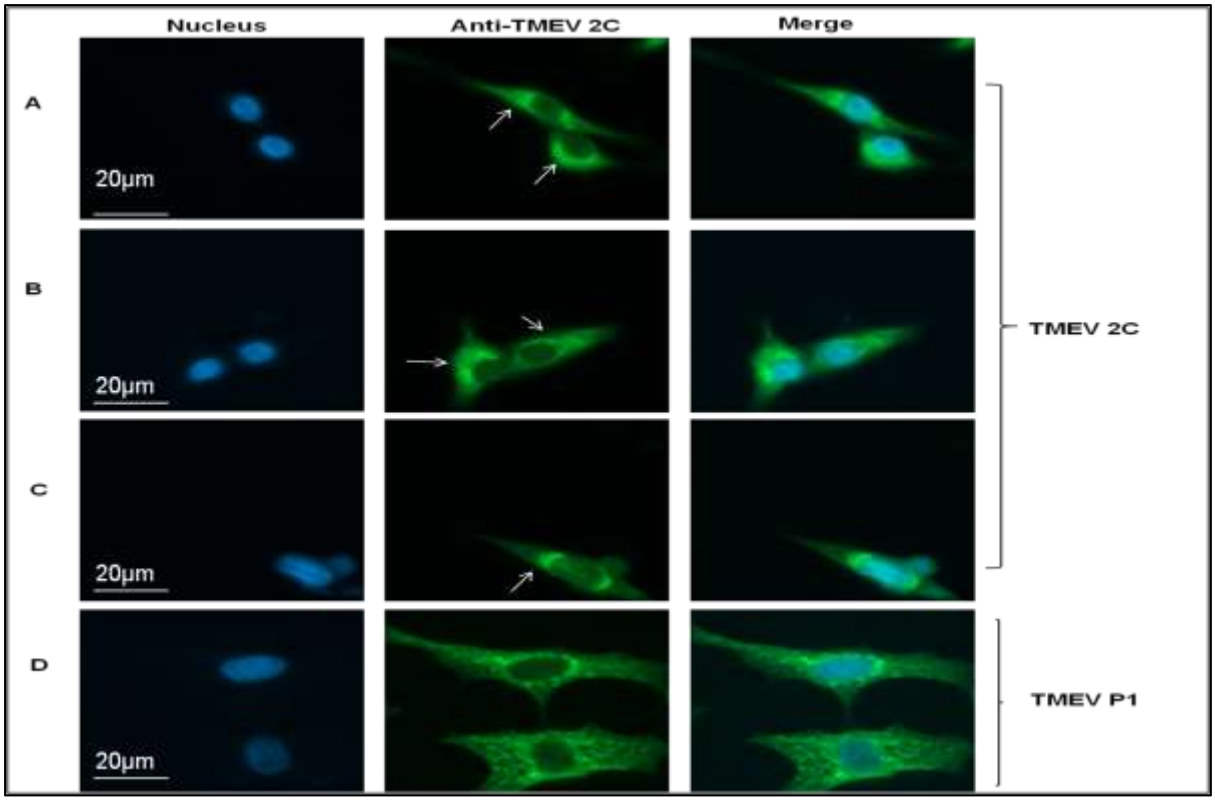

Figure 4.5: Detection of TMEV 2C and P1 in infected BHK-21 cells at 6.5 hrs post-infection. Panel A-C: Infected BHK-21 cells probed with anti-TMEV 2C antibodies (1:1000), primary antibodies were visualised with Alexa-Fluor 488-conjugated anti-rabbit antibodies. Arrows indicate TMEV replication complexes. **Panel D:** Infected BHK-21 cells probed with anti-TMEV P1 monoclonal antibodies (1:1000), primary antibodies were visualised with Alexa-Fluor 488-conjugated anti-mouse antibodies.

Cells were visualised using fluorescence microscopy. Panel A, B and C represent separate fields of TMEV-infected cells fixed at 6.5 hrs post-infection. The staining pattern of 2C is concentrated within a structure next to the nucleus as described by Jauka *et al.*, 2010. Panel D shows the distribution of TMEV P1. The signal appears to be both punctate and diffuse in the cytoplasm and also concentrated in the perinuclear region of the cells. The detection of TMEV 2C and P1 confirms that the infection process was successful.

Negative controls were conducted by staining cells with anti-TMEV $3C^{pro}$ antibodies and Alexa-Fluor 488-conjugated anti-rabbit antibodies alone in order to determine the specificity of the antibodies for staining virally-expressed $3C^{pro}$. Cells were viewed using confocal microscopy and the bright field channel was utilised to visualise cell morphology. The results are shown in figure 4.6 A and B below.

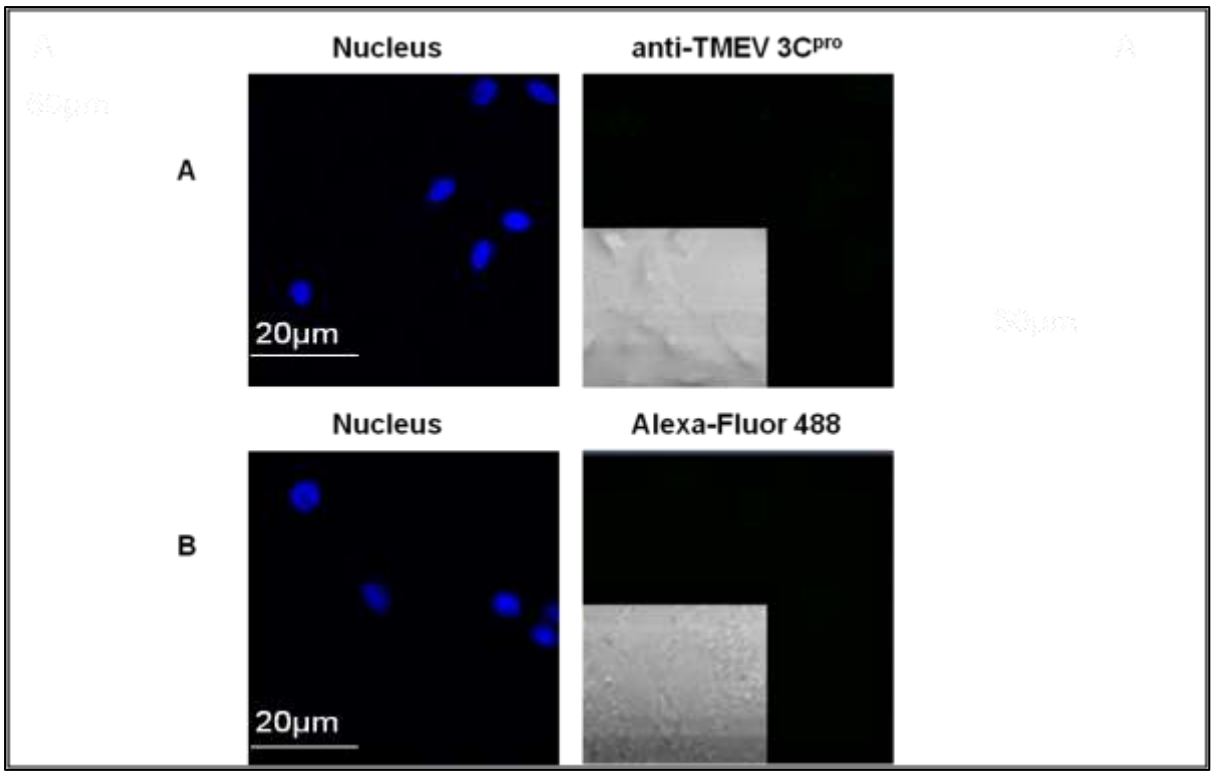

Figure 4.6: Negative controls for detection of 3C^{pro} in TMEV-infected cells. Panel A: Infected cells probed with anti-TMEV 3C^{pro} antibodies (1:1000) only. **Panel B:** Infected cells probed with Alexa-Fluor 488-conjugated anti-rabbit antibodies (1:500) only. Cells in both panels were visualised using the bright field channel in order to visualise cell morphology.

No signal is detected in cells probed with anti TMEV 3C^{pro} antibodies alone (Panel A) and with Alexa-Fluor 488-conjugated anti-rabbit secondary antibodies alone (Panel B). Most cells showed typical fibroblast morphology as shown by the bright field channel in both panels. Based on these results, BHK-21 cells were infected and probed with different dilutions of anti-TMEV 3C^{pro} antibodies in order to localise 3C^{pro} using fluorescence microscopy (figure 4.7).

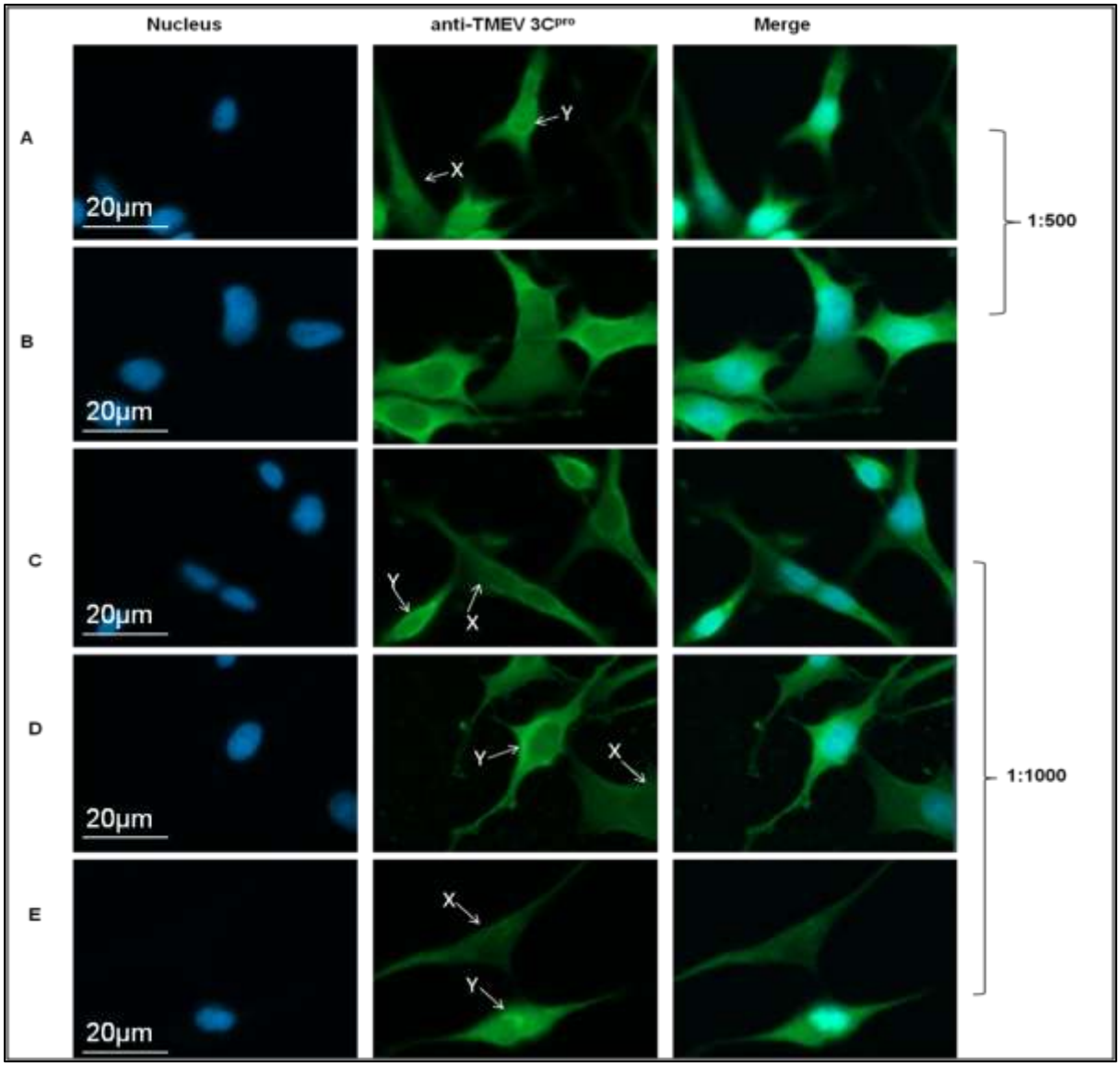

Figure 4.7: Detection of TMEV 3C^{pro} in infected BHK-21 cells at 6.5 hrs post-infection: Panel A and B: Infected cells labelled with anti-TMEV 3C^{pro} at 1:500 dilution. **Panel C, D and E:** Infected cells labelled with anti-TMEV 3C^{pro} at 1:1000 dilution. Primary antibodies were visualised with Alexa-Fluor 488-conjugated anti-rabbit antibodies at 1:500 dilution. Arrowhead X represents cells with faint 3C^{pro} staining and Arrowhead Y represent cells with stronger 3C^{pro} staining.

Panel A and B show separate fields of TMEV-infected cells fixed at 6.5 hrs post-infection and probed with anti-TMEV 3C^{pro} antibodies at a 1:500 dilution. Cytoplasmic staining is observed as well as concentrated staining in the perinuclear region. As can be seen by the arrowhead marked X, there are cells with faint staining. Panels C, D and E show separate fields of TMEV-infected cells fixed at 6.5 hrs post-infection and probed with anti-TMEV 3C^{pro} antibodies at a 1:1000 dilution.. A weaker signal observed at this dilution compared to the lower antibody dilution of 1:500 (Panel A and B). Cytoplasmic staining is observed as

well as concentrated staining around the perinuclear region in panel C and D, as can be seen by the arrowheads marked X, there are cells which have weaker staining for $3C^{pro}$ and arrowheads marked Y show cells which have a stronger staining signal for $3C^{pro}$.

4.4 Discussion

This chapter describes the testing of anti-TMEV $3C^{pro}$ antibodies for the ability to detect $3C^{pro}$ by Western analysis and indirect IF.

Antibodies generated against protein antigens are required for analytical techniques such as immunoblotting and immunohistochemistry in order to further study virus-host interactions. In the case of TMEV, polyclonal antibodies generated against the non-structural 2C protein were used to localise the protein to the Golgi apparatus of TMEV-infected cells where virus replication is suggested to occur (Jauka *et al*., 2010). In a similar study, anti-Hsp 90, anti-Hsp 70 and anti-TMEV 2C antibodies were used to study the role of molecular chaperones in TMEV infection (Mutsvunguma *et al*., 2011). Antibodies have been used to study the inhibitory role played by the Leader (L) protein in *Cardioviruses* in the formation of cytoplasmic aggregates caused by the exposure of infected cells to various environmental stresses and to localise the protein to the mitochondria of TMEV-infected cells (Borghese and Michiels, 2011; Sorgeloos *et al*., 2011). Antibodies have also been used to determine the role of $CD4^+$ T cells in the development of demyelinating diseases due to TMEV infection (as reviewed by Oleszak *et al*., 2004). Neutralising monoclonal antibodies to TMEV DA and GDVII strains were utilised to confirm the division of TMEV into two different subgroups (Nitayaphan *et al*., 1985). Furthermore a study by Yamada *et al*., (1990) was able to show that the production of a monoclonal antibody, H8, as a result to TMEV infection enhances demyelination of the CNS by binding to oligodendrocytes in brain cells.

Antigens are injected along with adjuvants in order to boost humoral and/or cell mediated immune response to the antigen for antibody production. The most widely utilised adjuvant for experimental antibody production is Freund's complete adjuvant (FCA) however its use has been limited due to its adverse effects on the host. FCA is comprised of mineral oils, a surfactant agent and heat-killed and dried *Mycobacterium tuberculosis*. Freund's incomplete adjuvant (FIA) differs from FCA in that it does not include the heat-killed *mycobacterium* (as reviewed by Cox and Coulter, 1997; Stills, 2005). Standard immunisation protocols involve injecting high doses of protein antigen with FCA and FIA for antibody production however,

this method becomes challenging when insufficient amounts of antigen are available (Lancefield *et al*., 1975; Bellstedt *et al*., 1987). Another method has been developed where acid-treated, naked bacteria are used as immune carriers for protein antigen and less than a milligram of protein antigen is required. This method involves adsorbing protein antigen to an acid-treated, naked bacteria suspension. The absorbed naked bacteria complexes are then emulsified with an equal volume of FCA and FIA and intravenously immunised into rabbits (Bellstedt *et al*., 1987). This technique was initially used for the production of antibodies against the lipid A portion of lipopolysaccharides (Galanos *et al*., 1971), and later used for the generation of highly specific antibodies against the human apolipoprotein A1 (Apo 1 or CEA) and TMEV 2C protein (Bellstedt *et al*., 1987; Jauka *et al*., 2010). In this study, Recombinant $3C^{pro}$ antigen was prepared under denaturing conditions and used for immunisation of rabbits using the above mentioned technique. Day 43 antiserum (anti-TMEV $3C^{pro}$ antibodies) was tested for detection of bacterial antigen and virally-expressed $3C^{pro}$ by Western analysis and indirect IF.

Crude anti-TMEV $3C^{pro}$ antibodies were able to detect as little as 107 ng of bacterially expressed antigen at a dilution of 1:100 000 by Western analysis. Pre-clearing of anti-TMEV $3C^{pro}$ antibodies using *E. coli* JM109 cell lysate reduced detection of contaminating protein bands and enhanced the signal for bacterial antigen.

Anti-TMEV $3C^{pro}$ antibodies were then used to detect virally-expressed $3C^{pro}$ in infected cell supernatants and total protein lysates by Western analysis. Anti-TMEV 2C antibodies were used as a positive control. Detection of a protein band resolved between 35 and 40 kDa for 2C was observed indicating that the cells were successfully infected. In a similar study, detection of TMEV 2C in infected cell lysates by Western analysis showed the detection of a protein of approximately 37 kDa present in both supernatant and pellet fractions (Jauka *et al*., 2010). No protein signal of the predicted size of $3C^{pro}$ was observed in either infected cell supernatants or total protein lysate samples.

In order for efficient interactions to occur between antigen and antibody, epitopes found on the antigen must be exposed to the surface for binding (Reverberi and Reverberi, 2007). This study showed that anti-TMEV $3C^{pro}$ antibodies were able to recognise bacterial antigen used for immunisation but not virally-expressed $3C^{pro}$ by Western analysis. There are a number of reasons why the antibodies could not detect virally-expressed protein. One reason could be that the antibodies were raised against denatured recombinant antigen as opposed to correctly

folded $3C^{pro}$, which would be produced in infected eukaryotic cells, suggesting that epitopes recognised by anti-TMEV $3C^{pro}$ antibodies on denatured antigen are buried within the virally-expressed protein in its final conformation. Other factors that may have been responsible for these results include pH changes, buffer composition and growth conditions all of which can affect antibody-antigen interactions by altering the epitope and affecting its ability to interact with the antibody (Reverberi and Reverberi, 2007). It is possible that these conditions may have caused an alteration to the epitope of virally expressed $3C^{pro}$ during the preparation of cell lysates for analysis. Thirdly, it may be possible that levels of virally-expressed $3C^{pro}$ were too low in the cell lysates to be detected by Western analysis. Furthermore, the binding of the non-structural 2C protein to $3C^{pro}$ at 5 hours-post infection may have altered important epitopes present on $3C^{pro}$ thus inhibiting the binding of the antibodies. Multiple sequence alignments of 2C with protease inhibitors have shown that 2C contains serine protease motifs scattered throughout its sequence, suggesting that 2C plays a regulatory role in protease activity. PV 2C was found to co-immunoprecipitate with viral 3C protease which resulted in the inhibition of proteolytic activity of 3C both *in vivo* and *in vitro* (Banerjee *et al*., 2004). In order to investigate this, TMEV-infected cells can be harvested at various time post-infection and analysed by Western analysis to determine a time point where $3C^{pro}$ is detected.

In the next study, anti-TMEV $3C^{pro}$ antibodies were tested for detection of $3C^{pro}$ in TMEV-infected cells by indirect IF. Imaging of negative control cells was performed using confocal microscopy. However, when follow up studies were conducted, focusing issues with the microscope were encountered and staining patterns for $3C^{pro}$, 2C and P1 could not be confirmed. Because of these issues, images were obtained using fluorescence microscopy.

Anti-TMEV 2C and P1 antibodies were used as positive controls in order to determine whether the cells were successfully infected. Cells stained with anti-TMEV 2C antibodies showed a staining pattern of 2C concentrated within a structure adjacent to the nucleus. In a study where TMEV 2C was localised, similar staining patterns were observed. The large structure was identified as the viral replication complex which is formed in the region of the Golgi apparatus (Jauka *et al*., 2010). Cells stained with anti-TMEV P1 antibodies showed a pattern which was both punctative and diffuse in the cytoplasm while at the same time appeared to be concentrated around the perinuclear region of the cells. The distribution is similar to that reported for Enterovirus 71 (Liu *et al*., 2013) and Coxsackie virus B3 (Wang *et al*., 2012). The detection of TMEV 2C and P1 confirmed that the infection process was successful.

No signal was detected in the negative controls as expected. The antibodies were then utilised for localising $3C^{pro}$ in TMEV-infected cells. A weaker signal was observed at an antibody dilution of 1:1000 compared to the lower antibody dilution of 1:500. In all cells imaged, cytoplasmic and perinuclear staining was observed, whereas nuclear staining was observed in one of the cells. Faint staining was observed in some of the cells imaged, suggesting that these cells may have been uninfected. Although further experiments are required to confirm antibody specificity, the distribution pattern observed for TMEV $3C^{pro}$ is similar to that described for HRV where $3C^{pro}$ and its precursors were localised in the nuclei, cytoplasm and perinuclear regions in infected HeLa cells at 4 hrs post-infection (Amineva *et al*., 2004). In a similar study, EMCV $3C^{pro}$ was localised to the nuclei and cytoplasm in infected HeLa cells harvested at 2, 3, 4 and 6 hrs post-infection (Aminev *et al*., 2003). In another study, the expression of FMDV $3C^{pro}$ alone in BSR T7/5 cells has shown a diffuse cytoplasmic staining pattern of the protein (Armer *et al*., 2008). Although the staining pattern observed using anti-TMEV $3C^{pro}$ antibodies is similar to staining patterns of other studies, further optimisation experiments are required to examine the specificity of the antibodies generated in this study. For example, mock-infected cells can be stained with various dilutions of anti-TMEV $3C^{pro}$ antibodies to test for background staining. Secondly, dilution studies of the antibodies can be conducted in order to determine the optimal staining concentration. Furthermore, pre-clearing of anti-TMEV $3C^{pro}$ antibodies with BHK-21 cell lysate could also be carried out to examine specificity. Due to time constraints, these experiments were not performed in this study.

In conclusion, crude and pre-cleared anti-TMEV $3C^{pro}$ antibodies were able to detect bacterially expressed antigen but were unable to detect virally-expressed protein in infected cell supernatant and total protein lysate samples by Western analysis. Further experiments are required to confirm the specificity of the antibodies for virally-expressed $3C^{pro}$ by indirect IF. The next chapter describes the general conclusions of this study and future work.

Chapter 5: General Conclusions and Future work

This study sought to generate polyclonal antibodies against TMEV VP1 and $3C^{pro}$ for use in localisation of the proteins in infected cells as tools to further study the role of Hsp 90 and Hsp 70 during TMEV replication and assembly. Molecular chaperones have been shown to play a role in viral entry, replication, assembly and exit and have been widely researched on a variety of viruses including picornaviruses. For example, GRP78 from the Hsp 70 family has been shown to play a role during the attachment and viral entry process of Coxsackievirus (CV) A9 (Triantafilou *et al*., 2002). Hsp 90 has been identified as a host factor which induces the activity of the RNA polymerase of Influenza A virus, leading to efficient transcription and replication of viral RNA (Momose *et al*., 2002). This chaperone has also been shown to be involved in Ebola virus replication (Smith *et al*., 2010). Another example is the role played by Hsc 70 during the virus assembly process of HIV-1 (Reviewed by Brenner and Wainberg, 1999). In *Enteroviruses*, Hsp 90 and Hsp 70 have been shown to maintain P1 in a processing conformation during virus assembly such that it can be recognised and cleaved by viral protease, $3C^{pro}$ (Macejak and Sarnow, 1992; Geller *et al*., 2007). This defines the requirement of molecular chaperones in the capsid assembly process of picornaviruses (Geller *et al*., 2007). Only one study has been conducted on the role played by Hsp 90 and Hsp 70 in the replication of TMEV (Mutsvunguma *et al*., 2011). No study has been conducted to investigate interactions between Hsp 90 and TMEV P1 during virus assembly. In order to study these specific interactions, antibodies against the antigenic capsid subunit, VP1 and $3C^{pro}$ are required. These antibodies can be used to study protein-protein interactions between VP1, $3C^{pro}$ and molecular chaperones. The distribution of both proteins in relation to Hsp 90 and Hsp 70 can also be studied in TMEV-infected cells.

In order to prepare purified antigen for immunisation purposes, bioinformatic analyses were conducted to determine predicted hydrophobic, hydrophilic and antigenic regions for VP1 and $3C^{pro}$. The Kyte and Doolittle Hydropathy plots for both proteins indicated that VP1 and $3C^{pro}$ have a distribution of amino acids which are predicted hydrophobic and hydrophilic throughout the protein sequence. The Hopp and Woods Hydrophilicity plots indicated that both proteins have a distribution of predicted antigenic and non-antigenic regions throughout the protein sequences. Structural analyses were also conducted for the prediction of linear B cell epitopes exposed on the molecular surfaces of both proteins. There were three predicted linear B cell epitopes exposed on the molecular surface of TMEV GDVII VP1, 1 (amino

acids 52-78), 2 (amino acids 195-209), 3 (amino acids 250-275) and three predicted B cell epitopes exposed on the molecular surface of TMEV GDVII $3C^{pro}$, 1 (amino acids 90-107), 2 (amino acids 130-136) and 3 (amino acids 145-152). Based on these results, the full length coding sequences of VP1 (880 bp) and $3C^{pro}$ (649 bp) were PCR amplified and cloned into pQE-80L to produce pBMVP1 and pBM$3C^{pro}$. The open reading frames for both recombinant plasmids were intact and no mutations were identified when VP1 and $3C^{pro}$ coding sequences were subjected to BLAST against the TMEV GDVII complete genome sequence (Acc no: X56019.1). The expression vector, pQE-80L was chosen as a vector system because cloning into this vector has been successful in our laboratory. TMEV 2C was cloned and expressed in pQE-80L for preparation of polyclonal antibodies against the non-structural 2C protein. Staining with anti-TMEV 2C antibodies localised the protein to the Golgi apparatus where it assists with the formation of replication complexes (Jauka *et al*., 2010).

Recombinant VP1 was expressed in *E. coli* JM109 cells by IPTG induction for 6 hrs. Solubility studies revealed that recombinant VP1 was present in the soluble fraction and treatment of cell lysate with Sarcosyl released most of recombinant VP1 into the soluble fraction. Culture volume was upscaled to 1 L for purification of recombinant VP1 under native conditions however recombinant VP1 co-purified with an unidentified protein which was present in higher concentrations. Because recombinant VP1 co-purified with an unidentified protein, a pET expression system was used to further attempt producing purified VP1 antigen for immunisation purposes. This system was chosen because it is widely used for the preparation of recombinant FMDV VP1 (Shi *et al*., 2012; Liu *et al*., 2011).

pETVP1 (1-741) was constructed and kindly donated by Dora Mwangola (B.Sc Honours student, Rhodes University). No mutations were identified when VP1 (1-741) sequence was subjected to BLAST against the TMEV GDVII complete genome sequence (Acc no: X56019.1). Recombinant VP1 (1-247) was expressed in *E. coli* BL21 (DE3) cells by IPTG induction for 6 hrs. The size of recombinant VP1 (1-247) was estimated to be 35 kDa and a protein band of that size was not observed by SDS-PAGE analysis. However Western analysis showed detection of a 6x His-tagged protein at approximately 35 kDa, suggesting that the recombinant protein was expressed in low levels possibly due to the presence of rare *E. coli* codons on the VP1 gene. Five rare codons for arginine (GGA) and 2 rare codons for CGG were identified. Two rare codons for isoleucine and thirteen rare codons for proline were identified. The presence of these particular rare *E. coli* codons in the TMEV VP1 (1-247) gene is not likely to be the cause for low expression levels as recombinant VP1 was

successfully expressed from pQE-80L in *E. coli* JM109 cells. Solubility studies resulted in the presence of two protein bands which were similar in size. The lower protein band was predominantly present in the insoluble fraction while the upper protein band was more concentrated in the soluble fraction. Separation of the protein bands by a longer electrophoresis time and Western analysis showed detection of two protein signals, making it difficult to determine which protein band represented VP1 (1-247). The presence of two protein bands resolved by SDS-analysis may have been caused by degradation of recombinant VP1 (1-247) due to continuous freeze-thawing of sample before analysis. Another reason could be the presence of the reducing agent, β-mercaptoethanol, in SDS-loading buffer.

Recombinant $3C^{pro}$ was expressed in *E. coli* JM109 cells by IPTG induction for 4 hrs. Solubility studies revealed that the recombinant protein was predominantly present in the insoluble fraction and treatment of cell lysate with Sarcosyl did not affect the solubility of recombinant $3C^{pro}$ because of the formation of insoluble inclusion bodies. Culture volume was upscaled to 1 L for purification of recombinant $3C^{pro}$ under denaturing conditions using 8M urea. Purified recombinant $3C^{pro}$ was eluted in the first fraction with trace amounts of co-eluting proteins. For immunisation purposes, urea present in the purified $3C^{pro}$ sample was removed by dialysis using PBS. During dialysis the purified $3C^{pro}$ antigen was observed to form a white precipitate, which was sent off as antigen for immunisation of rabbits. Even though immunisation with precipitated antigen is considered better than immunisation with soluble antigen, solubilisation of recombinant $3C^{pro}$ could have been attempted. Further studies can involve reducing the formation of protein aggregates by altering certain parameters during protein expression such as growth temperature, expression rate and host metabolism. These parameters are known to lead to low expression levels and high solubility of recombinant protein (Jonasson *et al*., 2002). A second approach can involve the expression of truncated $3C^{pro}$ peptides for immunisation purposes. Peptide-based immunisation is most commonly intended to induce a specific response to a range of pre-determined antigenic sites. An advantage of this technique is that only desired antigenic regions which will enhance an immune response are selected and antigens which may interfere with the immune response are avoided (Schunk and Macallum, 2005).

Day 43 antiserum (anti-TMEV $3C^{pro}$ antibodies) was tested for detection of bacterially expressed $3C^{pro}$ by Western analysis. Crude anti-TMEV $3C^{pro}$ antibodies detected as little as 107 ng of bacterially expressed antigen however the antibodies required pre-clearing due to

the presence of contaminating protein bands. Pre-cleared anti-TMEV $3C^{pro}$ antibodies were effective as there was a reduction in signal intensity for contaminating protein bands. When the antibodies were tested for detection of virally expressed $3C^{pro}$ in TMEV-infected cell supernatant and total protein lysates by Western analysis, no signal for a protein the size of $3C^{pro}$ was detected. This may be due to a number of reasons such as conformation of virally-expressed $3C^{pro}$, low concentrations of $3C^{pro}$ present in the cell lysates, physicochemical conditions such as buffer composition and pH changes or the inhibition of 2C on $3C^{pro}$ activity. Further studies will involve conducting a time course study where TMEV-infected cells are harvested at various time post-infection and analysed by Western analysis to determine a time point where $3C^{pro}$ is detected.

Lastly, anti-TMEV $3C^{pro}$ antibodies were tested for detection of $3C^{pro}$ in TMEV-infected cells by indirect IF. In all cells imaged, cytoplasmic and perinuclear staining was observed, whereas nuclear staining was observed in one of the cells. The distribution was similar to that described in section 4.4 for HRV, FMDV and EMCV $3C^{pro}$. Although the staining pattern observed for anti-TMEV $3C^{pro}$ antibodies is in agreement with staining patterns of other picornavirus $3C^{pro}$, further optimisation studies are required to confirm the specificity of the antibodies for virally-expressed $3C^{pro}$.

Antibody specificity refers to the ability of the antibody to bind to specific epitopes of the target antigen without cross-reacting with other proteins. The specificity of an antibody is determined by showing specific reactions with the target protein using various experiments. Testing for antibody specificity helps to avoid follow up experiments on false-positive results (Burry, 2000).

Future work is needed to confirm the distribution of virally-expressed $3C^{pro}$ in infected cells. Firstly, more dilution studies of the antibodies can be conducted in order to determine the optimal staining concentration. Secondly, cells can be mock-infected and stained with various dilutions of anti-TMEV $3C^{pro}$ antibodies to test for background staining. Background staining can also be tested for by conducting negative control studies where infected-cells are stained with anti-TMEV $3C^{pro}$ antibodies alone and Alexa-Fluor conjugated secondary antibodies alone using various dilutions. Thirdly, the antibodies can be tested at various time points post-infection to see if an increase in signal pattern is observed. Furthermore, antibodies can be pre-cleared with BHK-21 cell lysate and utilised to examine specificity towards virally-expressed $3C^{pro}$.

Once the antibodies have been successfully optimised, co-immunoprecipitation studies can be carried out in order to determine protein-protein interactions between $3C^{pro}$ and molecular chaperones. Secondly, the distribution of $3C^{pro}$ in relation to Hsp 90 and Hsp 70 can be observed in TMEV-infected cells. Lastly, the effect of Hsp 90 and Hsp 70 inhibition on TMEV capsid folding and assembly can also be studied.

Since problems were encountered during the preparation of purified VP1 antigen, future studies are intended to express truncated VP1 peptides in *E.coli* cells and prepare antigen for immunisation purposes. A second approach will involve purifying virus particles from TMEV-infected cells and using the purified particles for immunisation purposes in order to generate antibodies against TMEV capsid proteins.

In conclusion, this study described the preparation of antigen for the generation of polyclonal antibodies against TMEV VP1 and $3C^{pro}$. Due to problems encountered, antibodies against VP1 were not generated. Anti-TMEV $3C^{pro}$ antibodies detected bacterial antigen but were unable to detect viral antigen in TMEV-infected cells by Western analysis. A staining pattern similar to that observed for HRV, FMDV and EMCV $3C^{pro}$ was obtained however further optimisation studies need to be carried out to confirm the specificity of the antibodies for virally-expressed $3C^{pro}$ by indirect IF.

Chapter 6: References

1. **Adams MJ, King AMQ & Carstens EB** (2013) Ratification vote on taxonomic proposals to the International Committee on Taxonomy of Viruses (2013). *Archives of Virology*. DOI 10.1007/s00705-013-1688-5
2. **Aldabe R & Carrasco L** (1995) Induction of membrane proliferation by poliovirus proteins 2C and 2BC. *Biochemical and Biophysical Research Communications* **206,** 64-76
3. **Alfano C & McMacken R** (1989) Heat shock protein-mediated disassembly of nucleoprotein structures is required for the initiation of bacteriophage lambda DNA replication. *Journal of Biological Chemistry* **264**, 10709-10718
4. **Aminev AG, Amineva SP & Palmenberg AC** (2003) Encephalomyocarditis virus (EMCV) proteins 2A and 3BCD localize to nuclei and inhibit cellular mRNA transcription but not rRNA transcription. *Virus Research* **95**, 59–73.
5. **Amineva SP, Aminev AG, Palmenberg AC & Gern JE** (2004) Rhinovirus 3C protease precursors 3CD and 3CD' localize to the nuclei of infected cells. *Journal of General Virology* **85**, 2969-2979
6. **Andino R, Boddeker N, Silvera D & Gamarnik AV** (1999) Intracellular determinants of picornavirus replication. *Trends in Microbiology* **7**, 76-82
7. **Armer H, Moffat K, Wileman T, Belsham GJ, Jackson T, Duprex WP, Ryan M & Monaghan P** (2008) Foot-and-Mouth Disease Virus, but Not Bovine Enterovirus, Targets the Host Cell Cytoskeleton via the Non-structural Protein $3C^{pro}$. *Journal of Virology* **82**, 10556-10566
8. **Balbas P** (1997) Designing Expression Plasmid vectors in *E. coli*. In: Recombinant Gene Expression protocols, volume 62, edited by Tuan, R. S. Totowa, New Jersey: Human Press Inc, pp 11-27
9. **Banerjee R, Weidman MK, Echeverri A, Kundu P & Dasgupta A** (2004) Regulation of Poliovirus 3C Protease by the 2C Polypeptide. *Journal of Virology* **78,** 9243-9256
10. **Baneyx F** (1999) Recombinant protein expression in *Escherichia coli*. *Current Opinion in Biotechnology* **10**, 411-421
11. **Bedard KM & Semler BL** (2004) Regulation of picornavirus gene expression. *Microbes and Infection* **6**, 702-713

12. **Bienz K, Egger D, Troxler M & Pasamontes L** (1990) Structural organisation of Poliovirus RNA replication is mediated by viral proteins of the P2 genomic region. *Journal of Virology* **64**, 1156-1163
13. **Bienz K, Egger D, Pfister T & Troxler M** (1992) Structural and functional characterisation of the Poliovirus replication complex. *Journal of Virology* **66**, 2740-2747
14. **Bellstedt DU, Human PA, Rowland GF & Van der Merwe KJ** (1987) Acid-treated, naked bacteria as immune carriers for protein antigens. *Journal of Immunological Methods* **98,** 249-255
15. **Borghese F & Michiels T** (2011) The Leader protein of Cardioviruses Inhibits Stress Granule Assembly. *Journal of Virology* **85,** 9614-9622
16. **Brenner BG & Wainberg MA** (1999) Heat shock protein-based therapeutic strategies against human immunodeficiency virus type 1 infection. *Infectious diseases in Obstetrics and Gynaecology* **7,** 80-90.
17. **Buenz EJ & Howe CL** (2006) Picornaviruses and cell death. *Trends in Microbiology* **14,** 28-36
18. **Burman A, Clark S, Abrescia NGA, Fry EE, Stuart DI & Jackson T** (2006) Specificity of the VP1 GH Loop of Foot-and-Mouth Disease Virus for αv Integrins. *Journal of Virology* **80,** 9798-9810
19. **Burry RW** (2000) Controls for Immunocytochemistry. *Journal of Histochemistry and Cytochemistry* **59,** 6-12
20. **Bushell M, Wood W, Carpenter G, Pain VM, Morley SJ & Clemens SJ** (2001) Disruption of the interaction of mammalian protein synthesis eukaryotic Initiation factor 4B with the Poly (A) binding protein by Caspase- and Viral protease-mediated cleavages. *Journal of Biological Chemistry* **276,** 23922-23928
21. **Carrio MM & Villaverde A** (2002) Construction and deconstruction of bacterial inclusion bodies. *Journal of Biotechnology* **96,** 3-12
22. **Cameron K, Zang X, Seal B, Rodriguez M & Njenga CK** (2001) Antigens to viral capsid and non-capsid proteins are present in brain tissues and antibodies in sera of Theiler's virus-infected mice. *Journal of Virological Methods* **91**, 11-19
23. **Carrasco L, Guinea R, Irurzun A & Barco A** (2002) Effects of viral replication on cellular membrane metabolism and function. In: Molecular Biology of Picornaviruses, edited by Semler BL and Wimmer E. Washington D.C, USA: ASM press, pp 337-354

24. **Centeno NB, Planas-Iglesias J & Oliva B** (2005) Comparative modeling of protein structure and its impact on microbial cell factories. *Microbial Cell Factories* **4**, 20
25. **Chen D & Texada DE** (2006) Low-usage codons and rare codons of *Escherichia coli. Gene therapy and Molecular Biology* **10,** 1-12
26. **Chen S, Sullivan WP, Toft DO & Smith DF** (1998) Differential interactions of p23 and the TPR-containing proteins Hop, Cyp40, FKBP52 and FKBP51 with Hsp90 mutants. *Cell stress and Chaperones* **3,** 118–129
27. **Cho MW, Teterina N, Bienz K & Ehrenfeld E** (1994) Membrane rearrangement and vesicle induction by recombinant poliovirus 2C and 2BC in human cells. *Journal of Virology* **202**, 129-145
28. **Chouki A, Ung S, Wychowski C & Dubbuisson J** (1998) Involvement of endoplasmic reticulum in the folding of hepatitis C virus glycoproteins. *Journal of Virology* **72,** 3851-3858
29. **Chromy LR, Pipas JM & Garcea RL** (2003) Chaperone-mediated in vitro assembly of polyomavirus capsids. *Proceedings of the National Academy of Sciences of the United States of America* **100,** 10477-10482
30. **Clark ME, Härmmele T, Wimmer E & Dasgupta A** (1991) Poliovirus proteinase 3C converts an active form of transcription factor IIIC to an inactive form: a mechanism for inhibition of host cell polymerase Ill transcription by poliovirus. *European Molecular Biology Organisation Journal* **10**, 2941-2947
31. **Clark ED** (1998) Refolding of recombinant proteins. *Current opinion in Biotechnology* **9,** 157-163
32. **Collen T, Dimarchi R & Doel TR** (1991) A T cell epitope in VP1 of foot-and-mouth disease virus is immunodorminant for vaccinated cattle. *Immunology* **146**, 749-755.
33. **Cox JC & Coulter AR** (1997) Adjuvants –A classification and review of their modes of action. *Vaccine.* **15,** 248-256
34. **Crossley R & Holberton DV** (1983) Selective extraction with Sarkosyl and repolymerization In Vitro of cytoskeleton proteins from Giardia. *Journal of Cell Science* **62,** 419-438
35. **Curry S, Roque-Rosell N, Zunszain PA & Leatherbarrow RJ** (2007) Foot-and-mouth disease virus 3C protease: Recent structural and functional insights into an antiviral target. *Journal of Biochemistry and Cell biology* **39**, 1-6

36. **Das S, Laxminarayana SV, Chandra N, Ravi V & Desai A** (2009) Heat shock protein 70 on Neuro2a cells is a putative receptor for Japanese encephalitis virus. *Virology* **385**, 47–57
37. **Dodd DA, Giddings Jr TH & Kirkegaard K** (2001) Poliovirus 3A protein limits interleukin-6 (II-6), IL-8 and interferon-beta secretion during viral infection. *Journal of Virology* **75,** 8158-8165
38. **Domingo E, Baranowski E, Escarmis C & Sobrino F** (2002) Foot and Mouth Disease Virus. *Comparative Immunology ,Microbiology and Infectious diseases* **25,** 297-308
39. **Doolittle RF** (1981) Similar Amino Acid Sequences: Chance or Common Ancestry? *Science* **214**, 149-159
40. **Dubuisson J & Rice CM** (1996) Hepatitis C virus glycoprotein folding: disulfide bond formation and association with Calnexin. *Journal of Virology* **70,** 778-786
41. **Dubuisson J** (1998) The role of chaperone proteins in the assembly of envelope proteins of hepatitis C virus. *Bulletin et memories de l'Academie royale de medicine de Belgique* **153,** 343-349
42. **Ellis J** (1987) Proteins as molecular chaperones. *Nature* **328,** 378-379
43. **Falk MM, Grigera PR, Bergmann IE, Zibert A, Multhaup G & Beck E** (1990) Foot-and-mouth disease virus protease 3C induces specific proteolytic cleavage of host cell histone H3. *Journal of Virology* **64,** 748–756.
44. **Fendrick A, Monto A, Nightengale B & Sarnes M** (2003) The economic burden of non influenza-related viral respiratory infections in the United states. *Archives of internal medicine* **163,** 487-494
45. **Fink AL** (1998) Protein aggregation: Folding aggregates, inclusion bodies and amyloid. *Folding and Design* **3,** 9-23
46. **Fink AL** (1999) Chaperone-mediated protein folding. *Physiological Reviews* **79,** 425-449
47. **Flint SJ, Enquist LW, Racaniello VR & Skalka AM** (2009) Principles of Virology. Third edition. Washington, DC: ASM Press.
48. **Fraga S** (1982) Theoretical prediction of protein antigenic determinants from amino acid sequence. *Canadian Journal of chemistry* **60**, 2606-2610
49. **Frydman J** (2001) Folding of newly translated protein in vivo: The role of molecular chaperones. *Annual Review of Biochemistry* **70**, 603-647

50. **Galanos C, Lüderitz O & Westphal O** (1971) Preparation and properties of antisera against the lipid A component of bacterial lipopolysaccharides. *European Journal of Biochemistry* **24, 116-122**
51. **Geller R, Vignuzzi M, Andino R & Frydman J** (2007) Evolutionary constraints on chaperone-mediated folding provide an antiviral approach refractory to development of drug resistance. *Genes & Development* **21,** 195-205
52. **Ghildyal R, Jordan B, Li D, Dagher H, Bardin PG, Gern JE & Jans DA** (2009) Rhinovirus 3C protease can localize and alter active and passive nucleocytoplasmic transport. *Journal of Virology* **83,** 8349-7352
53. **Grant RA, Filman DJ, Fujinami RS, Icenogle JP & Hogle JM** (1992) Three-dimensional structure of Theiler's virus. *Proceedings of the National Academy of Sciences of the United States of America* **89,** 2061-2065
54. **Grubman MJ & Baxt B** (2004) Foot-and-Mouth Disease. *Clinical Microbiology Reviews* **17,** 465-493
55. **Gullberg M, Tolf C, Jonsson N, Polacek C, Precechtelova J, Badurova M, Sojka M, Mohlin C, Israelsson S, Johansson K, Bopegamage S, Hafenstein S & Lindberg AM** (2010) A single coxsackievirus B2 capsid residue controls cytolysis and apoptosis in rhabdomyosarcoma cells. *Journal of Virology* **84**, 5868–5879
56. **Guerrero CA, Bouyssounade D, Zarate S, Isa P, Lopez T, Espinosa R, Romero P, Mendez E, Lopez S & Arias CF** (2002) Heat shock cognate protein 70 is involved in rotavirus cell entry. *Journal of Virology* **76**, 4096–4102
57. **Harlow E & Lane D** (1988) Using Antibodies: A Laboratory Manual. Cold Spring: Harbor Laboratory press
58. **Hartl FU & Hayer-Hartl M** (2002) Molecular Chaperones in the Cytosol: From Nascent Chain to Folded Protein. *Science* **295,** 1852-1858
59. **Hillisch A, Pineda LF & Hilgenfeld R** (2004) Utility of Homology Models in the Drug Discovery Process. *Drug Discovery Today* **15**, 659-69
60. **Hopp T**P **& Woods KR** (1981) Prediction of potential antigenic determinants from amino acid sequences. *Proceedings of the National Academy of Sciences of the United States of America* **78,** 3824-3828
61. **Hughes AL** (2004) Phylogeny of the picornaviridae and differential evolutionary divergence of picornavirus proteins. *Infections, Genetics and Evolution* **4,**143-152

62. **Inoue A, Choe Y & Kim B** (1993) Analysis of antibody responses to predominant linear epitopes on Theiler's murine encephalomyelitis virus. *Journal of Virology* **68**, 3324-3333
63. **Jackson T, Ellard FM, Ghazaleh RA, Brookes SM, Blakemore WE, Corteyn AH, Stuart DI, Newman JW & King AM** (1996) Efficient infection of cells in culture by type O Foot-and-Mouth Disease Virus requires binding to cell surface Heparan sulphate. *Journal of Virology* **70,** 5282-5287
64. **Jana S & Deb JK** (2005) Strategies for efficient production of heterologous proteins in *Escherichia coli*. *Applied Microbiology and Biotechnology* **67,** 289-298
65. **Jauka T, Mutsvunguma L, Boshoff A, Edkins AL & Knox C** (2010) Localisation of Theiler's murine encephalomyelitis virus 2C to the Golgi apparatus using antibodies generated against the peptide region. *Journal of Virological Methods* **168**, 162-169
66. **Joachims M, Harris KS & Etchison D** (1995) Poliovirus protease 3C mediates cleavage of Microtubule-Associated Protein 4. *Journal of Virology* **211**, 451-461
67. **Joachims M, Van Breugel PC & Lloyd RE** (1999) Cleavage of Poly (A)-binding protein by *Enterovirus* Proteases Concurrent with inhibition of translation *in vitro. Journal of Virology* **73,** 718-727
68. **Johnson GD, Davidson RS, McNamee KC, Russell G, Goodwin D & Holborow EJ** (1981) Fading of immunofluorescence during microscopy: a study of the phenomenon and its remedy. *Journal of Immunological Methods* **55,** 231-242
69. **Jonasson P, Liljeqvist S, Nygren P & Stahl S** (2002) Genetic design for facilitated production and recovery of recombinant proteins in Escherichia coli. *Journal of Biotechnology and Applied Biochemistry* **35,** 91-105
70. **Kane JF** (1995) Effects of rare codon clusters on high-level expression of heterologous proteins in Escherichia coli. *Current Opinion in Biotechnology* **6**, 494-500
71. **Kim B, Choe Y, Crane M & Jue C** (1992) Identification and Localisation of a number of predominant conformation-independent antibody epitopes of Theiler's murine encephalomyelitis virus. *Immunology letters* **31**, 199-205
72. **Knowles NJ, Hovi T, Hyyoia T, King AMQ, Lindberg AM, Pallansch MA, Palmenberg AC, Simmonds P, Skern T, Stanway G, Yamashita T & Zell R** (2012) Virus taxonomy: classification and nomenclature of viruses: ninth report of the

International Committee on Taxonomy of Viruses – Part II: The positive sense single stranded RNA viruses – Picornaviridae. Elsevier Inc, pp. 855-880

73. **Knox C, Moffat K, Ali S, Ryan M & Wileman T** (2005) Foot and Mouth disease virus replication sites form next to the nucleus and close to the Golgi apparatus, but exclude marker proteins with host membrane compartments Printed in Great Britain. *Journal of General Virology* **86**, 687-696
74. **Kong W, Ghagde G & Roos R** (1994) Involvement of cardiovirus leader in host cell restricted virus expression. *Proceedings of the national academy of sciences of the United States of America* **91**, 1796-1800
75. **Kumar M & Mitra D** (2005) Heat shock protein 40 is necessary for human immunodeficiency virus-1 Nef-mediated enhancement of viral gene expression and replication. *Journal of Biological Chemistry* **280,** 40041-40050
76. **Kyte J & Doolittle RF (1982)** A simple method for displaying the hydropathic character of a protein. *Journal of Molecular Biology* **157,** 105
77. **Lancefield RC, McCarty M & Everly WN** (1975) Multiple mouse protective antibodies directed against Group B Streptococci. *Journal of Experimental Medicine* **142,** 165-172
78. **Larsen JE, Lund O & Nielsen M** (2006) Improved method for predicting linear B-cell epitopes. *Immunome Research* **2,** 1-7
79. **Li JP & Baltimore D** (1990) An intragenic revertant of poliovirus 2C mutant has an uncoating effect. *Journal of Virology* **64,** 1102-1107
80. **Lin J, Chen T, Weng K, Chang S, Chen L & Shih S** (2009) Viral and Host proteins involved in picornavirus lifecycle. *Journal of Biomedical Science* **16,** 1-14
81. **Lipton HL** (1975) Theiler's virus infection in mice: an unusual biphasic disease process leading to demyelination. *Infection Immunology* **11**, 1147-1155
82. **Lipton HL & Friedman A** (1980) Purification of Theiler's Murine Encephalomyelitis Virus and analysis of structural virion polypeptide profile with virulence. *Journal of Virology* **33,** 1165-1172
83. **Liu JS, Kuo SR, Makhov AM, Cyr DM, Griffith JD, Broker TR & Chow LT** (1998) Human Hsp70 and Hsp40 chaperone proteins facilitate human papillomavirus-11 E1 protein binding to the origin and stimulate cell-free DNA replication. *Journal of Biological Chemistry* **273**, 30704–30712
84. **Liu X, Wang Y, Zang Y, Fang Y, Pan L, LÜ J, Zhou P, Zhang Z, Qi-wei C, Wang G, Wang J, Lou H & Jiang S** (2011) Cloning, codon-optimized expression

and homology modelling of structural protein VP1 from foot and mouth disease virus. *African Journal of Microbiology* **5**, 486-495

85. **Liu Q, Huang X, Ku Z, Wang T, Liu F, Cai Y, Li D, Leng Q & Huang Z** (2013) Characterization of Enterovirus 71 capsids using subunit protein-specific polyclonal antibodies. *Journal of Virological Methods* **187,** 127-131
86. **Luckow VA** (1991) Cloning and expression of heterologous genes in insect cells with baculovirus vectors. In: Recombinant DNA technology and applications, edited by Prokop A & Bajpai RK. New York: McGraw-Hill Publishers, pp 97-152
87. **Macejak DG & Sarnow P** (1992) Association of heat shock protein 70 with Enterovirus capsid precursor P1 in infected human cells. *Journal of Virology* **66**, 1520-1527
88. **Marcotte LL, Wass AB, Gohara DW, Pathak HB, Arnold JJ, Filman DJ, Cameron CE & Hogle JM** (2007) Crystal structure of poliovirus 3CD protein, virally encoded protease and precursor to the RNA-dependent RNA polymerase. *Journal of Virology* **81,** 3583-3596
89. **Mason PW, Rieder E & Baxt B** (1994) RGD sequence of foot-and-mouth disease virus is essential for infecting cells via the natural receptor but can be bypassed by an antibody-enhancement pathway. *Proceedings of the National Academy of Sciences of the United states of America* **91,** 1932-1936
90. **Miller LK** (1988) Baculoviruses as gene expression vectors. *Annual Review of Microbiology* **42,** 117-199
91. **Minor PD, Ferguson M, Evans DMA, Almond JW & Icenogle JP** (1986) Antigenic structures of Polioviruses of Serotypes 1, 2 and 3. *Journal of General Virology* **67,** 1283-1291
92. **Mirzayan C & Wimmer E** (1994) Biochemical studies on Poliovirus Polypeptide 2C: Evidence for ATPase Activity. *Virology* **199,** 176-187
93. **Moffat K, Howell G, Knox C, Belsham GJ, Monaghan P, Ryan MD & Wileman T** (2005) Effects of Foot-and-Mouth Disease Virus non-structural Proteins on the Structure and Function of the Early Secretory Pathway: 2BC but not 3A Blocks Endoplasmic Reticulum –to-Golgi Transport. *Journal of Virology* **79,** 4382-4395
94. **Momose F, Naito T, Yano K, Sugimoto S, Morikawa Y & Nagata K** (2002) Identification of Hsp 90 as a stimulatory host factor involved in influenza virus RNA synthesis. *Journal of Biological Chemistry* **277**, 45306-45314.

95. **Mosimann SC, Cherney MM, Sia S, Poltch S & James MNG** (1997) Refined X-ray crystallographic structure of the poliovirus 3C gene product. *Journal of Molecular Biology* **273,** 1032-1047

96. **Murray L, Luke G, Ryan, MD, Wileman T & Knox C** (2009) Amino acid substitutions within the 2C coding sequence of Theiler's Murine Encephalomyelitis virus alter virus growth and affect protein distribution. *Virus Research* **144**, 74–82

97. **Mutsvunguma LZ, Moetlhoa B, Edkins AL, Luke GA, Blatch GL & Knox C,** (2011) Theiler's murine encephalomyelitis virus infection induces a redistribution of heat shock proteins 70 and 90 in BHK-21 cells, and is inhibited by novobiocin and Geldanamycin. *Cell stress and Chaperones* **15**, 505-515

98. **Nitayaphan S, Toth MM & Roos RP** (1985) Neutralizing monoclonal antibodies of Theiler's Murine encephalomyelitis viruses. *Journal of Virology* **53,** 651-657

99. **Norder H, De Palma AM, Selisko B, Costenaro L, Papageorgiou N, Arnan C, Coutard B, Lantez V, De Lamballaeri X, Baronti C, Sola m, Tan J, Neyts J, Canard B, Coll m, Gorbalenya AE & Hilgenfeld R** (2011) Picornavirus non-structural proteins as targets for new anti-virals with broad activity. *Antiviral Research* **89,** 204-218

100. **Novy R, Drott D, Yaeger K & Mierendorf R** (2001) Overcomming the codon bias of E. coli for enhanced protein expression. *inNovations* **12**, 1-3

101. **Odorico M & Pellequer J** (2003) BEPITOPE: predicting the location of continuous epitopes and patterns in proteins. *Journal of Molecular Recognition* **16,** 20-22

102. **Olezak EL, Chang JR, Friedman H, Katsetos CD & Platsoucas CD** (2004) Theiler's virus infection: A Model for Multiple Sclerosis. *Clinical Microbiology Reviews* **17,** 174-207

103. **Olson NH, Kolatkar PR, Oliveira MA, Cheng RH, Greve JM, McClelland A, Baker TS & Rossman MG** (1993) Structure of a human rhinovirus complexed with its receptor molecule. *Proceedings of the National Academy of Sciences of the United States of America* **90,** 507-511

104. **Orbeste MS, Maher K, Kilpatrick DR, Flemister MR, Brown BA & Pallansch MA** (1999) Typing of Human Enteroviruses by partial sequencing of VP1. *Journal of Clinical Microbiology* **37,** 1288-1293

105. **Pathak HB, Arnold JJ, Wiegand PN, Hargittai MRS & Cameron CE** (2007) Picornavirus genome replication: Assembly and Organization of the VPg

Uridylylation ribonucleoprotein (initiation) complex. *Journal of Biological Chemistry* **282,** 16202-16213

106. **Palomares LA, Sandino E & Ramirez OT** (2004) Production of recombinant proteins In Recombinant gene Expression: Reviews and Protocols, Second edition, edited by Balbas, P & Lorence, A. Totowa, New Jersey: Human Press Inc, pp 3-52

107. **Ponomarenko JV & van Regenmortel MHV** (2009) B-cell epitope prediction. In: Structural Bioinformatics, second edition, edited by Gu J & Bourne PE. USA: John Wiley and Son Inc, pp 849-879

108. **Premanand B, Kiener TK, Meng T, Tan YR, Jia Q, Chow VTK & Kwang J** (2012) Induction of protective immune response against EV71 in mice by baculovirus encoding a novel expression cassette for capsid protein VP1. *Antiviral Research* **95,** 311-315

109. **Prodromou C, Siligardi G, O'Brien R, Woolfson DN, Regan L, Panaretou B, Ladbury JE, Piper PW & Pearl LH** (1999) Regulation of Hsp90 ATPase activity by tetratricopeptide repeat (TPR)- domain cochaperones. *European Molecular Biology Organisation Journal* **18**, 754-762

110. **Prodromou C, Roe SM, O'Brien R, Ladbury JE, Piper PW & Pearl LH** (1997) Identification and structural characterization of the ATP/ADP-binding site in the Hsp90 molecular chaperone. *Cell* **90**, 65-75

111. **Racaniello VR** (2007) Picornaviridae: The viruses and their replication. In: Fields Virology, fifth edition, edited by Knipe DM, Howley PM, Griffin DE, Lamb RA, Martin MA, Roizman B & Strauss SE. Philadelphia, USA: Lippincott Williams and Wilkins Publishers, pp 796-826

112. **Reverberi R & Reverberi L** (2007) Factors affecting the antigen-antibody reaction. *Blood Transfusion* **5,** 227-240

113. **Reyes-Del Valle J, Chavez-Salinas S, Medina F & Del Angel RM** (2005) Heat shock protein 90 and heat shock protein 70 are components of dengue virus receptor complex in human cells. *Journal of Virology* **79**, 4557–4567

114. **Rodriguez PL & Carrasco L** (1995) Poliovirus protein 2C contains two regions involved in RNA binding activity. *Journal of Biological Chemistry* **270,** 10105-10112

115. **Rossky PJ** (2008) Protein denaturation by Urea: Slash and Bond. *Proceedings of the National Academy of Sciences of the United States of America* **105,** 16825-16826

116. **Ryan MD & Flint M** (1997) Virus-encoded proteinases of the picornavirus super-group. *Journal of General Virology* **78,** 699-723

117. **Eswar N, Eramian D, Webb B, Shen MY & Sali A** (2008) Protein structure modelling with MODELLER. *Methods Molecular Biology* **426,** 145-159

118. **Samudzi R, Leman PA, Paweska JT, Swanepoel R & Burt FJ** (2012) Bacterial expression of Crimean-Congo haemorrhagic fever virus nucleoprotein and its evaluation as a diagnostic reagent in an indirect ELISA. *Journal of Virological Methods* **179**, 70-76

119. **Sandoval IV & Carrasco L** (1997) Poliovirus infection and expression of the poliovirus 2B provoke the disassembly of the Golgi complex, the organelle target for the antipoliovirus drug Ro-090179. *Journal of Virology* **71**, 4679-4693

120. **Savolainen C, Blomqvist S, Mulders MN & Hovi T** (2002) Genetic clustering of all 102 human rhinovirus prototype strains: serotype 87 is close to human enterovirus 70. *Journal of General Virology* **83,** 333–340

121. **Schueler-Furman O & Baker D** (2003) Conserved residue clustering and protein structure prediction. In: Proteins: Structure, function and Bioinformatics, Issue 52. USA: Willey Periodicals Inc, pp 225-235

122. **Schunk MK & Macallum GE** (2005) Applications and Optimization of Immunization Procedures. *Institute of Laboratory Animal Research Journal* **46,** 241-257

123. **Semler BL** (2011) Picornaviruses. In: Fundamentals of molecular virology, second edition, by Acheson NH, edited by Witt K. USA: John Wiley and Sons Inc publishers, pp 125-137

124. **Sharma R, Raychaudhuri S & Dasgupta S** (2004) Nuclear entry of poliovirus-polymerase precursor 3CD implications for host cell transcription shut-off. *Journal of Virology* **35,** 195-205

125. **Sharma P, Gaur SN & Arora N** (2013) *In Silico* Identification of IgE-binding epitopes of Osmotin protein. *PLOS ONE* **8,** e54755

126. **Shi Q, Gao G, Zhang Y, Zheng C, Xiang H & Xuan H** (2012) Cloning of structural protein VP1 gene of Foot and Mouth Disease Virus and its Expression in Escherichia coli. *Advances in Biomedical Sciences* **9,** 117-122

127. **Singh SM & Panda AK** (2005) Solubilization and refolding of bacterial inclusion body proteins. *Journal of Bioscience and Bioengineering* **99,** 303-310

128. **Smith DR, McCarthy A, Chrovian A, Olinger G, Stossel A, Geisbert TW, Hensley LE & Connor JH** (2010) Inhibition of heat-shock-protein 90 reduces Ebola virus replication. *Antiviral Research* **87,** 187-194

129. **Söding J, Biegert A & Lupas AN** (2005) The HHpred Interactive Server for Protein Homology Detection and Structure Prediction. *Nucleic Acids Research **33,***(Web Server Issue), W244-8

130. **Søresen HP & Mortesen KK** (2005) Advanced genetic strategies for recombinant protein expression in *Escherichia coli*. *Journal of Biotechnology* **115**, 113-128

131. **Sorgeloos F, Vertommen D, Rider MH & Michiels T** (2011) Theiler's L protein is targeted to the Mitochondrial Outer Membrane. *Journal of Virology* **85,** 3690-3694

132. **Stanway G** (1990) Structure, function and evolution of picornaviruses. *Journal of General Virology* **71,** 2483-2501

133. **Stills HF** (2005) Adjuvants and antibody production: Dispelling the Myths associated with Freund's Complete and Other adjuvants. *Institute of Laboratory Animal Research Journal* **46**, 281-293

134. **Sullivan CS & Pipas JM** (2001) The virus-chaperone connection. *Virology* **287**, 1-8

135. **Sweeney TR, Roque-Rosell N, Birtley JR, Leatherbarrow RJ & Curry S** (2007) Structural and mutagenic analysis of foot-and-mouth disease virus 3C protease reveals the role of the beta-ribbon in proteolysis. *Journal of Virology* **81,** 115-124

136. **Terpe K** (2006) Overview of bacterial expression systems for heterologous protein production: for molecular and biochemical fundamentals to commercial systems. *Applied Microbiology and Biotechnology* **72**, 211-222

137. **Theiler M & Gard S** (1940) Encephalomyelitis of mice. 1. Characteristics and pathogenesis of the virus. *Journal of Experimental Medicine* **72**, 49-67

138. **Thompson D, Muriel P, Russell D, Osborne P, Bromley A, Rowland M, Creigh-Tyte S & Brown C** (2002) Economic costs of the Foot and mouth disease outbreak in the United Kingdom in 2001. *Review of Science and Technology* **21,** 675-687

139. **Triantafilou M, Triantafilou K, Wilson KM, Takada Y, Fernandez N & Stanway G** (2002) GRP78, a coreceptor for coxsackievirus A9, interacts with major histocompatibility complex class I molecules which mediate internalization. *Journal of Virology* **76**, 633-643

140. **Vance LM, Moscufo N, Chow M & Heinz BA** (1997) Poliovirus 2C region functions during Encapsidation of Viral RNA. *Journal of Virology* **71,** 8759-8765

141. **van Marwijk J** (2010) Biological synthesis of gold nanoparticles by *Thermus scotoductus* SA-01. PHD dissertation, Department of Microbial, Biochemical and Food biotechnology. University of the Free State. Bloemfontein, RSA, pp 93-95

142. **van Pesch V, van Eyll O & Michiels T** (2001) The Leader Protein of Theiler's Virus Inhibits Immediate-Early Alpha / Beta Interferon Production. *Journal of Virology* **75**, 7811-7817

143. **Verma R, Boleti E & George AJT** (1998) Antibody engineering: Comparison of bacterial, yeast, insect and mammalian expression systems. *Journal of Immunological Methods* **216,** 165-181

144. **Wang J, Liang C, Peng J, Shieh J, Jong M, Lin Y, Sieber M & Liang S** (2003) Induction of immunity in swine by purified recombinant VP1 of foot-and-mouth disease virus. *Vaccine* **21,** 3721-3729

145. **Wang T, Yu B, Lin L, Zhai X, Han Y, Qin Y, Guo Z, Wu S, Zho X, Wang Y, Tong L, Zhang F, Si X, Zhao W & Zhong Z** (2012) A functional nuclear localization sequence in the VP1 capsid protein of coxsackievirus B3. *Journal of Virology* **433**, 513-521

146. **Waxman L, Whitney M, Pollok BA, Kuo LC & Darke PL** (2001) Host cell factor requirement for hepatitis C virus enzyme maturation. *Proceedings of the national academy of sciences of the United States of America* **98**, 13931–13935

147. **Weidman MK, Sharma R, Raychaunhuri S, Kundu P, Tsai W & Dasgupta A** (2003) The interaction of cytoplasmic RNA viruses with the nucleus. *Virus Research* **95,** 75-85

148. **Whitley D, Steven SP & Jordan WD** (1999) Heat Shock Proteins: A review of the molecular chaperones. *Journal of Vascular Surgery* **29**, 748-751

149. **Whitesell L & Lindquist SL** (2005) HSP90 and the chaperoning of cancer. *Nature review of Cancer* **5**,761–772

150. **Wimmer E, Helen CUT & Cao X** (1993) Genetics of poliovirus. *Annual Review of Genetics* **27,** 353-436

151. **World health Organization** (2002) The global poliomyelitis eradication initiative: number of endemic countries at lowest ever. *Weekly Epidemiological Record* **77,** 414-415

152. **Wychowski C, van der Werf S, Siffert O, Crainic R, Bruneau P & Girard M** (1983) A poliovirus type 1 neutralization epitope is located within amino acid

residues 93 to 104 of viral capsid polypeptide VP1. *European Molecular Biology Organisation Journal* **2,** 2019-2024

153. **Xiao A, Wong J & Luo H** (2010) Viral interaction with molecular chaperones: role in regulating viral infection. *Archives of Virology* **155,** 1021-1031

154. **Xiao Y, Lu Y & Chen Y H** (2001) Epitope vaccine as a new strategy against HIV-1 mutation. *Immunology letter* **77,** 3-6

155. **Yalamanchili P, Banerjee R & Dasgupta A** (1997a) Poliovirus encoded protease $2A^{pro}$ cleaves the TATA-binding protein but does not inhibit host cell RNA polymerase II transcription in vitro. *Journal of Virology* **71**, 6881- 6886

156. **Yalamanchili P, Datta U & Dasgupta A** (1997b) Inhibition of host cell transcription by poliovirus: cleavage of transcription factor CREB by poliovirus-encoded protease $3C^{pro}$. *Journal of Virology* **71**, 1220-122

157. **Yalamanchili P, Weidman K & Dasgupta A** (1997c) Cleavage of transcriptional activator Oct-1 by poliovirus encoded protease $3C^{pro}$. *Journal of Virology* **239**, 176-185

158. **Yamada M, Zurbriggen A & Fujinami RS** (1990) Monoclonal antibody to Theiler's Murine Encephalomyelitis Virus defines a determinant on myelin and oligodendrocytes and augments demyelination in experimental allergic encephalomyelitis. *Journal of **E**xperimental Medicine* **171,** 1893-1907

159. **Yau WW, Kirkland JJ & Bly DD** (1979) Modern Size-Exclusion Liquid Chromatography: Practice of Gel Permeation and Gel filtration Chromatography. United States of America: John Wiley & Sons, Inc, pp 1-2

160. **Ypma-Wong MF, Dewalt PG, Johnson VH, Lamb JG & Semler BL** (1988) Protein 3CD is the major poliovirus proteinases responsible for cleavage of the P1 capsid precursor. *Virology* **166,** 265-270

161. **Zhang SP, Zubay G & Goldman E** (1991) Low-usage codons in *Escherichia coli*, yeast, fruit fly and primates. *Gene* **105,** 61-72

162. **Zuehlke A & Johnson JL** (2010) Hsp90 and co-chaperones twist the functions of diverse client proteins. *National Institute of Health* 93, 211-217

163. **Zamora M, Marissen WE & Lloyd RE** (2002) Multiple elf4GI-specific protease activities present in uninfected and polio-infected cells. Journal of Virology 76, 165-177

164. **Zarate S, Cuadras MA, Espinosa R, Romero P, Juarez KO, Camacho-Nuez M, Arias CF & Lopez S** (2003) Interaction of rotaviruses with Hsc 70 during cell entry is mediated by VP5. *Journal of Virology* **77,** 7254-7260

165. **Zurbriggen A, Hogle JM & Fujinami RS** (1989) Alteration of amino acid 101 within the capsid protein VP-1 changes the pathogenicity of TMEV. *Journal of Experimental Medicine* **170,** 2037-2049

166. **Zylicz M & Georgopoulos C** (1984) Purification and properties of the *Escherichia coli* DnaK replication protein. *Journal of Biological Chemistry* **259**, 8820–8825

167. **Zylicz M, Ang D, Liberek K & Georgopoulos C** (1989) Initiation of lambda DNA replication with purified host- and bacteriophage-encoded proteins: the role of the DnaK, DnaJ and grpE heat shock proteins. *European Molecular Biology Organisation Journal* **8**, 1601-1608

168. **Zylicz M, Yamamoto T, McKittrick N, Sell S & Georgopoulos C** (1985) Purification and properties of the DnaJ replication protein of *Escherichia coli*. *Journal of Biological Chemistry* **260**, 7591–7598

Internet References

1. Novagen pETsystem manual (2003): www.novagen.co.za, accessed: 20-02-2013

2. Promega online manual (2003): www.promega.com, accessed: 20-02-2013

3. Proteintech™: Making better antibodies with whole proteins as nature intended (2010): www.ptglab.com, accessed: 14-03-2013

4. ProSci Inc: Antibody production and services: www.prosci-inc.com, accessed: 14-03-2013

5. Qiagen user-manual (2001); www.**qiagen**/knowledge-and-Support/Resource-Center/, accessed: 20-02-2013

6. Santa cruz Biotechnology, Inc: www.scmt.com, accessed: 10-03-2013

7. Takara-bio Inc online manual (2011): www.takarabioeurope.com, accessed: 17-03-2013

8. Zuchner T: Ultrasensitive Protein Detection Unit, Universität Leipzig (2005) : www.uni-leipzig.com, accessed: 11-03-2013